GAR

Global Assessment Report on Disaster Risk Reduction

Atlas

Unveiling Global Disaster Risk

Augmented Reality

UNISDR
United Nations Office for Disaster Risk Reduction

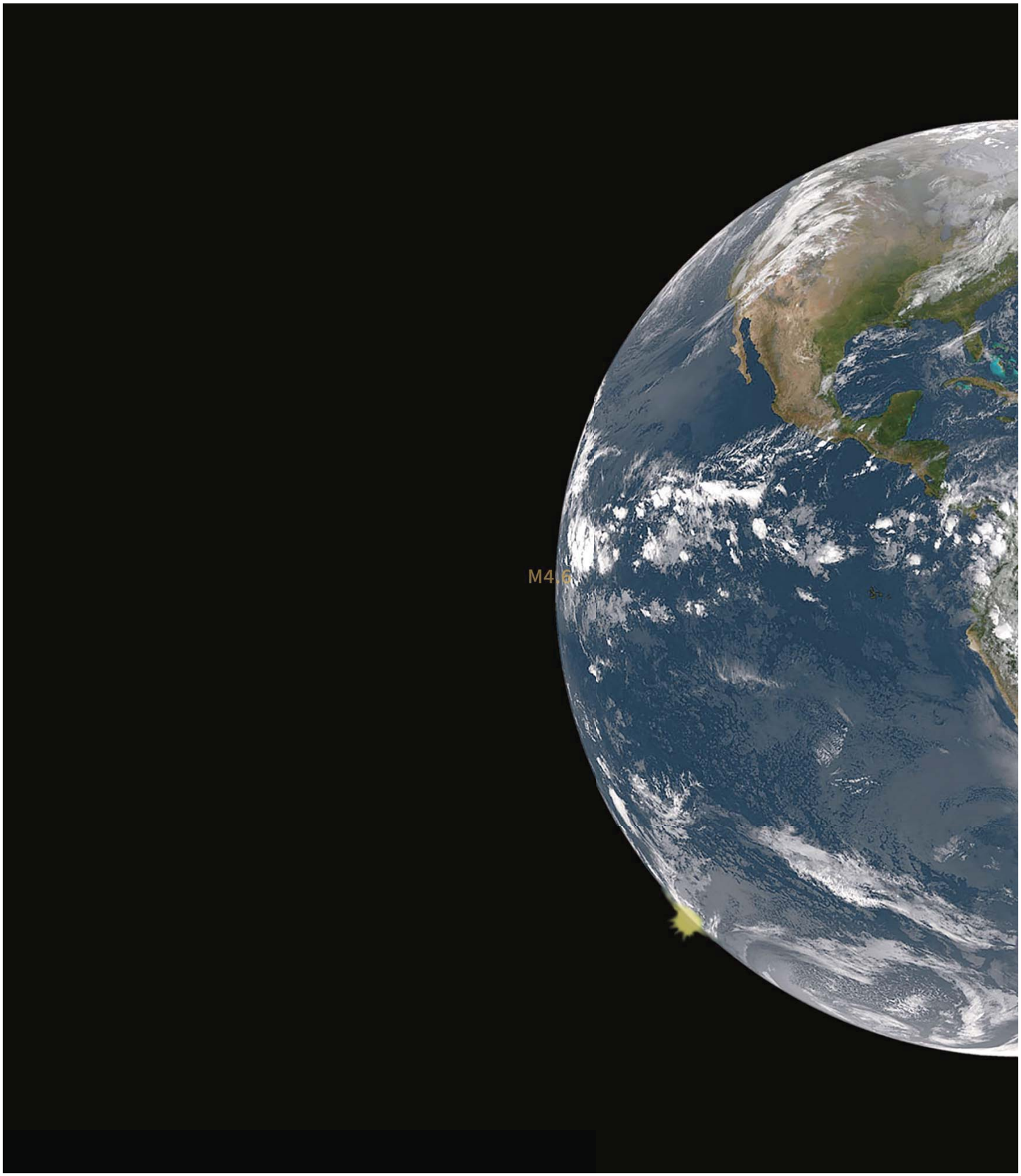
M4.6

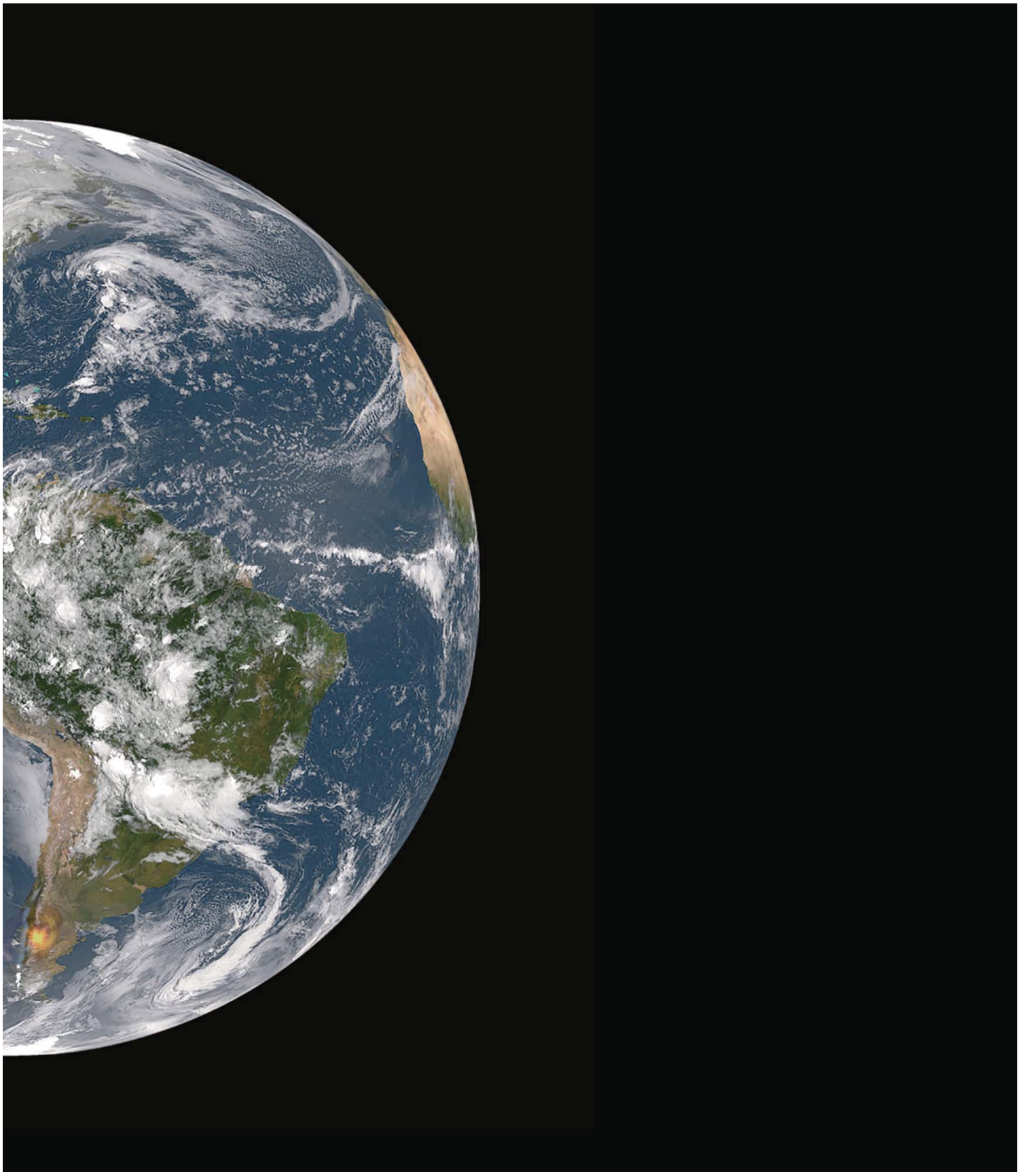

United Nations Office for Disaster Risk Reduction (UNISDR) acknowledges the financial resources generously made available by the European Commission, the German Federal Ministry for Economic Cooperation and Development, Willis Towers Watson and RMS and the in-kind and substantive contributions provided by INGENIAR LTDA, which made possible the publication of the GAR Atlas. United Nations Office for Disaster Risk Reduction (UNISDR) is also grateful to the organisations whose logos are displayed below who collaborated in the development of the UNISDR-led Global Risk Model and in the design of the GAR Atlas and accompanying GfT application.

Federal Ministry
for Economic Cooperation
and Development

Willis Towers Watson

Atlas

Unveiling Global Disaster Risk

Augmented Reality

UNISDR
United Nations Office for Disaster Risk Reduction

Download on the App Store

GET IT ON Google Play

The *GAR Atlas: Unveiling Global Disaster Risk* is an augmented reality publication. It has been designed to be read and explored using an IOS or Android tablet. Most of the information contained in the *GAR Atlas* can only be accessed in this way.

After downloading the free GAR for Tangible Earth (GfT) application from the QRcode above or from the App Store (http://unisdr.org/go/gar/apple-store) or Google play (http://unisdr.org/go/gar/android-store), activate the camera icon on the application and point your tablet or smartphone at any of the maps in your *GAR Atlas*.

Your *GAR Atlas* will now start to shimmer and the hidden veins of global disaster risk will start to come into focus. From the bare minimalist cartography on the printed page the world of disaster risk comes to life. Suddenly, and depending on the function you choose, you can be immersed in a swirling world of cloud cover and real time weather conditions or be threatened by the tracks of tropical cyclones or the releases of seismic energy. The *GAR Atlas* then becomes a vehicle for showing how the planet is far from static but dynamic and very much alive.

While the cartography in the printed atlas provides basic disaster risk metrics, using the *GAR Atlas* function on the GfT application enables you to access and explore much more detailed risk information for each country and territory. This includes a detailed risk profile, including the absolute and relative Annual Average Loss (AAL), a Loss Exceedance Curve (LEC) and, where available, data on historical disaster losses. Furthermore, additional information is provided on Average Annual Mortality for earthquakes, financing gaps as well as on the social, economic and environmental drivers of risk and resilience.

Furthermore, in each country, you can explore a range of case studies from the GAR series and beyond. The Earth Diary provides the latest news published on Prevention Web, "serving the information needs of the disaster reduction community".

Other augmented reality features in the *GAR Atlas* include hydro-meteorological, geological and anthropogenic data, which is brought together in an easy-to compare or "mash-up" format. As such the *GAR Atlas* provides not only interactive risk scenarios; it is sufficiently data-rich that the user can explore and create scenarios on their own, searching by time, place, risk driver, hazard, disaster event profile, and more.

Users of the GfT application may also explore the same data on a new media platform ; « ARTe » (the AR Tangible-earth system on normal analogue globes) through which we present the content of Gft in a brand-new way.

The new version of the GfT application also uses the latest technology for "speech recognition (SR)". It understands and carries out instructions and will also read information such as case studies for you. For example, simply press the button "SR", and say "*What's new in* Fiji" and press it back. Of course you can select any country or major cities you want, using this sentence: "*What's new in …*". In addition, the latest real-time disaster alerts are available on the GfT application through the GDACS "Global Disaster Alert and Coordination System.

GfT is fun, educational, and empowering.

** Limited numbers of ATRe (real 3D globes) will be available from UNISDR*

The Global Assessment Report on Disaster Risk Reduction (GAR) Atlas includes enhanced content. Augmented reality (AR) icons link the report to its companion application, GAR for Tangible Earth (GfT), and provide the reader with additional information and multimedia content.

To use these features, first point the camera on your GfT-installed tablet or smartphone at the desired icon, then press the AR button when it appears. A variety of dynamic information functions designed to enrich the reading experience will then play on your device.

The Earth Icon
Links the user to a dynamic 3D globe, enabling geospatial data relevant to the subject in the text.

The Web Link Icon
Links to external websites that provide details relevant to the subject in the text.

The Tablet Icon
Opens dynamic animations and additional information on the static print charts in GAR.

The Video Icon
Links to videos of UNISDR and partners relevant to the subject in the text.

Disclaimers

The views expressed in this publication do not necessarily reflect the views of the United Nations Secretariat.

The designations employed and the presentation of the material do not imply the expression of any opinion whatsoever on the part of the United Nations Secretariat concerning the legal status of any country, territory, city or area, or of its authorities, or concerning the delineation of its frontiers or boundaries.

Mention of a commercial company or product in this document does not imply endorsement by United Nations Office for Disaster Risk Reduction (UNISDR) or the authors. The use of information from this document for publicity or advertising is not permitted. Trademark names and symbols are used in an editorial fashion with no intention on infringement of trademark or copyright laws.

The boundaries and names shown and the designations used on the maps on this site do not imply official endorsement or acceptance by the United Nations.

This publication may be freely quoted but acknowledgment of the source is requested.

Citation: UNISDR (2017). GAR Atlas: Unveiling Global Disaster Risk, Geneva, Switzerland: United Nations Office for Disaster Risk Reduction (UNISDR).

Design and layout: AXIS and ELP, Tokyo, Japan.

Printing: Imprimerie Gonnet, Belley, France.

Forewords

The *GAR Atlas: Unveiling Global Disaster Risk* is being published by UNISDR two years after UN Member States agreed on an ambitious set of actions and targets to reduce disaster losses significantly, in the shape of the Sendai Framework for Disaster Risk Reduction. In 2015 too, the 2030 Agenda for Sustainable Development was adopted. It recognises that disaster risk reduction is essential to ending poverty and fostering sustainable development and well-being for all. The *GAR Atlas* provides a set of tools and practices to achieve these goals based on the strong evidence presented in the series of United Nations Global Assessment Reports on Disaster Risk Reduction, and on an increasingly sophisticated understanding of disaster risk.

As the world gears up to implement fully the Sendai Framework, the results of the UNISDR-led Global Risk Model are more important than ever. They show clearly that, across the globe, countries have to concern themselves with potential losses from disasters, and that disaster losses are disproportionately higher in resource-strapped poorer countries. Countries and regions which can least afford reduced financial and human capacity to invest in resilience continue to lose the most.

This is not news. And yet, true understanding of the scale and patterns of risk associated with key hazards such as earthquakes, tsunamis, floods, tropical cyclones, droughts and heatwaves remains limited. At UNISDR, we are committed to increasing this understanding as a vital step towards achieving effective disaster risk management. The German poet Goethe's insight that "you only see what you know" applies here. We hope that making disaster risk visible, in the form of this unique set of global and regional maps, will be a significant step in the right direction.

Robert Glasser
Special Representative of the Secretary-General for Disaster Risk Reduction,
Head, United Nations Office for Disaster Risk Reduction (UNISDR)

March 2017

Forewords

It was not until the sixteenth century that we had the first world map with recognizable continents and oceans. Over the next four hundred years, as coastlines and lakes were surveyed with increasing accuracy, as satellite observations replaced trigonometric surveys, we discovered new metrics to be plotted, giving us global maps of topography and geology; maps of temperatures, rainfall, sunshine, and wind speeds; maps of climate zones, vegetation types, human settlements, and energy usage – and more.

Risk is real. Although we cannot readily see risk, we can measure it by understanding how the probability of damaging winds, floods, or shaking compounds with the exposure of settlements and livelihoods and lives. Using vulnerability functions that link the hazard to the damage, we can calculate and map risk.

Thanks to the work of the UNISDR, we have the first global map of the potential for harm to the built environment from a range of sources, including earthquake shaking, tsunami, volcanic eruption, wind, and flood. This map is measured using a constant metric of percentage loss of value at consistent levels of probability, which makes it possible to compare the impact of a cyclone in Bangladesh to an earthquake in Peru or understand the risk cost of a tsunami with that of a storm surge, just to name a few.

To be most useful, we do not just want to know the risk at a single location, but how risk correlates across multiple locations that can be impacted in the same disaster. This is what was achieved in the catastrophe modeling revolution of the late 1980s, leading to data-rich models and software tools that are used by insurers and (re)insurers worldwide. Now, these same capabilities are being made available to countries and cities in order for them to manage and reduce their catastrophe risks. Extending the use of catastrophe models to all countries at risk is a key step in using these models to identify the benefits of alternative policies around risk reduction.

We know that catastrophe losses in any one country, and even worldwide, are too volatile to be able to measure progress by comparing one decade with another. Instead we will need to measure progress through employing catastrophe models, in the same way that insurers use risk models to measure the price of risk. The UNISDR's accomplishment in delivering a global multi-hazard perspective of catastrophe risk is to be commended. This is an important milestone in developing a safer world.

Robert Muir-Wood
Chief Research Officer, RMS

March 2017

Forewords

For nearly two centuries Willis Towers Watson has been arranging protection of people and property from natural disasters. Over the last decade we have worked with the United Nations Office for Disaster Reduction to expand the awareness and resilience of communities and assets to these growing threats and we are delighted to support the production of this ground breaking global risk atlas and the unique team and capabilities that lay behind it.

What gets measured can get managed and the UNISDR is to be congratulated for taking the methods, metrics and models that have transformed the capability of the reinsurance industry to better understand these risks and applying them to serve a wider community. The creation of this globally consistent and comparable risk assessment across a wide range of perils is a remarkable achievement of data access, integration and visualisation. These knowledge facilities will help governments, companies and NGOs save millions of lives and livelihoods, and billions of dollars, in the decades ahead and one day we hope and expect that people will look back and say these maps helped change the world.

Rowan Douglas, CBE, FRGS
CEO Capital, Science & Policy Practice
Willis Towers Watson
Chairman, Willis Research Network

March 2017

Contents

iv **Forewords**

iv United Nations Office for Disaster Risk Reduction, UNISDR
v Risk Management Solutions, RMS
vi Willis Towers Watson

9 **Section 1: Introduction**

10 **1.1** The GAR Atlas
11 **1.2** Maps that change the world
12 **1.3** The hidden veins of disaster risk
12 **1.4** Chance would be a fine thing
18 **1.5** The GAR Global Risk Model

19 **Section 2: The world of disaster risk**

47 **Section 3: Disaster risk implications for social and economic development**

47 **3.1** Fiscal resilience challenged
52 **3.2** Assessing the impact of disaster mortality
60 **3.3** A holistic approach to understanding disaster risk and resilience
64 **3.4** The implications for sustainable development

71 **Section 4: Applications of the Global Risk Model**

71 **4.1** How climate change modifies disaster risk
73 **4.2** Estimating the risk from volcanic ash
76 **4.3** Modelling extensive risk
77 **4.4** Local level applications
77 **4.4.1** Volcanic risk in Nariño, Colombia
78 **4.4.2** Earthquake risk in Lorca, Spain
78 **4.5** Estimating risk scenarios using the Global Risk Model
78 **4.5.1** The April 2015 Nepal Earthquake
78 **4.5.2** The August 2016 Amatrice, Italy Earthquake
79 **4.5.3** Estimating risk during an unfolding event: Hurricane Matthew, October 2016

81 **Section 5: Probabilistic hazard and risk assessment methodology**

81 **5.1** Probabilistic hazard analysis
81 **5.1.1** Probabilistic seismic hazard analysis
91 **5.1.2** Probabilistic tsunami hazard analysis
101 **5.1.3** Probabilistic tropical cyclonic wind and storm surge hazard analysis
116 **5.1.4** Probabilistic riverine flooding hazard analysis
125 **5.2** Development of the Global Exposure Database
125 **5.3** Physical vulnerability of exposed assets
126 **5.4** Probabilistic multi-hazard risk assessment
129 **5.5** Aggregated multi-hazard probable maximum losses

cxxxi **References**

cxxxiii **Acknowledgements**

GAR Atlas: Unveiling Global Disaster Risk

Section 1: Introduction

1.1 The GAR Atlas

On the 2 February 2017, the United Nations General Assembly adopted a set of indicators to measure progress against the seven Global Targets of the Sendai Framework for Disaster Risk Reduction 2015-2030 (Sendai Framework)[i].

The outcome indicators associated with Targets A – D[ii] now provide for the first time a way of measuring whether disaster loss and damage has actually been reduced by 2030. Importantly, and again for the first time, the same indicators have been adopted to monitor progress against relevant targets of the Sustainable Development Goals (SDGs).

Under the Hyogo Framework for Action[iii], which guided international action until 2015, significant progress was made in improving preparedness and response to disasters and in strengthening the institutional capacities, policy and legislative frameworks and strategies to do so. Over much of the same period, however, global disaster loss and damage continued to increase (Figure 1.1)[iv]. As such, if the Outcome and Goal of the Sendai Framework and its Global Targets are to be achieved, countries will need to transform their approach to managing disaster risk[v].

The Hyogo Framework was predominantly concerned with managing disasters. Only one of its four Priorities for Action (Priority for Action 4) focused on addressing underlying risk drivers. In contrast, the Sendai Framework is primarily a framework for managing disaster risk. It therefore represents a change in perspective: from managing disasters towards managing underlying risk.

The reduction of poverty, the improvement and access to health and education for all, the achievement of sustainable and equitable economic growth and the protection of the health of the planet depend on the management of disaster risk in the day-to-day development decisions of governments, companies, investors, civil society organisations, households and individuals. Strengthened disaster risk reduction, therefore, is essential to make development sustainable.

Priority for Action 1 of the Sendai Framework deals with understanding risk. Given that all development decisions, whether they are related to capital investment, social expenditure or environmental protection, have the potential to either reduce or increase risk, understanding the risk and trade-offs inherent in each activity is fundamental to both disaster risk reduction and sustainable development. Risk metrics are critical to inform and to identify the costs, benefits and trade-offs implicit in each decision[vi]. In particular, this is critical to the first aspect of the Goal of the Sendai Framework, which calls for the prevention of new disaster risk.

The *GAR Atlas* contributes to improving our understanding of risk and provides a powerful rationale for pursuing development pathways that prevent the creation of new risk, reduce existing risk and strengthen resilience.

The *GAR Atlas* presents the output of a Global Risk Model (GRM) that can estimate the disaster risk associated with different kinds of hazard faced by national economies throughout the world. The model uses a state-of-the-art probabilistic approach analogous to that applied by the catastrophe modelling and insurance industry over recent decades. This model has been developed by a consortium of leading scientific and technical organisations, under the coordination of UNISDR. Initial results from the model have already been previewed in GAR13 and GAR15[vii].

The *GAR Atlas* displays the risk associated with earthquakes, tsunamis, riverine flooding, cyclonic winds and storm surge with a global level of observation and a national level of resolution. By using the same methodology, arithmetic and exposure model to calculate the risk for all these hazards, the GAR Atlas provides globally comparable multi-hazard risk metrics and enables comparisons of risk levels between countries and regions and across hazard types. For example, the values associated with earthquake risk in Indonesia and flood risk in Colombia, and their relevance for national economies, can now be compared because they have been calculated using the same methodological framework.

Figure 1.1 Conflicting evidence on progress: gradual progress across the Hyogo Framework's Priorities for Action (left) but increasing physical damage (right).

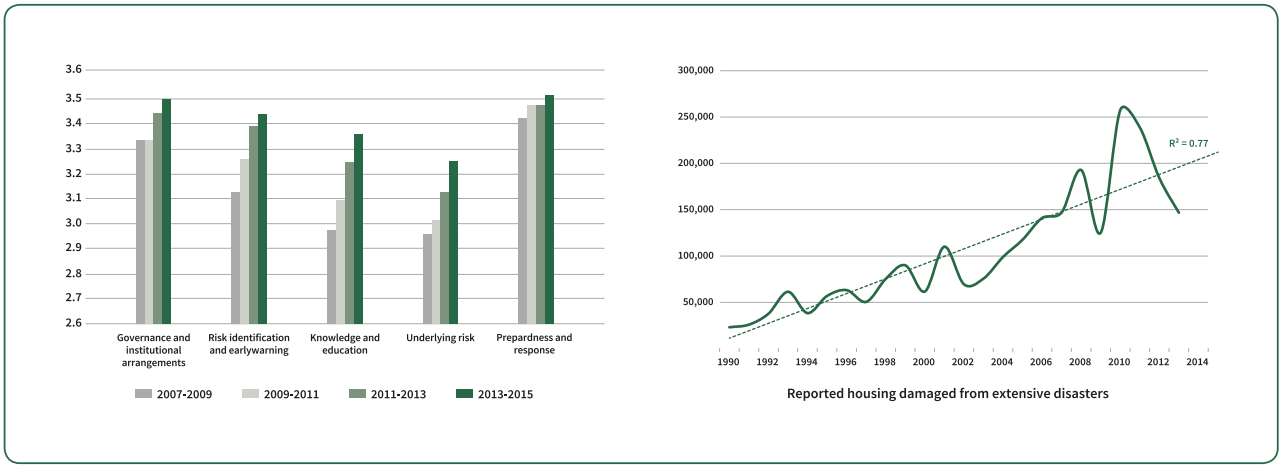

Source: UNISDR

In this way, the *GAR Atlas* facilitates a better understanding of the global risk landscape, enabling the estimation of the order of magnitude of probable losses in each country, and taking into account the risk contributions from different hazards. The *GAR Atlas* is the first of its kind that is non-proprietary, completely open and with multi-hazard global coverage.

The *GAR Atlas* thus enables governments, the private sector, the international community and indeed anyone concerned with development to access risk metrics that up to now have generally only been available to the insurance and reinsurance industry. This fills a major gap in understanding risk. Most probabilistic risk assessments have been developed commercially for the insurance industry and cover risk from specific hazards, mainly in higher-income countries. However, they are rarely accessible and are based on proprietary models. While more and more public-domain risk models are now being developed, the use of different methodologies and datasets makes comparison difficult. By providing a first level risk assessment for all countries, the *GAR Atlas* offers a framework for filling in what are still blank spaces on a world map of risk.

By making global patterns of disaster risk explicit, by facilitating access to risk metrics and by exploring the interactions between risk and development, it is hoped that the *GAR Atlas* will contribute to the implementation of the Sendai Framework and the SDGs and will stimulate the creation of a new generation of risk models at more detailed scales and in all countries of the world[viii].

1.2 Maps that change the world

Quantum physicist David Bohm proposed that meaning, along with energy and matter, is intrinsic to reality. For Bohm, the act of interpreting the universe is at the same time an act of creation[ix].

In 15th century Florence, artists such as Masolino da Panicale and Brunelleschi first established the principles of linear perspective, an innovative approach to representing three-dimensional space. The adoption of linear perspective, however, not only changed the representation and interpretation of space: ultimately it radically transformed the perception of both time and space. Whereas medieval artists appeared immersed in the universe they represented, the fixed viewpoint of linear perspective art had the effect of separating subject and object and of externalising and objectifying space and time. Given that perceptions of space and time are encoded in all social and economic practices and relations[x], the invention of linear perspective played a critical role in the construction of space in the centuries that followed.

Similarly, when 2nd century Alexandrian scientist Ptolemy depicted a spherical earth on a two-dimensional map using parallels of latitude and meridians of longitude he introduced a new way of representing geographic space, which had a similarly incisive influence on how space was occupied and transformed.

In the 6th century BCE, Anaximander (Figure 1.2) had already highlighted the relationship between distinct continents, seas and oceans and a vision of the inhabited world as a two-dimensional disc. But it was Ptolemy´s mathematical grid that really revolutionised cartography, first in the medieval Islamic world and later in Renaissance Europe.

In 1154, Muhammad al-Idrisi produced the *Tabula Rogeriana,* which for the next three centuries was to remain the most accurate map of the world. The *Tabula Rogeriana* used Ptolemy's mathematical grid to divide the inhabited world into seven climate zones, each of which were further divided into ten sections or fractions. The geography of each of these sections was described in detail in Ibn Khaldun's monumental *Al-Muqaddimah* in the 14th century.

A fusion between Ptolemy's principles of cartography and the Florentine principles of linear perspective then enabled Renaissance mapmakers to accurately fix the location of any place in the world, as well as its distance and direction to any other place, through a system of unchanging coordinates. By the time the *Atlas Major* was published in 1634 (Figure 1.3) most of the world, as we know it today, had already been accurately represented in maps.

These cartographic innovations, taken together with the invention of the chronometer in the 18th century, objectified and externalised time and space so that it could be observed, mapped, measured and

Figure 1.2 Anaximander's world map from the 6th Century BCE[xi]

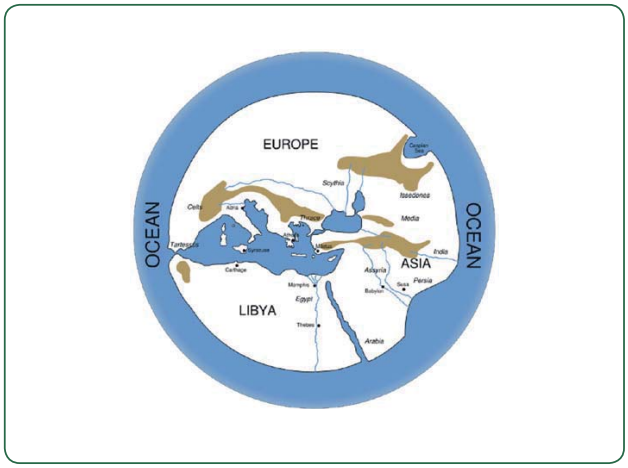

Figure 1.3 Atlas Major of 1634[xii]

analysed in a seemingly scientific and factual way. This new vision of space and time also underpinned, facilitated and permeated dramatic transformations of the world's social, economic, territorial and environmental landscape.

Maps, therefore, have the power not only to interpret, but to transform and create the landscape. Maps, indeed, can change the world.

1.3 The hidden veins of disaster risk

Legendary Jamaican sound engineer and producer Lee Perry once stated that dub versions are the X-ray of a song[xiii]. By subverting and disrupting both the song as object and the artist as subject, hidden musical veins, that were only implicit in the original songs, came to the surface and flowed through swirling, spacious dubscapes.

A change of focus from managing disasters as events to managing the underlying processes that create risk requires a similar process of deconstruction and reassembly, one that makes explicit and visible the hidden veins of disaster risk.

Whether in the media, research or policy discourse, disasters often continue to be characterised as unexpected, unforeseeable, overwhelming and fundamentally exogenous events. Over the years this objectification of disasters as decontextualised events and as *externalities* has been gradually codified into increasingly structured disaster management organisations and systems[xiv].

There is a growing consensus, however, now reflected in the Sendai Framework, that disaster risk is endogenous to a range of underlying social, economic, territorial and environmental processes and drivers and is constructed and accumulated over time. Disaster risk is normally described as a compound variable, constructed through the relationships between three other variables: *hazard, exposure* and *vulnerability.*

In turn, hazard, exposure and vulnerability are also dependent variables. Hazard, for instance, is a complex expression of probability that is built from both socially constructed as well as physical variables. Exposure is a reflection of how social relations of production unfold in territory and geography, concentrating people and assets in certain locations. Vulnerability, or the susceptibility to damage of certain structures due to certain hazards, is likewise configured through a range of social, economic, political and cultural conditions.

From that perspective, disasters in any given time and place are a result of multiple causes and conditions; crystallisations of *realised risk,* when what are often implicit processes of risk accumulation suddenly become manifest. Risk, similarly, has no independent existence but is a value that represents the interdependence of multiple social, economic, environmental and territorial relationships and interactions occurring over different spatial and temporal scales. This is a view coherent with both Nagarjuna's concept of interdependent origination as well as with Alexander von Humboldt's *invention of nature*[xv].

Box 1.1 Basic definitions

Disaster Risk: The potential loss of life, injury, destroyed or damaged assets which could occur to a system, society or a community in a specific period of time, determined probabilistically as a function of hazard, exposure, vulnerability and capacity.

Hazard: A process, phenomenon or human activity that may cause loss of life, injury or other health impacts, property damage, social and economic disruption or environmental degradation.

Exposure: The situation of people, infrastructure, housing, production capacities and other tangible human assets located in hazard-prone areas.

Vulnerability: The conditions determined by physical, social, economic and environmental factors or processes, which increase the susceptibility of an individual, a community, assets or systems to the impacts of hazards.

Underlying disaster risk drivers: Processes or conditions, often development-related, that influence the level of disaster risk by increasing levels of exposure and vulnerability or reducing capacity.

Source: United Nations, 2016
It is recommended that these definitions are read together with their annotations in the report.
United Nations, 2016

1.4 Chance would be a fine thing

The genius of writer Graham Greene was his capacity to be able to distil the whole experience of the tropics into the smell of one rotten guava[xvi]. In the same way, a probabilistic risk metric presented in the *GAR Atlas,* the Annual Average Loss (AAL), condenses in a single number the multiple interdependencies and complexities that configure disaster risk into a single numerical value. Visualising those values in a cartographic form is a way of making explicit the hidden veins of disaster risk. Only when disaster risk can be made visible and can be measured can it be properly managed.

The concept of probability is rooted in the Latin word *probare.* The etymology of the term suggests a double meaning: one aspect of it refers to a view into the future, while the other one is an interpretation of the past, one is concerned with opinions, the other with what we actually know[xvii].

The mathematical study of probability, as the likelihood of an event occurring, has its origins not in disaster risk modelling, but in the rather more Dionysian pursuit of gambling. Gambling, and the stakes and chances involved in it, has occupied human minds for millennia. The term *hazard* itself is derived from *al zahr* – the Arabic word for dice. The first scientific treatises on probability date back to the reflections of Blaise Pascal and Pierre de Fermat in the 17th century, eventually giving birth to systematic probability analysis[xviii].

The basic premise of probability analysis is that more things *might* happen in the future than actually *will* happen. Examining disaster risk from a probabilistic perspective therefore mixes future possibilities with present realities. The possibilities refer, in this case, to the hazardous events, which could happen, although their characteristics in terms of location, timing, duration and intensity are unknown. Realities

refer to the present conditions of exposure and vulnerability within which hazardous events occur.

Probabilistic disaster risk assessment was first introduced by the insurance industry following Hurricane Andrew in Florida in 1992, which at the time was the most destructive hurricane in the history of the United States of America, with total damage exceeding USD 15.5 billion[xix].

Until then, premiums for catastrophe insurance were generally calculated using traditional actuarial approaches that made use of projections of historical patterns of disaster loss and damage. Hurricane Andrew highlighted, with lamentable consequences for the insurance industry, the limitations of that approach. The possibility that a hurricane like Andrew might occur had not been priced into insurance premiums in South Florida. As a result more than 930,000 policyholders lost coverage after 11 insurance companies went bankrupt[xx].

While historical losses can explain the past, they do not necessarily provide a good guide to the future. Catalogues of observed and recorded hazardous events are generally incomplete, while very severe events may only occur over return periods that are longer than historical records. For example, even if a full century of historical data exists on extreme flooding and drought events in a country, any model derived from that data would not be able to forecast the previous extremes that had occurred over the past 1,000 years (Figure 1.4). As such, most disasters that could happen have not happened yet[xxi].

After Hurricane Andrew, the increasing availability of computation power and capacity made it possible for the first time to process the large volumes of data necessary to model hazard, exposure and vulnerability, ushering in the era of probabilistic disaster risk modelling, or catastrophe modelling as it is known in the insurance industry.

Probabilistic models simulate those future disasters which, based on scientific evidence, could possibly occur, reproducing the physics of the phenomena and recreating the intensity of a large number of synthetic hazardous events. In doing so, they provide a more complete picture of the full spectrum of future potential losses than is possible with only historical data. The scientific data and knowledge used is still incomplete, meaning that all models have a degree of inherent uncertainty. However, provided that this uncertainty is recognised, probabilistic models can provide much better guidance on the likely *order of magnitude* of probable losses compared to projections from historical data.

In these models, probability refers to the likely frequency of occurrence or the return period of losses associated with certain hazards. The concept of return period is often misunderstood. If a loss has a 500-year return period, this does not mean that the loss only occurs every 500 years, nor does it mean that if the loss occurred today, it would not recur for another 500 years. Rather it means that the loss occurs once every 500 years on average. For example, if four extreme losses occur in the space of a century followed by nineteen centuries without such extreme losses, the return period would still be 500 years.

The main output of probabilistic risk models is the loss exceedance curve (LEC), which relates different loss values with their exceedance rates, usually expressed in years. From the LEC several risk metrics can be derived.

The Average Annual Loss (AAL) is a compact metric with a low sensitivity to uncertainty. It corresponds to the expected average loss per year considering all the events that could occur over a long time frame, including very intensive losses over long return periods. When normalised by exposed value or capital stock it is known as the *pure risk premium* in the insurance industry. The Probable Maximum Loss (PML) represents the maximum loss that could be expected within a given return period. For example, the PML can be used to determine the size of reserves that governments or insurance companies should have available to buffer losses.

Box 1.2 Highlights the different stages of probabilistic risk modelling used in the Global Risk Model.

Figure 1.4 The small sample size of hazard events records

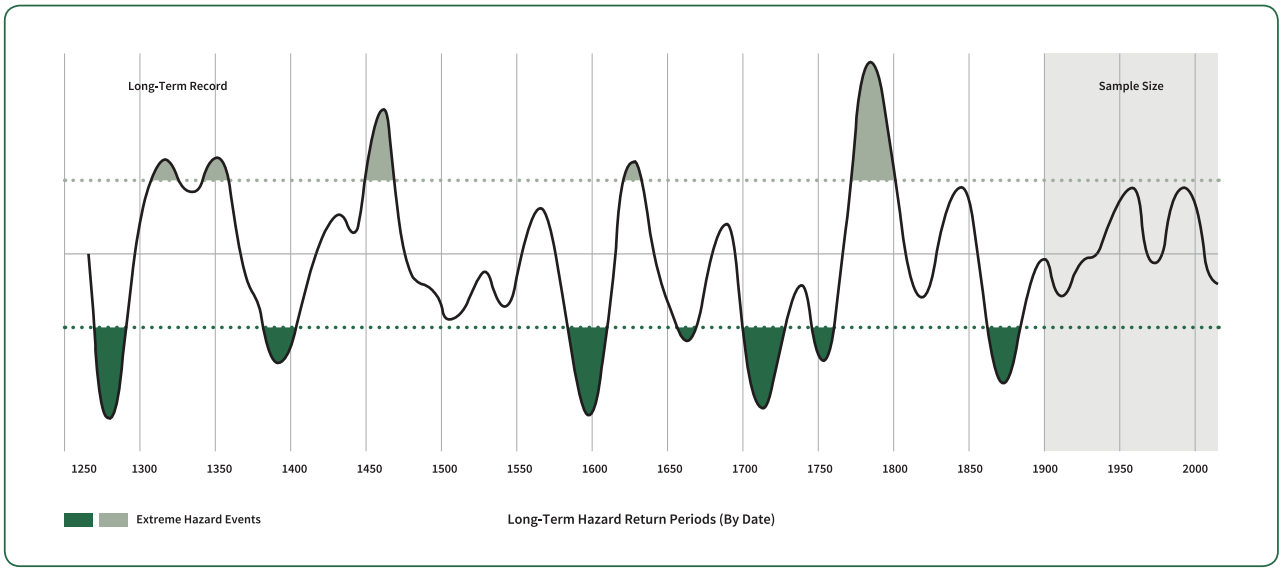

Source: UNISDR, 2015a

Box 1.2 Assessing risk using a fully probabilistic approach

The objective of a fully probabilistic risk assessment is to estimate the probability of occurrence of future losses associated with different hazards for given portfolios of vulnerable and exposed assets.

The required input data are:

Hazard: Generation of a simulated event set for each hazard.

Figure 1.5 Simulated events.

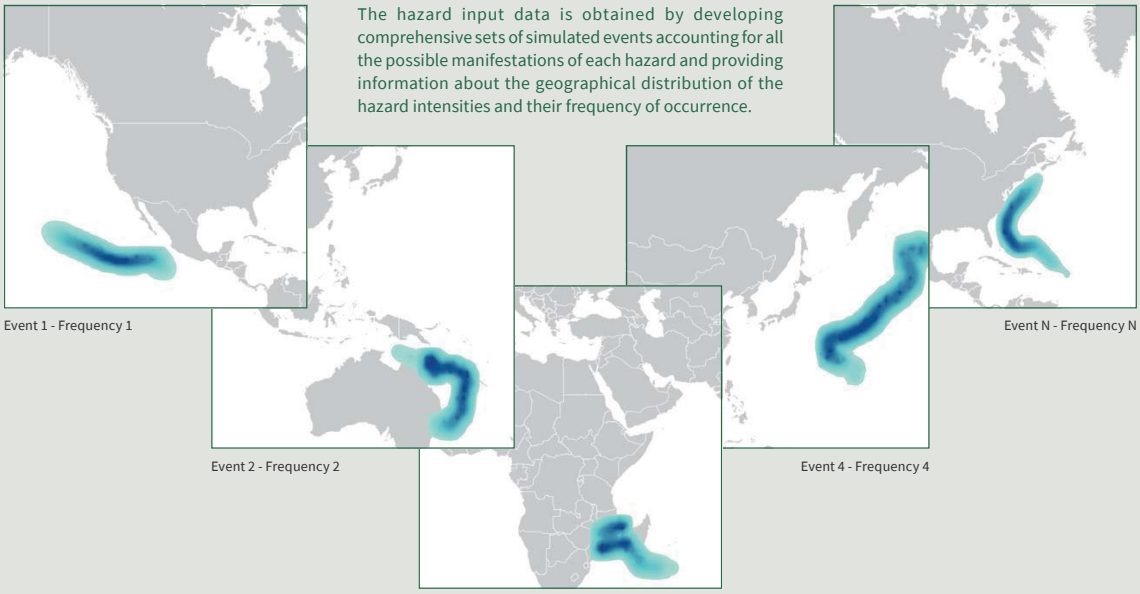

Source: Cardona et al. 2015

Exposure: Assembly of a database with an accurate representation and characterisation of the assets exposed and susceptible to damage due to the occurrence of at least one of the considered hazards.

In the *GAR Atlas*, public and private buildings located in urban and rural areas globally were mapped at 5x5km resolution level inland and 1x1km resolution level in coastal areas.

Source: UNISDR

Figure 1.6 Example of exposure information.

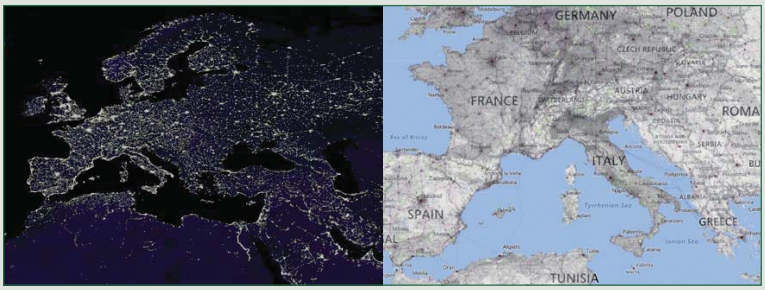

Earth at night[xxii]

Distribution of exposure database entries in Europe

Each 5x5km (or 1x1km in coastal locations) pixel contains information about the distribution of building classes, their structural characteristics, use and value.

Figure 1.7 Example of exposure characterization.

Source: UNISDR

Vulnerability: Development, for each building class and for each hazard, of vulnerability models that provides relationships between hazard intensities and expected losses in a continuous, qualitative and probabilistic manner.

Figure 1.8 Example of vulnerability functions for different building classes and different hazards. Adapted from Cardona et al. 2015

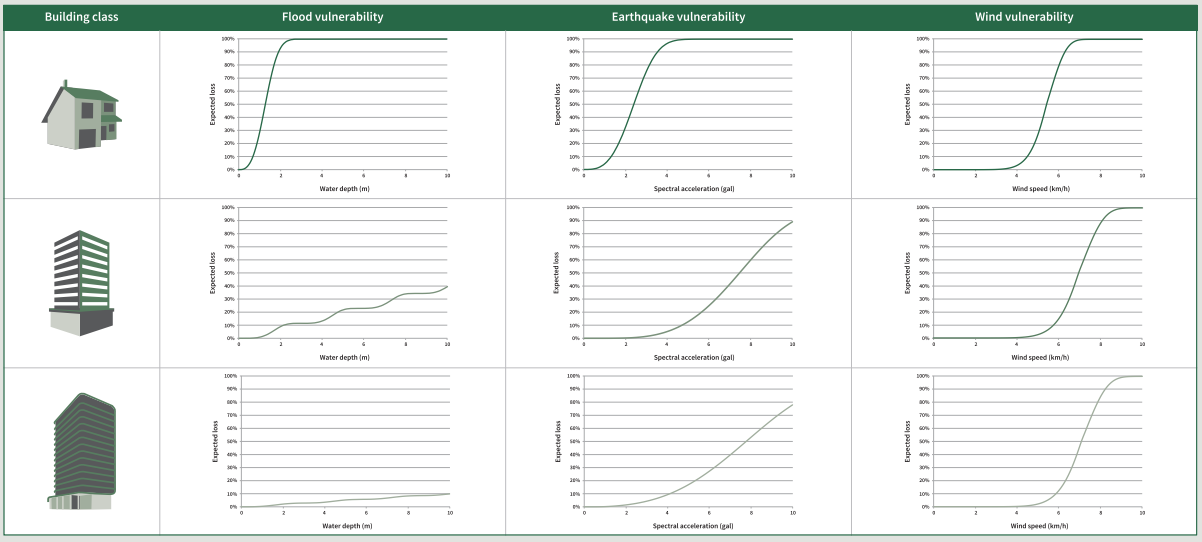

Probabilistic risk assessment: the convolution between the hazard and vulnerability inputs.

The associated damage and loss for each asset included in the exposure database is then calculated for each event included in the stochastic sets. The distribution of probable future losses is then obtained from the exceedance rates for each loss value, enabling the definition of a loss exceedance curve (LEC) and the derivation of risk metrics such as Average Annual Loss (AAL) as shown in Figure 1.10 and Probable Maximum Loss (PML) for each country.

Probabilistic Risk Assessment

Figure 1.9 Combination between the hazard, exposure and vulnerability inputs

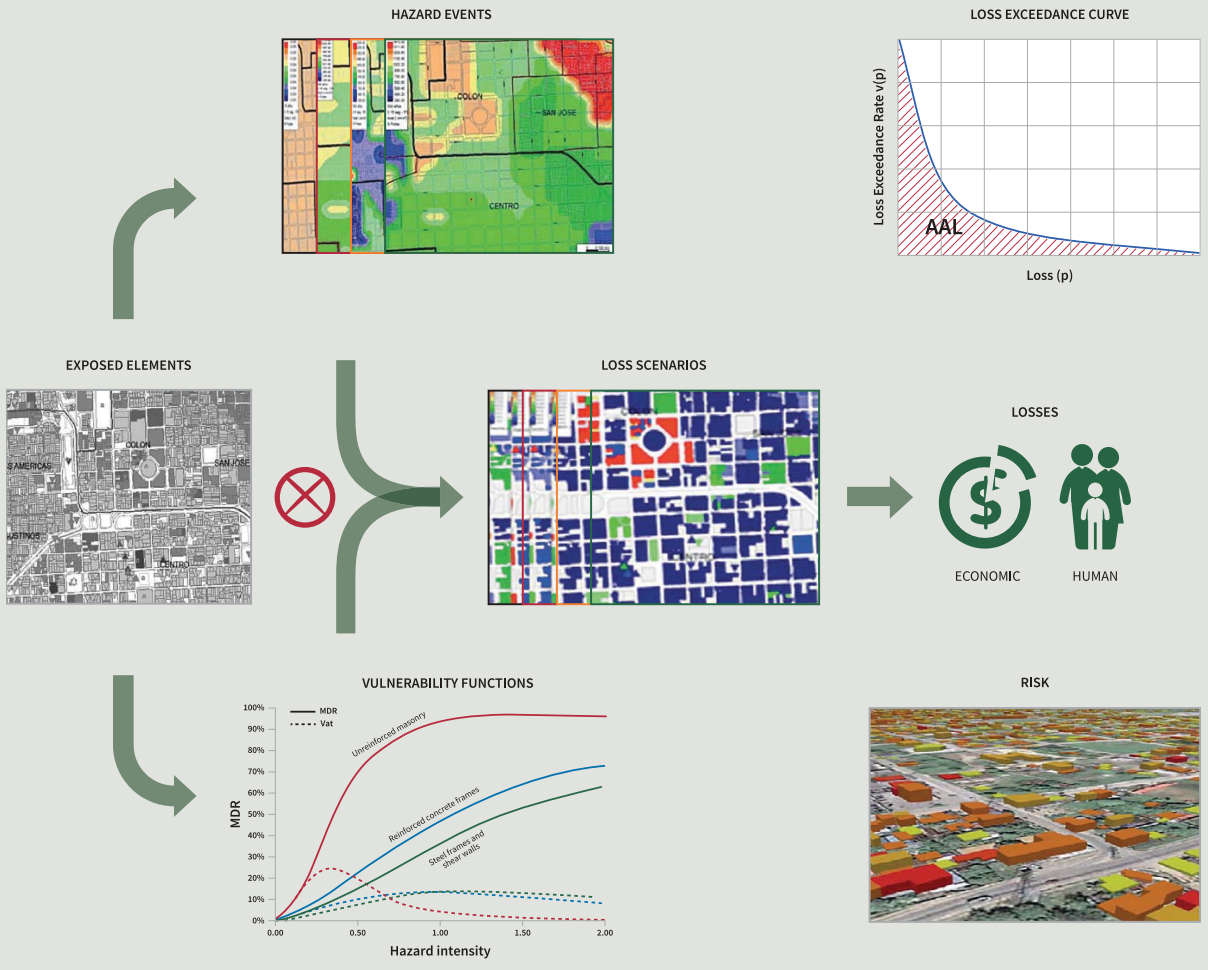

Figure 1.10 Global multi-hazard AAL relative to capital stock

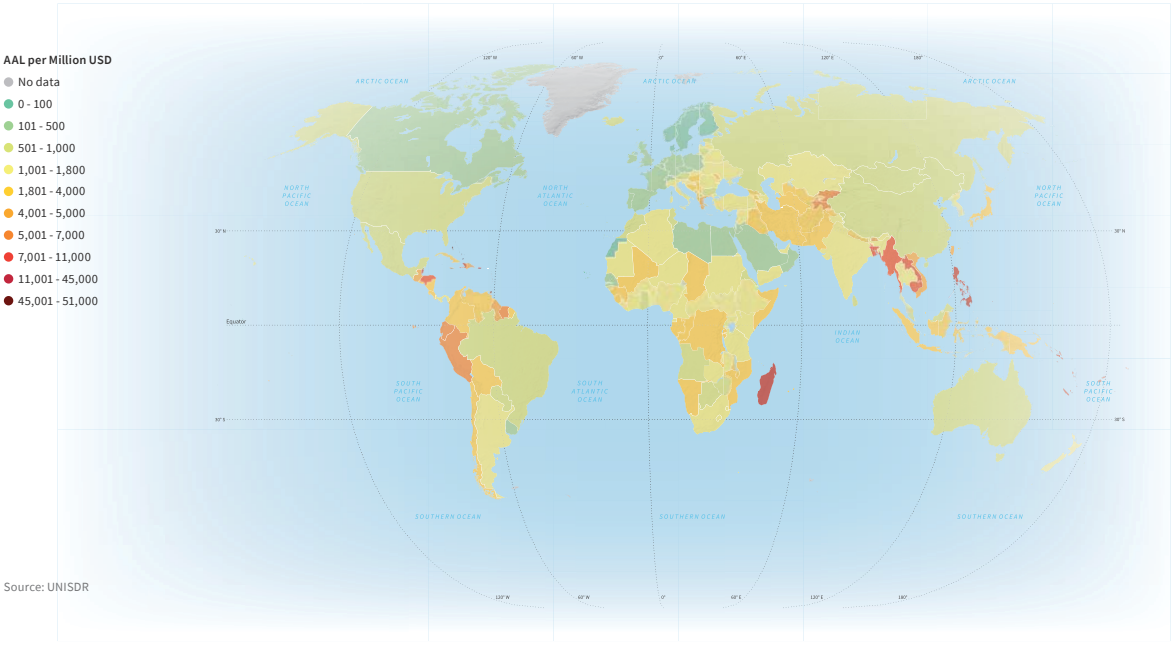

Source: UNISDR

Scale

Using exactly the same methodology, probabilistic risk assessments can be developed at sub-national, urban or local scales, using more detailed input data on hazard, exposure and vulnerability. Even though assessments can be carried out on a building-by-building scale, uncertainties will always exist and need to be taken into account.

Figure 1.11 Seismic Annual Average Loss in Medellin, Colombia

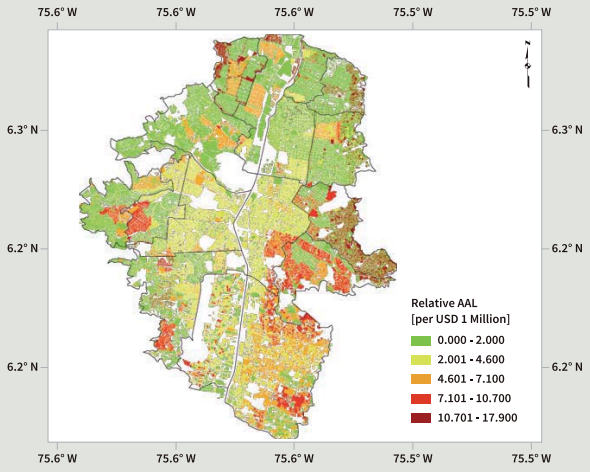

Source: Salgado-Gálvez et al. 2014

1.5 The GAR Global Risk Model

In the GAR Global Risk Model (GRM), probabilistic hazard models have been developed for five major hazards: earthquakes, tropical cyclone winds and storm surge, tsunamis and riverine flooding worldwide. In addition, *proof of concept models* have been developed for volcanic ash fall in the Asia-Pacific region, and for the impact of climate change on hurricane wind hazard in the Caribbean.

A global exposure model has been developed at a 1x1km resolution along coastlines and 5x5km elsewhere, with information on the structural characteristics, use and the value of the building stock exposed to hazardous events. Appropriate vulnerability functions have been selected on the basis of expert knowledge in each region.

The open-source multi-hazard risk platform CAPRA[xxiii] was specially enhanced for the GRM and has been used to calculate risk. A more detailed technical description of the modelling process is provided in Section 5 of the *GAR Atlas.*

By covering most of the principal hazards that affect the built environment in all world regions, the GRM provides a first cut estimate of global disaster economic risk. However, these estimates are still very conservative. Other hazards, such as drought, have not yet been assessed globally, meaning that risk to the agriculture sector (including livestock, forestry and fisheries) is not represented in the risk metrics. It is planned to address risk in the agricultural sector in the next phase of the GRM, which will allow for a more complete assessment of global disaster risk.

Similarly, the approach taken allows estimations of direct economic loss, understood as the *monetary value of total or partial destruction of physical assets existing in the affected area*[xxiv]. As the metrics do not include indirect economic loss, the estimates are again very conservative. For example, in the 2010 Haiti earthquake and the 2014 Serbia floods, direct economic loss in the built environment only represented 47 per cent and 31 per cent respectively of total losses[xxv].

Similarly, the risk estimates provided by the GRM do not include extensive risk, associated with large number of localised, low-severity but frequently occurring events and which cannot be modeled probabilistically at the global level. In some countries, extensive risk may represent a significant proportion of the AAL. As discussed in Section 4 of the *GAR Atlas,* extensive risk can be most effectively estimated using empirical approaches based on national disaster loss and damage records. As of March 2017, only around 90 countries have such records, which means that a global estimate of extensive risk is currently not yet possible.

In order to monitor progress against the Global Targets of the Sendai Framework it is expected that many more countries will collect this data in the coming years and that its coverage and quality will be improved. This should allow the integration of extensive risk into the GRM.

As a global model, the GRM models risk at a relatively coarse grain resolution. As such, the risk metrics presented in the *GAR Atlas* are designed to identify broad patterns of risk and their development implications rather than to inform development decisions at the local level. While the resolution of the GRM can be increased to focus in on specific areas, this leads to commensurate increases in the uncertainty of the results.

However, as highlighted in Section 4 of the *GAR Atlas,* the GRM can provide a global framework for the development of more detailed risk models, using a similar methodology and higher-resolution data. Even with this limitation, and again as highlighted in Section 4, the GRM has proved capable of generating credible event scenarios in the same order of magnitude as reported losses in the case of a number of recent disasters.

From that perspective, the *GAR Atlas* can be considered an *Atlas Major* of global disaster risk. Our current understanding of the global distribution and attributes of disaster risk are probably analogous to a 16th century world map. As better data and advanced modelling techniques come on stream, risk metrics will gradually become more accurate and currently unexplored facets of global risk will become visible. In the interim, the *GAR Atlas* gives us a sense of the overall scale, distribution and patterns of disaster risk, with a global level of observation and a national level of resolution. As in the case of early world maps, it is hoped that the *GAR Atlas* will encourage risk-explorers to find new pathways and map new geographies of risk.

---

i. UNISDR 2015a

ii. United Nations 2016

iii. UNISDR 2005

iv. UNISDR 2009, 2011,2013, 2015b

v. UNISDR 2015a

vi. UNISDR 2015a

vii. UNISDR 2013, 2015b

viii. The metrics provided by the *GAR Atlas* have already been used in a number of applications. For example: Disaster Risk Indicators for the Americas (CIMNE and INGENIAR, 2015), INFORM (IASC and European Commission, 2015), ThinkHazard (GFDRR, 2016), Disaster risk integrated operational risk model (The Economist Intelligent Unit, 2016), Unbreakable : Building the Resilience of the Poor in the Face of Natural Disasters (Hallegate et al. 2017), Salgado-Gálvez (2016a)

ix. Bohm and Peat 1987

x. Harvey 1989

xi. http://www.atlasandboots.com/maps-that-changed-our-world-view/ and http://www.smithsonianmag.com/history/the-waldseemuller-map-charting-the-new-world-148815355/?no-ist=&page=2

xii. http://www.atlasandboots.com/maps-that-changed-our-world-view/ and http://www.smithsonianmag.com/history/the-waldseemuller-map-charting-the-new-world-148815355/?no-ist=&page=2

xiii. Veal 2007

xiv. Oliver-Smith et al. 2016

xv. Wulf 2015

xvi. Garcia Marquez 1984

xvii. Bernstein 1996

xviii. Bernstein 1996

xix. AIR 2002

xx. McChristian 2012

xi. UNISDR 2013

xxii. http://cdn1.theweek.co.uk/sites/theweek/files/styles/theweek_gallery_main_image/public/121206earthnip_6_0.jpg?itok=ac4op1Ek

xxiii. Cardona et al. 2012

xxiv. United Nations 2016

xxv. UNISDR 2015b

Section 2

The world of disaster risk

This Section of the *GAR Atlas* illustrates how direct disaster economic loss in the built environment is distributed across countries and territories.

Box 2.1 Basic definitions

> **Direct economic loss:** the impact of total or partial destruction of physical assets existing in the affected area. Direct economic loss is nearly equivalent to physical damage.
>
> Source: United Nations 2016.
>
> *It is recommended that these definitions are read together with their annotations in the report of the open-ended intergovernmental expert working group on indicators and terminology relating to disaster risk reduction*

Two different risk metrics are used: absolute risk, represented by Annual Average Loss (AAL), and relative risk, represented by the AAL as a percentage of the value of capital stock. Risk maps are presented for the world and for each region for both metrics and for specific hazards: earthquake, riverine flood, cyclonic wind and storm surge, and tsunami hazard.

The AAL is the average amount that each country could expect to lose each year over the long term. It is one of the metrics that provides basic information for national planning, economic forecasts, budgeting and accounting when dealing with disaster risk.

The multi-hazard global AAL amounts to USD 293 billion[1]. This is equivalent to the GDP of relatively small, but strong economies such as Singapore or Denmark. It is higher than the value of social expenditure in South Asia and Sub-Saharan Africa combined, or of the value of public investment in Italy.

Globally, the distribution of AAL reflects the value and vulnerability of the assets concentrated on cyclone- or tsunami-prone coastlines, along seismic fault lines or in flood-prone river basins. In absolute terms, global AAL is concentrated in large, higher-income, hazard-exposed economies, such as Japan and the United States of America. In these countries, although overall physical vulnerability is relatively low, the exposed value is very high, which in turn leads to high absolute risk values.

The global AAL has been calculated with respect to the total value of a country's commercial and residential buildings, schools and hospitals. However, the capital stock figures used in the calculation also include the value of infrastructure such as roads, telecommunications and water supply. Given that in highly-developed economies these figures reflect the density of high-value infrastructure (underground railways, airports, expressways, etc.) it is likely that the estimated AAL figures for some of these economies may be higher than could be inferred from only the value of residential and non-residential buildings.

In contrast, in some low- and middle-income countries, the estimated AAL may be closer to the overall value of capital stock, given the lower density of high value infrastructure. As mentioned in Section 1, the estimated AAL values do not include an estimation of extensive risk, which may be significant in these countries.

When the AAL is expressed relative to the value of capital stock, global risk is distributed in a very different way. In general, the value of exposed capital stock is usually significantly less in lower-income countries compared to higher-income countries. However, its vulnerability is often significantly higher, which translates into higher relative risk.

In the case of small island developing states (SIDS) in all income geographies, normally a very high proportion of their capital stock may be exposed. This again translates into very high levels of relative risk, even though absolute risk may be very small, from a global perspective.

Large and diversified economies are more likely to be resilient to even high absolute AAL values given that these values represent only a very small share of their capital stock. However, in countries like Japan, where both absolute and relative AAL are high, economic viability depends on continued and major investments in disaster risk reduction.

Fast-growing economies are likely to be able to cope with high levels of relative AAL better than stagnant or sluggish economies, as losses could be quickly replaced by new capital investment. However, unless this new investment is risk-informed it could actually drive future increases in risk. In the latter case, as countries would struggle to make new capital investments, disasters may set back development for years or even decades. Thus in both kinds of economy, high levels of AAL may compromise the ability to achieve sustainable development.

In order to provide insight into the construction of risk, additional information is provided for the ten countries with highest risk globally and the five countries with highest risk in each region with respect to four underlying risk drivers: income level, social progress, environmental performance, and the rate of urban growth.

Correlations between these drivers and absolute or relative AAL can only be inferred in very general terms. Today's disaster risk is the result of decisions and actions taken in the social, economic, environmental and governance context of the past. Similarly, decisions and actions in today's context will influence the direction of future risk but are not necessarily reflected in present risk values.

Map 2.1 Global absolute AAL associated with earthquakes

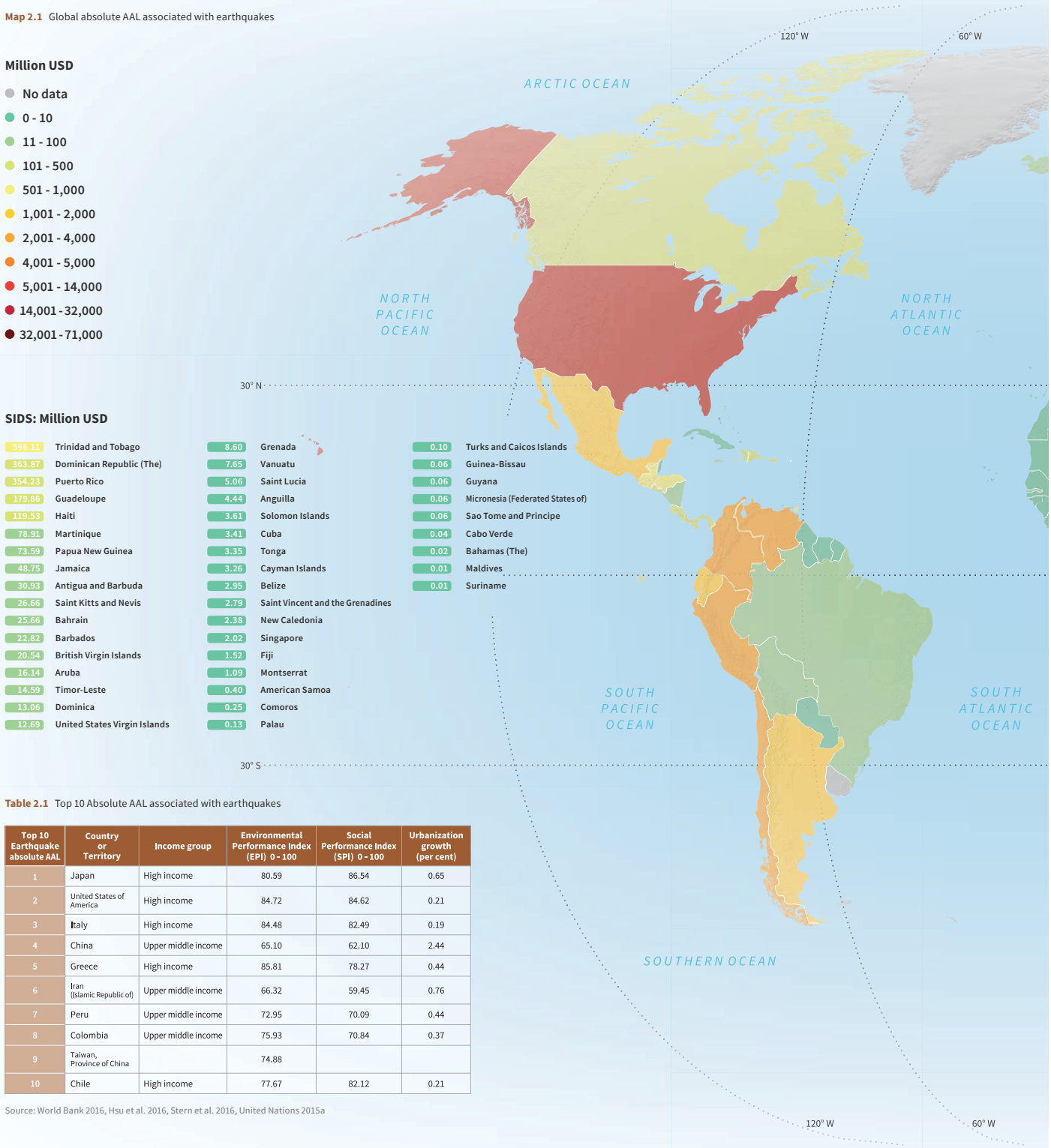

Table 2.1 Top 10 Absolute AAL associated with earthquakes

Top 10 Earthquake absolute AAL	Country or Territory	Income group	Environmental Performance Index (EPI) 0 - 100	Social Performance Index (SPI) 0 - 100	Urbanization growth (per cent)
1	Japan	High income	80.59	86.54	0.65
2	United States of America	High income	84.72	84.62	0.21
3	Italy	High income	84.48	82.49	0.19
4	China	Upper middle income	65.10	62.10	2.44
5	Greece	High income	85.81	78.27	0.44
6	Iran (Islamic Republic of)	Upper middle income	66.32	59.45	0.76
7	Peru	Upper middle income	72.95	70.09	0.44
8	Colombia	Upper middle income	75.93	70.84	0.37
9	Taiwan, Province of China		74.88		
10	Chile	High income	77.67	82.12	0.21

Source: World Bank 2016, Hsu et al. 2016, Stern et al. 2016, United Nations 2015a

0°
60° E
120° E
180°
ARCTIC OCEAN
ARCTIC OCEAN
NORTH PACIFIC OCEAN
30° N
INDIAN OCEAN
SOUTH PACIFIC OCEAN
30° S
SOUTHERN OCEAN
SOUTHERN OCEAN
0°
60° E
120° E
180°
Earthquake Absolute AAL

Map 2.2 Global AAL associated with earthquakes relative to capital stock

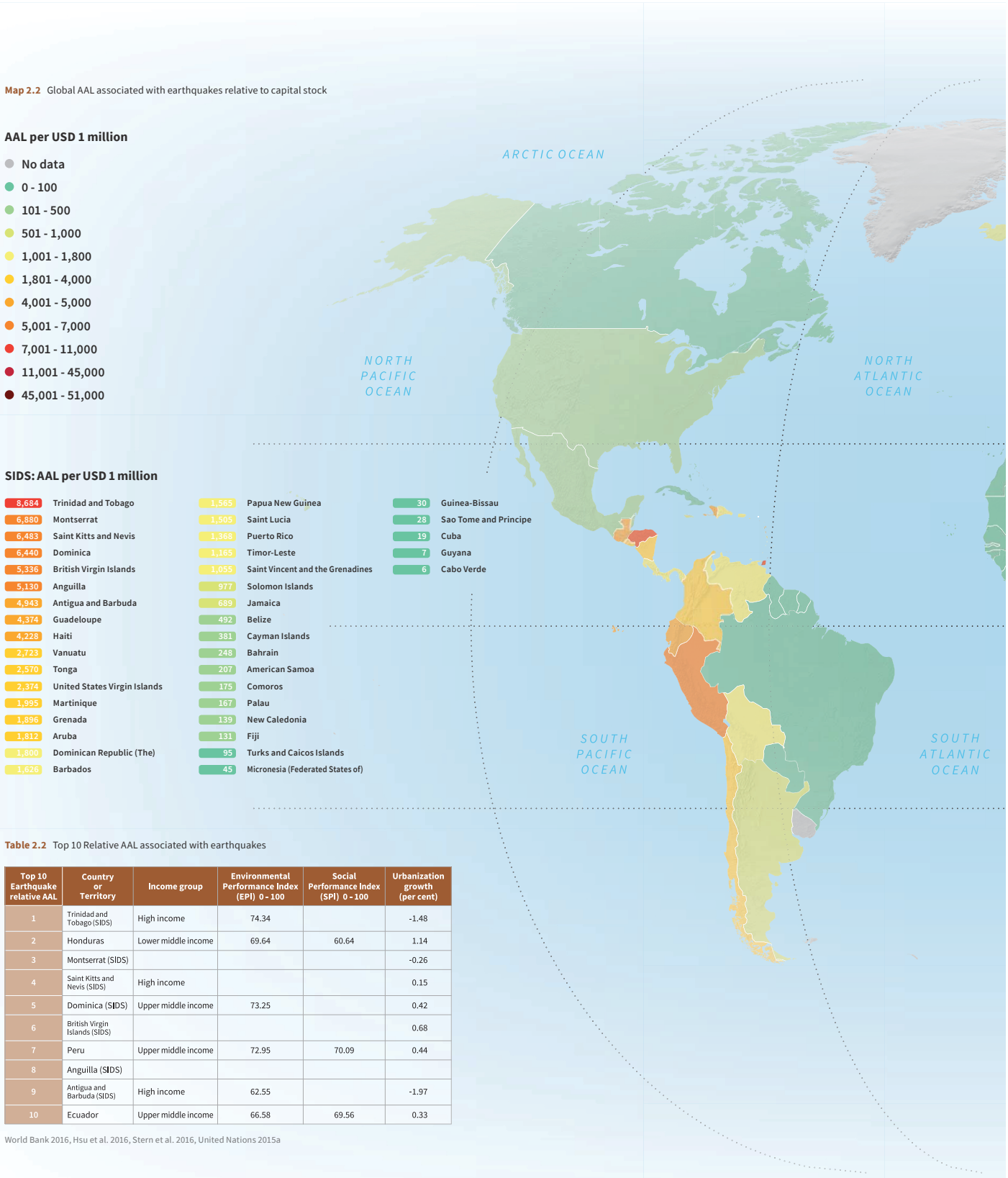

Table 2.2 Top 10 Relative AAL associated with earthquakes

Top 10 Earthquake relative AAL	Country or Territory	Income group	Environmental Performance Index (EPI) 0 - 100	Social Performance Index (SPI) 0 - 100	Urbanization growth (per cent)
1	Trinidad and Tobago (SIDS)	High income	74.34		-1.48
2	Honduras	Lower middle income	69.64	60.64	1.14
3	Montserrat (SIDS)				-0.26
4	Saint Kitts and Nevis (SIDS)	High income			0.15
5	Dominica (SIDS)	Upper middle income	73.25		0.42
6	British Virgin Islands (SIDS)				0.68
7	Peru	Upper middle income	72.95	70.09	0.44
8	Anguilla (SIDS)				
9	Antigua and Barbuda (SIDS)	High income	62.55		-1.97
10	Ecuador	Upper middle income	66.58	69.56	0.33

World Bank 2016, Hsu et al. 2016, Stern et al. 2016, United Nations 2015a

ARCTIC OCEAN
ARCTIC OCEAN
NORTH PACIFIC OCEAN
INDIAN OCEAN
SOUTH PACIFIC OCEAN
SOUTHERN OCEAN
Earthquake Relative AAL

Map 2.3 Global absolute AAL associated with tsunami

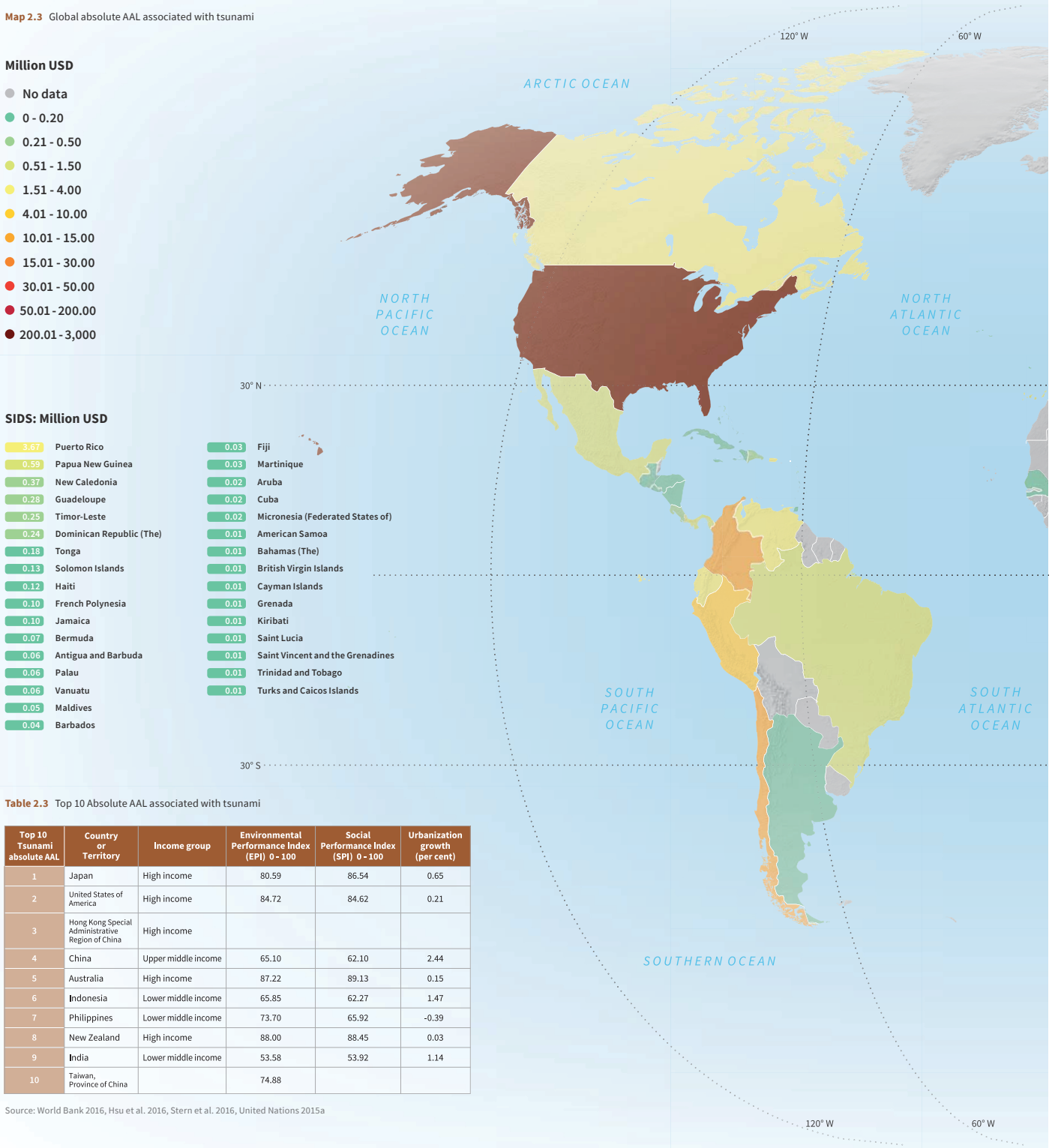

Table 2.3 Top 10 Absolute AAL associated with tsunami

Top 10 Tsunami absolute AAL	Country or Territory	Income group	Environmental Performance Index (EPI) 0 - 100	Social Performance Index (SPI) 0 - 100	Urbanization growth (per cent)
1	Japan	High income	80.59	86.54	0.65
2	United States of America	High income	84.72	84.62	0.21
3	Hong Kong Special Administrative Region of China	High income			
4	China	Upper middle income	65.10	62.10	2.44
5	Australia	High income	87.22	89.13	0.15
6	Indonesia	Lower middle income	65.85	62.27	1.47
7	Philippines	Lower middle income	73.70	65.92	-0.39
8	New Zealand	High income	88.00	88.45	0.03
9	India	Lower middle income	53.58	53.92	1.14
10	Taiwan, Province of China		74.88		

Source: World Bank 2016, Hsu et al. 2016, Stern et al. 2016, United Nations 2015a

Tsunami **Absolute** AAL

Map 2.4 Global AAL associated with tsunami relative to capital stock

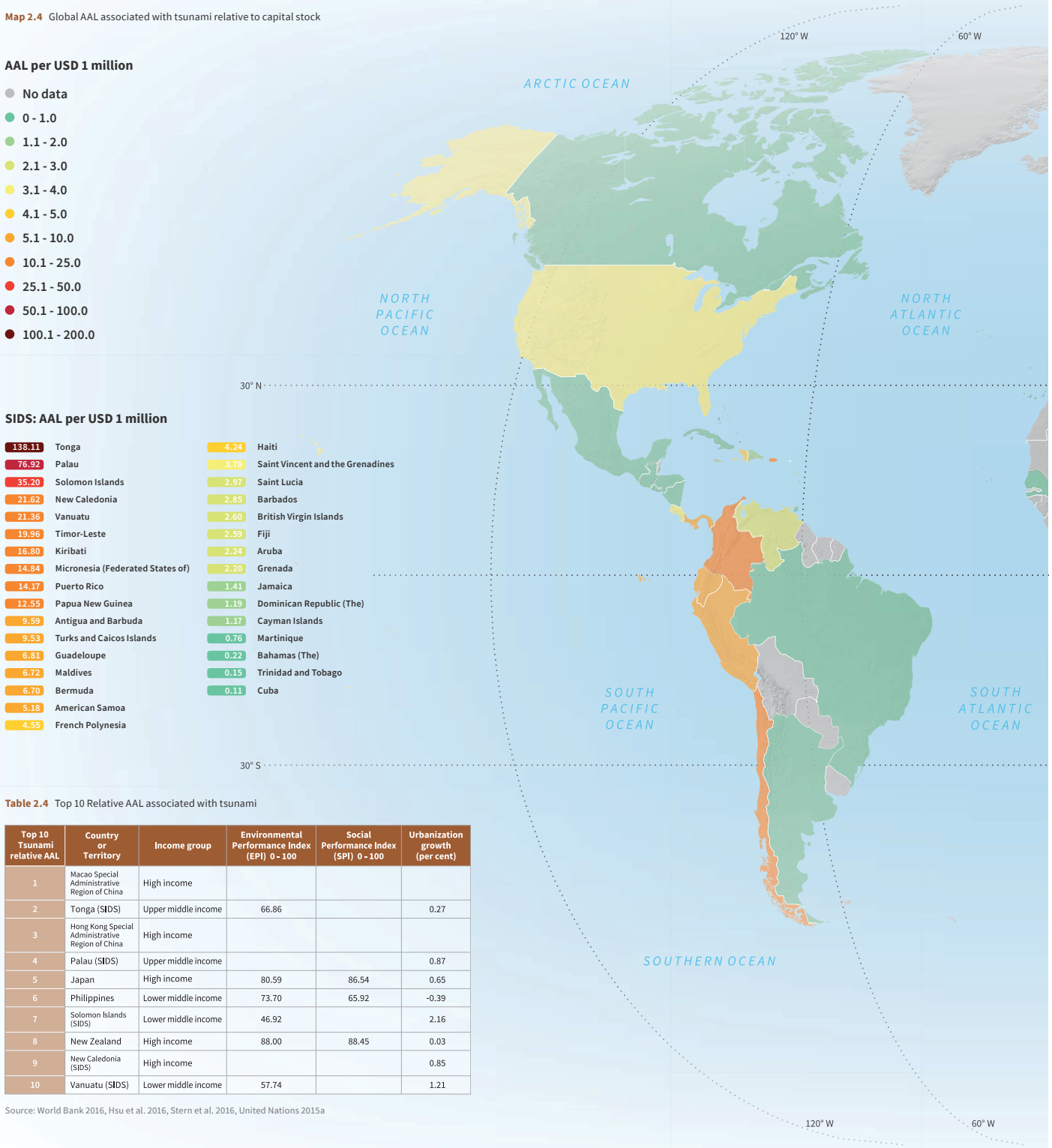

Table 2.4 Top 10 Relative AAL associated with tsunami

Top 10 Tsunami relative AAL	Country or Territory	Income group	Environmental Performance Index (EPI) 0 - 100	Social Performance Index (SPI) 0 - 100	Urbanization growth (per cent)
1	Macao Special Administrative Region of China	High income			
2	Tonga (SIDS)	Upper middle income	66.86		0.27
3	Hong Kong Special Administrative Region of China	High income			
4	Palau (SIDS)	Upper middle income			0.87
5	Japan	High income	80.59	86.54	0.65
6	Philippines	Lower middle income	73.70	65.92	-0.39
7	Solomon Islands (SIDS)	Lower middle income	46.92		2.16
8	New Zealand	High income	88.00	88.45	0.03
9	New Caledonia (SIDS)	High income			0.85
10	Vanuatu (SIDS)	Lower middle income	57.74		1.21

Source: World Bank 2016, Hsu et al. 2016, Stern et al. 2016, United Nations 2015a

0°
60° E
120° E
180°
ARCTIC OCEAN
ARCTIC OCEAN
NORTH PACIFIC OCEAN
30° N
INDIAN OCEAN
SOUTH PACIFIC OCEAN
30° S
SOUTHERN OCEAN
SOUTHERN OCEAN
0°
60° E
120° E
180°
Tsunami Relative AAL

Map 2.5 Global absolute AAL associated with tropical cyclones (wind and storm surge)

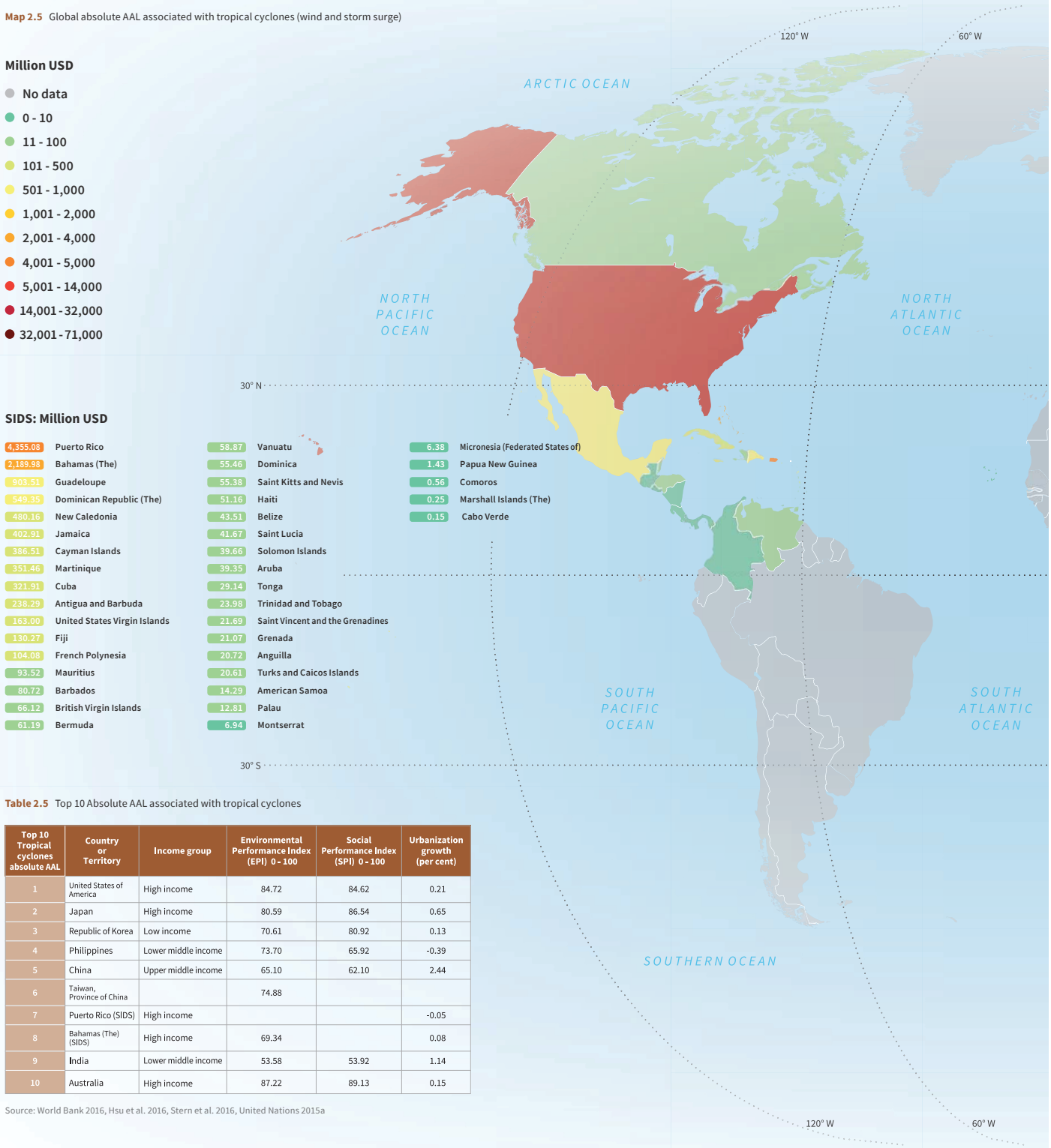

Table 2.5 Top 10 Absolute AAL associated with tropical cyclones

Top 10 Tropical cyclones absolute AAL	Country or Territory	Income group	Environmental Performance Index (EPI) 0 - 100	Social Performance Index (SPI) 0 - 100	Urbanization growth (per cent)
1	United States of America	High income	84.72	84.62	0.21
2	Japan	High income	80.59	86.54	0.65
3	Republic of Korea	Low income	70.61	80.92	0.13
4	Philippines	Lower middle income	73.70	65.92	-0.39
5	China	Upper middle income	65.10	62.10	2.44
6	Taiwan, Province of China		74.88		
7	Puerto Rico (SIDS)	High income			-0.05
8	Bahamas (The) (SIDS)	High income	69.34		0.08
9	India	Lower middle income	53.58	53.92	1.14
10	Australia	High income	87.22	89.13	0.15

Source: World Bank 2016, Hsu et al. 2016, Stern et al. 2016, United Nations 2015a

Tropical Cyclones **Absolute** AAL

Map 2.6 Global AAL associated with tropical cyclones (wind and storm surge) relative to capital stock

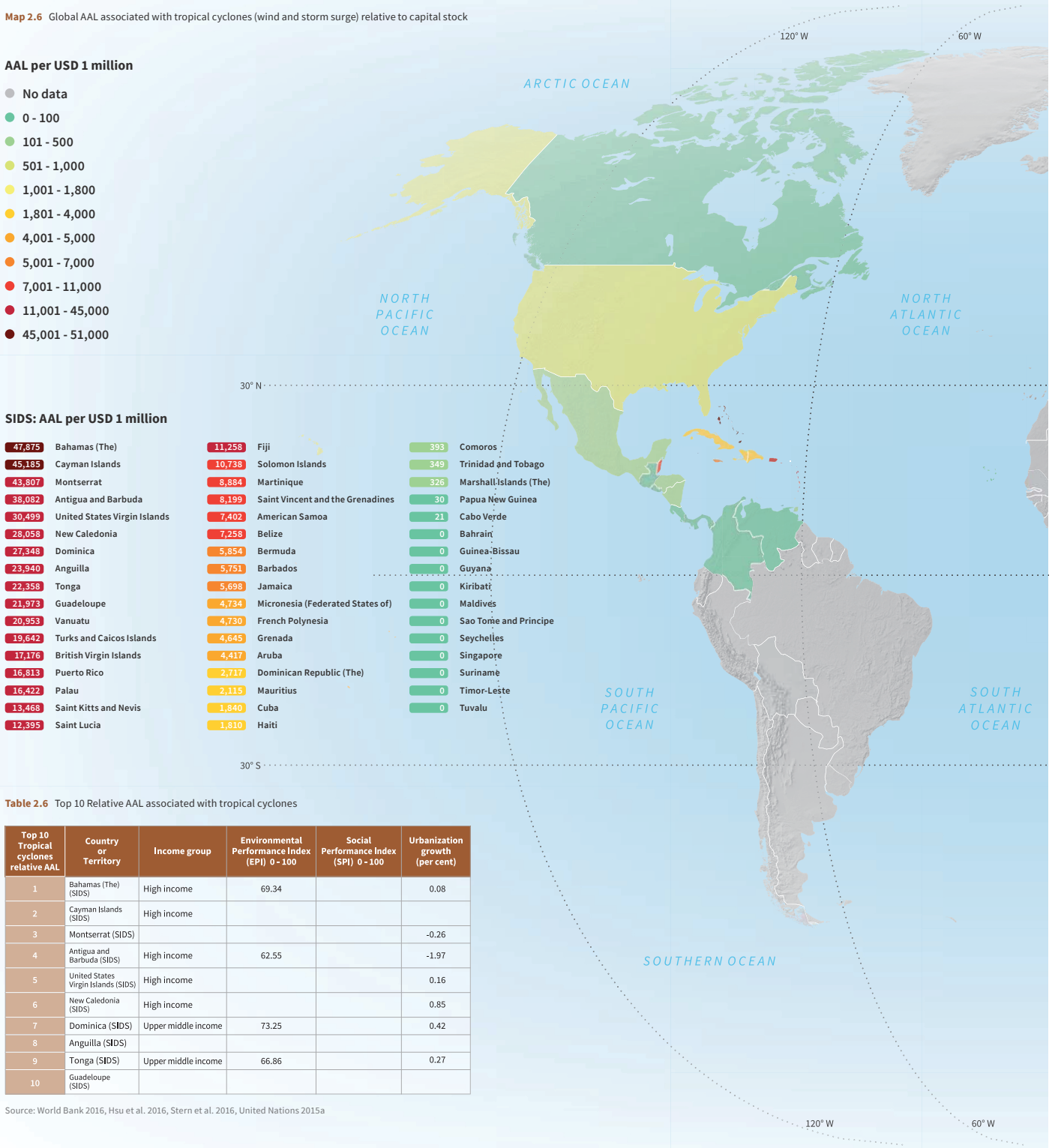

SIDS: AAL per USD 1 million

47,875	Bahamas (The)	11,258	Fiji	393	Comoros
45,185	Cayman Islands	10,738	Solomon Islands	349	Trinidad and Tobago
43,807	Montserrat	8,884	Martinique	326	Marshall Islands (The)
38,082	Antigua and Barbuda	8,199	Saint Vincent and the Grenadines	30	Papua New Guinea
30,499	United States Virgin Islands	7,402	American Samoa	21	Cabo Verde
28,058	New Caledonia	7,258	Belize	0	Bahrain
27,348	Dominica	5,854	Bermuda	0	Guinea-Bissau
23,940	Anguilla	5,751	Barbados	0	Guyana
22,358	Tonga	5,698	Jamaica	0	Kiribati
21,973	Guadeloupe	4,734	Micronesia (Federated States of)	0	Maldives
20,953	Vanuatu	4,730	French Polynesia	0	Sao Tome and Principe
19,642	Turks and Caicos Islands	4,645	Grenada	0	Seychelles
17,176	British Virgin Islands	4,417	Aruba	0	Singapore
16,813	Puerto Rico	2,717	Dominican Republic (The)	0	Suriname
16,422	Palau	2,115	Mauritius	0	Timor-Leste
13,468	Saint Kitts and Nevis	1,840	Cuba	0	Tuvalu
12,395	Saint Lucia	1,810	Haiti		

Table 2.6 Top 10 Relative AAL associated with tropical cyclones

Top 10 Tropical cyclones relative AAL	Country or Territory	Income group	Environmental Performance Index (EPI) 0 - 100	Social Performance Index (SPI) 0 - 100	Urbanization growth (per cent)
1	Bahamas (The) (SIDS)	High income	69.34		0.08
2	Cayman Islands (SIDS)	High income			
3	Montserrat (SIDS)				-0.26
4	Antigua and Barbuda (SIDS)	High income	62.55		-1.97
5	United States Virgin Islands (SIDS)	High income			0.16
6	New Caledonia (SIDS)	High income			0.85
7	Dominica (SIDS)	Upper middle income	73.25		0.42
8	Anguilla (SIDS)				
9	Tonga (SIDS)	Upper middle income	66.86		0.27
10	Guadeloupe (SIDS)				

Source: World Bank 2016, Hsu et al. 2016, Stern et al. 2016, United Nations 2015a

0°
60° E
120° E
180°
ARCTIC OCEAN
ARCTIC OCEAN
NORTH PACIFIC OCEAN
30° N
INDIAN OCEAN
SOUTH PACIFIC OCEAN
30° S
SOUTHERN OCEAN
SOUTHERN OCEAN
0°
60° E
120° E
180°
Tropical Cyclones Relative AAL

Map 2.7 Global absolute AAL associated with riverine floods

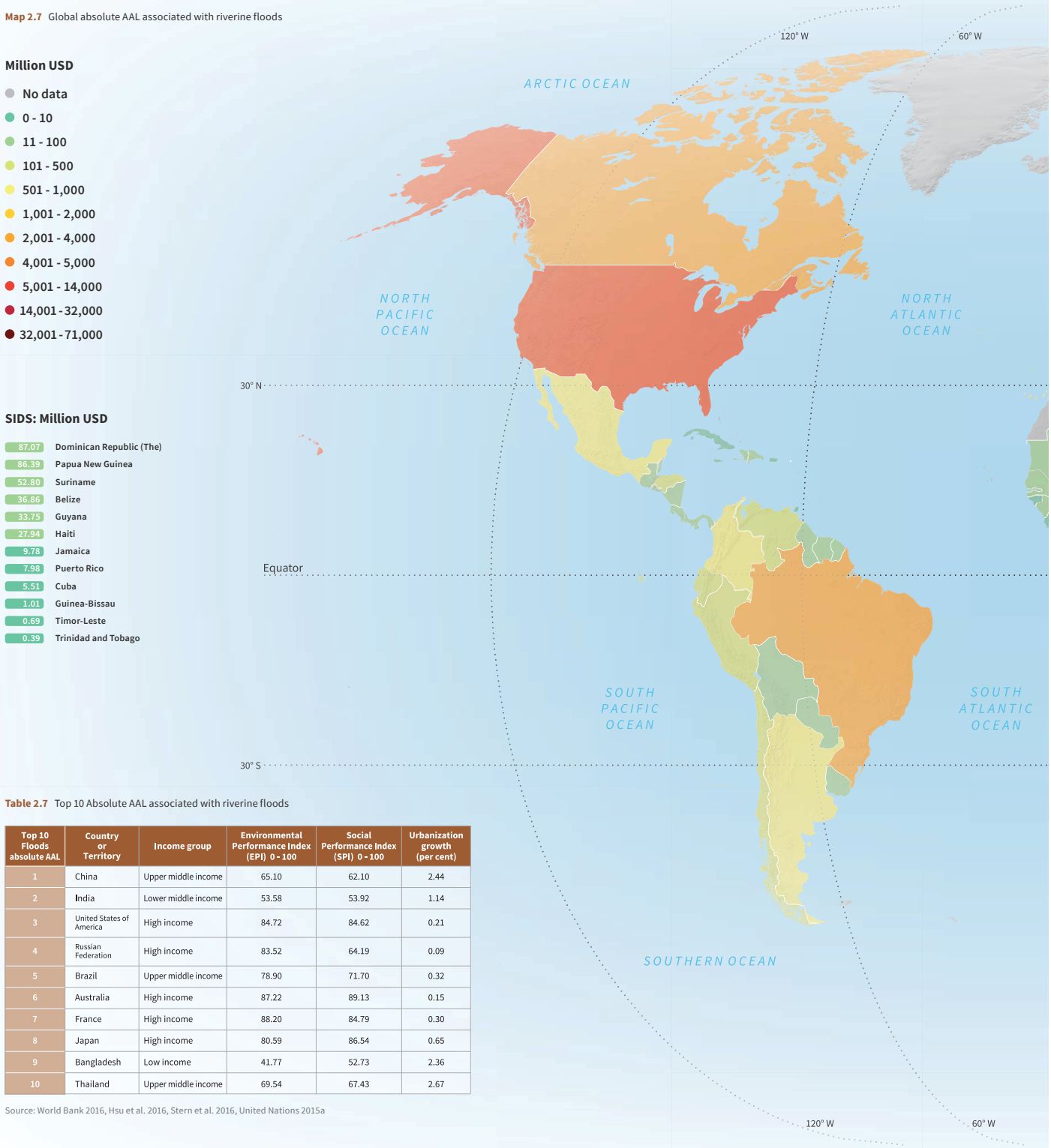

Table 2.7 Top 10 Absolute AAL associated with riverine floods

Top 10 Floods absolute AAL	Country or Territory	Income group	Environmental Performance Index (EPI) 0 - 100	Social Performance Index (SPI) 0 - 100	Urbanization growth (per cent)
1	China	Upper middle income	65.10	62.10	2.44
2	India	Lower middle income	53.58	53.92	1.14
3	United States of America	High income	84.72	84.62	0.21
4	Russian Federation	High income	83.52	64.19	0.09
5	Brazil	Upper middle income	78.90	71.70	0.32
6	Australia	High income	87.22	89.13	0.15
7	France	High income	88.20	84.79	0.30
8	Japan	High income	80.59	86.54	0.65
9	Bangladesh	Low income	41.77	52.73	2.36
10	Thailand	Upper middle income	69.54	67.43	2.67

Source: World Bank 2016, Hsu et al. 2016, Stern et al. 2016, United Nations 2015a

0°
60° E
120° E
180°
ARCTIC OCEAN
ARCTIC OCEAN
NORTH PACIFIC OCEAN
30° N
INDIAN OCEAN
SOUTH PACIFIC OCEAN
30° S
SOUTHERN OCEAN
SOUTHERN OCEAN
0°
60° E
120° E
180°
Riverine Floods Absolute AAL

Map 2.8 Global AAL associated with riverine floods relative to capital stock

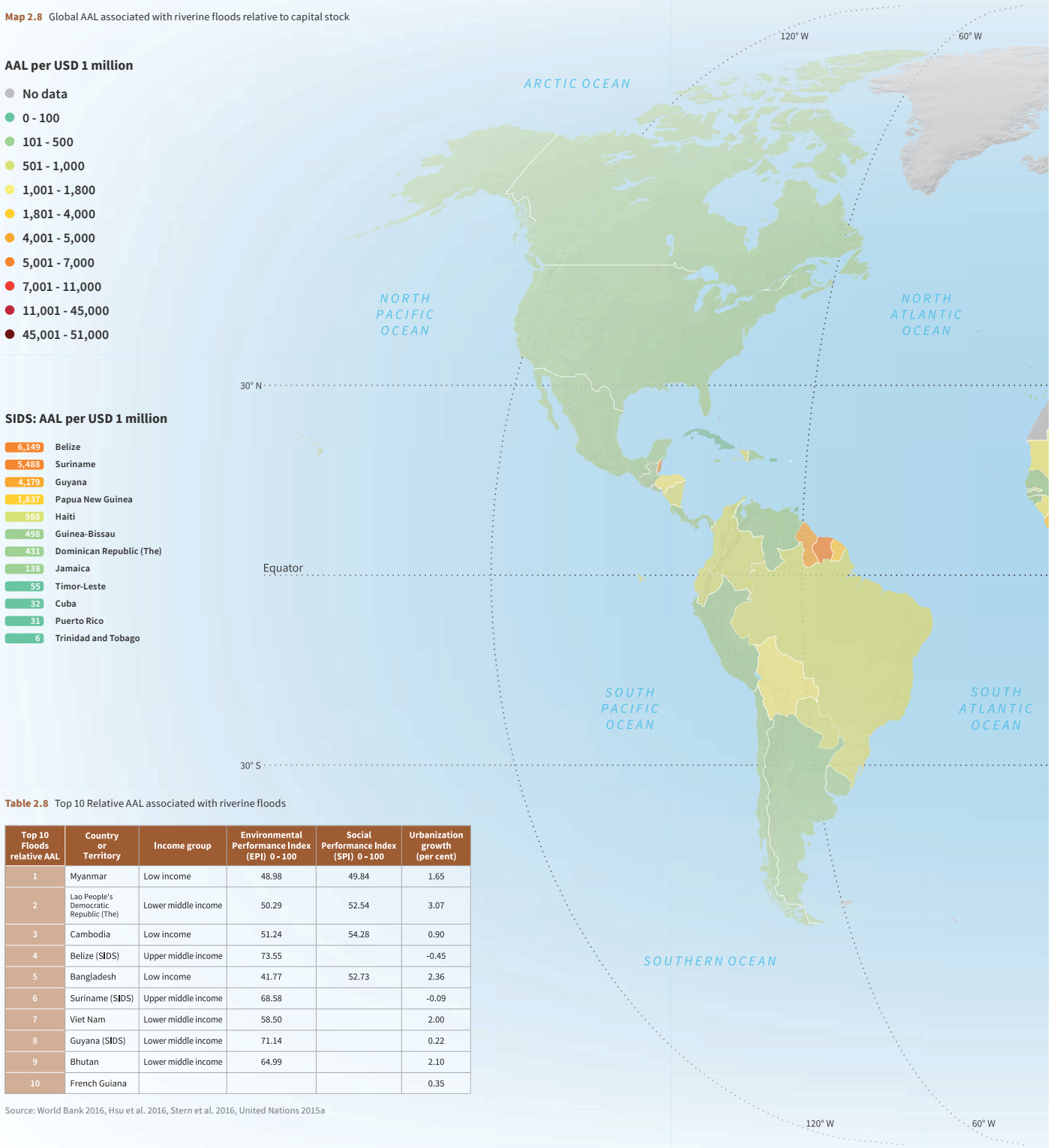

Table 2.8 Top 10 Relative AAL associated with riverine floods

Top 10 Floods relative AAL	Country or Territory	Income group	Environmental Performance Index (EPI) 0 - 100	Social Performance Index (SPI) 0 - 100	Urbanization growth (per cent)
1	Myanmar	Low income	48.98	49.84	1.65
2	Lao People's Democratic Republic (The)	Lower middle income	50.29	52.54	3.07
3	Cambodia	Low income	51.24	54.28	0.90
4	Belize (SIDS)	Upper middle income	73.55		-0.45
5	Bangladesh	Low income	41.77	52.73	2.36
6	Suriname (SIDS)	Upper middle income	68.58		-0.09
7	Viet Nam	Lower middle income	58.50		2.00
8	Guyana (SIDS)	Lower middle income	71.14		0.22
9	Bhutan	Lower middle income	64.99		2.10
10	French Guiana				0.35

Source: World Bank 2016, Hsu et al. 2016, Stern et al. 2016, United Nations 2015a

0°
60° E
120° E
180°
ARCTIC OCEAN
ARCTIC OCEAN
NORTH PACIFIC OCEAN
30° N
INDIAN OCEAN
SOUTH PACIFIC OCEAN
30° S
SOUTHERN OCEAN
SOUTHERN OCEAN
0°
60° E
120° E
180°
Riverine Floods Relative AAL

Map 2.9 Global absolute multi-hazard AAL

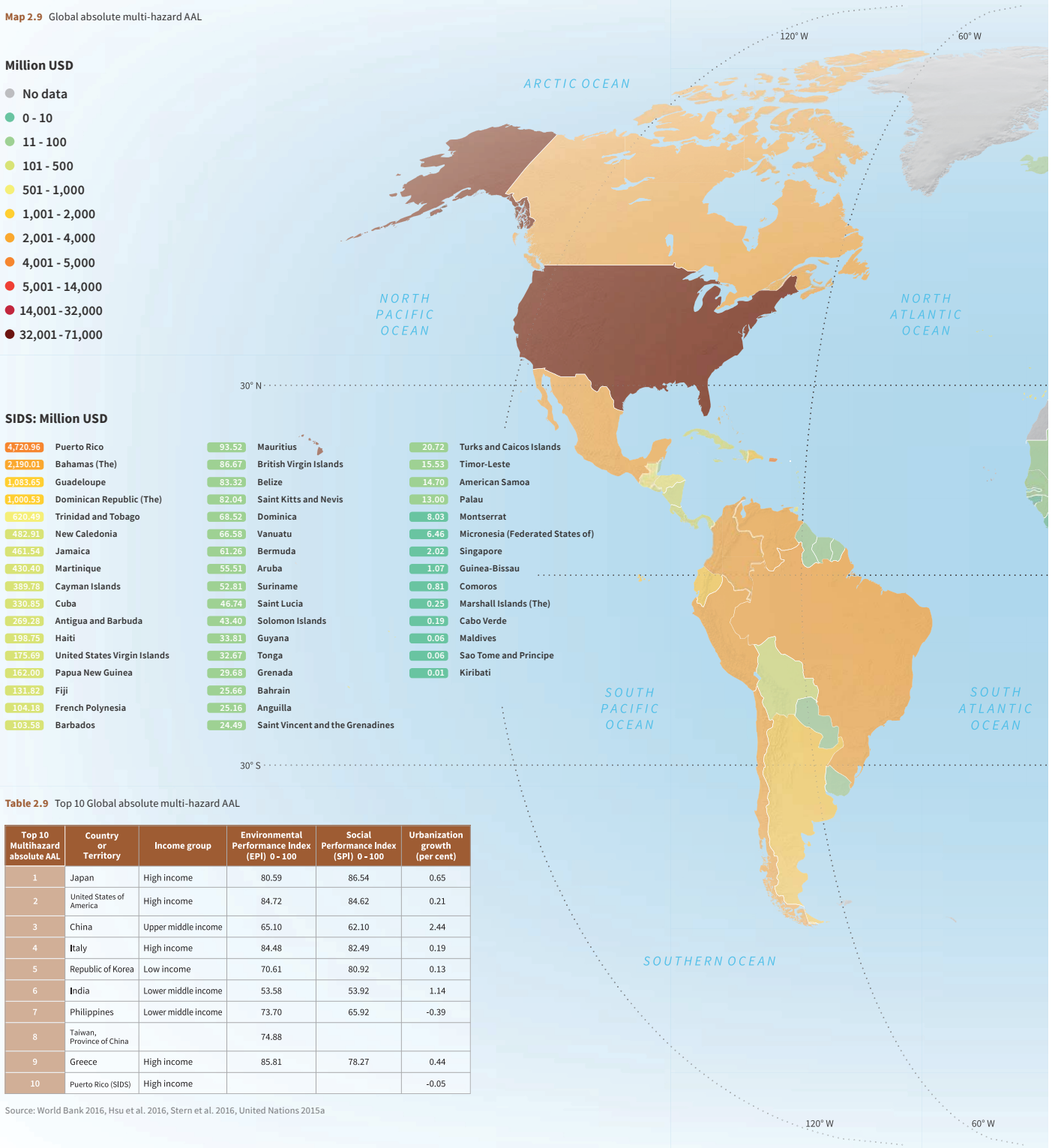

SIDS: Million USD

4,720.96	Puerto Rico	93.52	Mauritius	20.72	Turks and Caicos Islands
2,190.01	Bahamas (The)	86.67	British Virgin Islands	15.53	Timor-Leste
1,083.65	Guadeloupe	83.32	Belize	14.70	American Samoa
1,000.53	Dominican Republic (The)	82.04	Saint Kitts and Nevis	13.00	Palau
620.49	Trinidad and Tobago	68.52	Dominica	8.03	Montserrat
482.91	New Caledonia	66.58	Vanuatu	6.46	Micronesia (Federated States of)
461.54	Jamaica	61.26	Bermuda	2.02	Singapore
430.40	Martinique	55.51	Aruba	1.07	Guinea-Bissau
389.78	Cayman Islands	52.81	Suriname	0.81	Comoros
330.85	Cuba	46.74	Saint Lucia	0.25	Marshall Islands (The)
269.28	Antigua and Barbuda	43.40	Solomon Islands	0.19	Cabo Verde
198.75	Haiti	33.81	Guyana	0.06	Maldives
175.69	United States Virgin Islands	32.67	Tonga	0.06	Sao Tome and Principe
162.00	Papua New Guinea	29.68	Grenada	0.01	Kiribati
131.82	Fiji	25.66	Bahrain		
104.18	French Polynesia	25.16	Anguilla		
103.58	Barbados	24.49	Saint Vincent and the Grenadines		

Table 2.9 Top 10 Global absolute multi-hazard AAL

Top 10 Multihazard absolute AAL	Country or Territory	Income group	Environmental Performance Index (EPI) 0 - 100	Social Performance Index (SPI) 0 - 100	Urbanization growth (per cent)
1	Japan	High income	80.59	86.54	0.65
2	United States of America	High income	84.72	84.62	0.21
3	China	Upper middle income	65.10	62.10	2.44
4	Italy	High income	84.48	82.49	0.19
5	Republic of Korea	Low income	70.61	80.92	0.13
6	India	Lower middle income	53.58	53.92	1.14
7	Philippines	Lower middle income	73.70	65.92	-0.39
8	Taiwan, Province of China		74.88		
9	Greece	High income	85.81	78.27	0.44
10	Puerto Rico (SIDS)	High income			-0.05

Source: World Bank 2016, Hsu et al. 2016, Stern et al. 2016, United Nations 2015a

0°
60° E
120° E
180°
ARCTIC OCEAN
ARCTIC OCEAN
NORTH PACIFIC OCEAN
30° N
INDIAN OCEAN
SOUTH PACIFIC OCEAN
30° S
SOUTHERN OCEAN
SOUTHERN OCEAN
0°
60° E
120° E
180°
Multi-hazard Absolute AAL

Map 2.10 Global multi-hazard AAL relative to capital stock

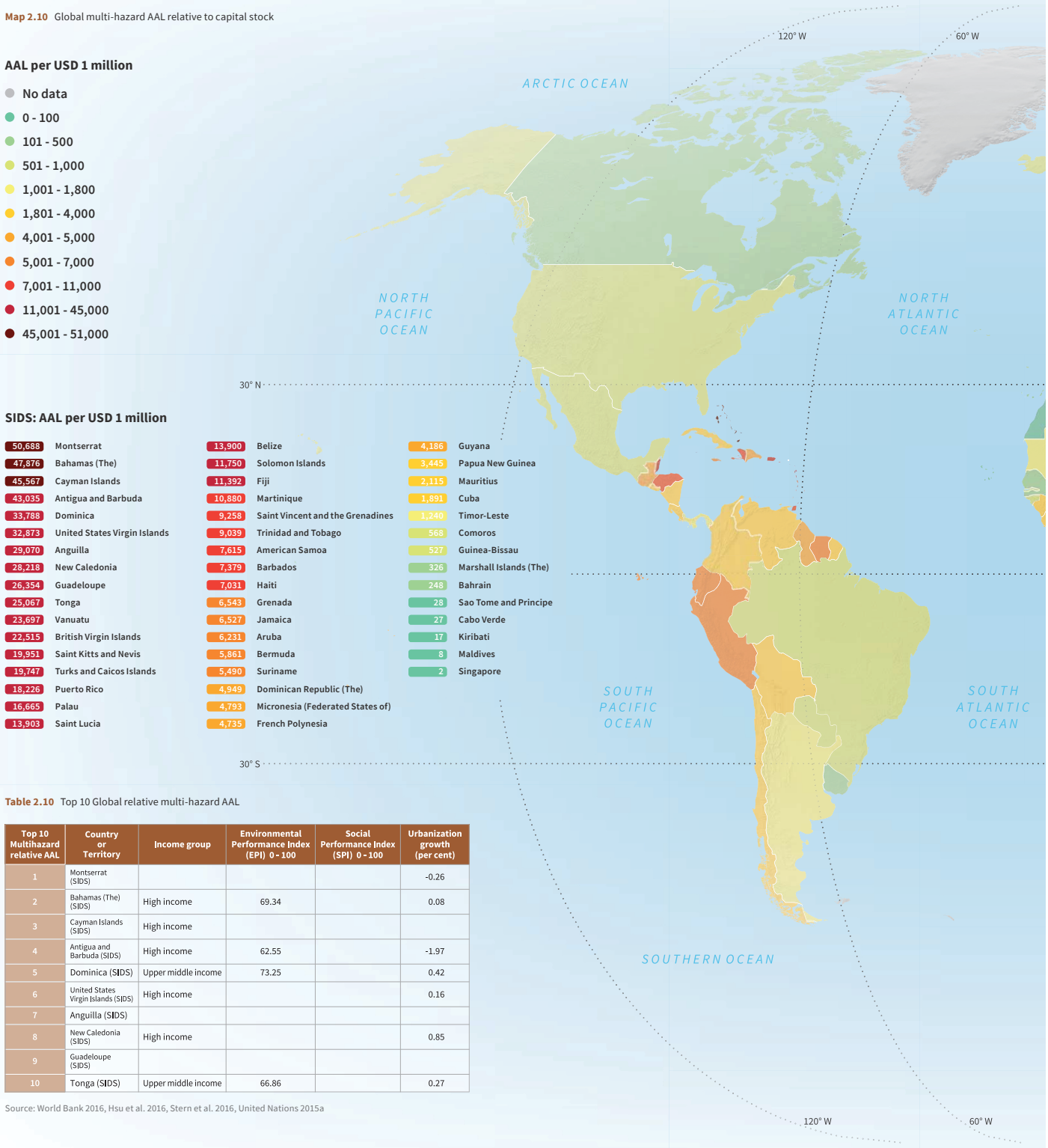

Table 2.10 Top 10 Global relative multi-hazard AAL

Top 10 Multihazard relative AAL	Country or Territory	Income group	Environmental Performance Index (EPI) 0 - 100	Social Performance Index (SPI) 0 - 100	Urbanization growth (per cent)
1	Montserrat (SIDS)				-0.26
2	Bahamas (The) (SIDS)	High income	69.34		0.08
3	Cayman Islands (SIDS)	High income			
4	Antigua and Barbuda (SIDS)	High income	62.55		-1.97
5	Dominica (SIDS)	Upper middle income	73.25		0.42
6	United States Virgin Islands (SIDS)	High income			0.16
7	Anguilla (SIDS)				
8	New Caledonia (SIDS)	High income			0.85
9	Guadeloupe (SIDS)				
10	Tonga (SIDS)	Upper middle income	66.86		0.27

Source: World Bank 2016, Hsu et al. 2016, Stern et al. 2016, United Nations 2015a

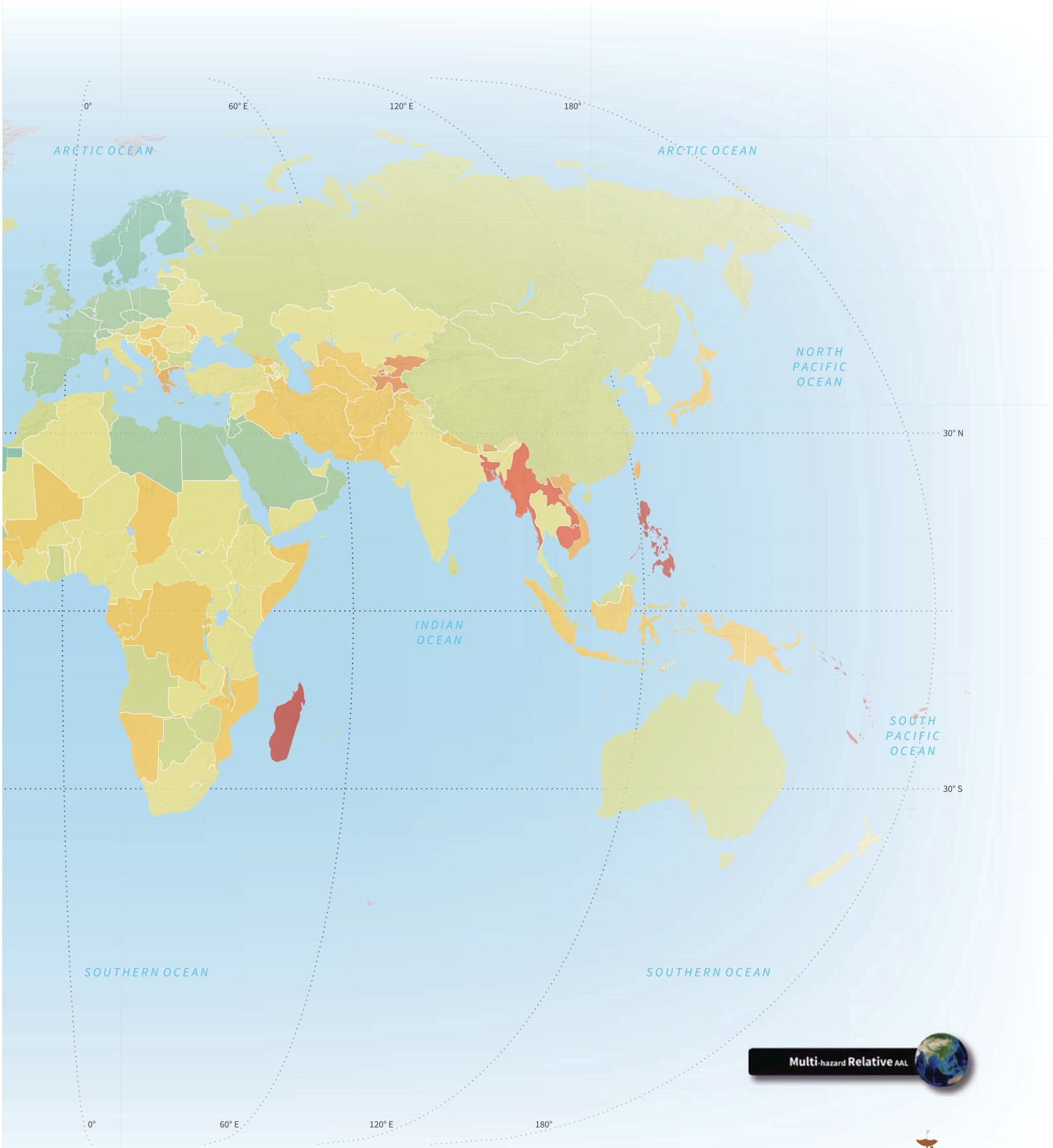
0°
60° E
120° E
180°
ARCTIC OCEAN
ARCTIC OCEAN
NORTH PACIFIC OCEAN
30° N
INDIAN OCEAN
SOUTH PACIFIC OCEAN
30° S
SOUTHERN OCEAN
SOUTHERN OCEAN
0°
60° E
120° E
180°
Multi-hazard Relative AAL

Map 2.11 Multi-hazard AAL relative to capital stock - East Asia and the Pacific

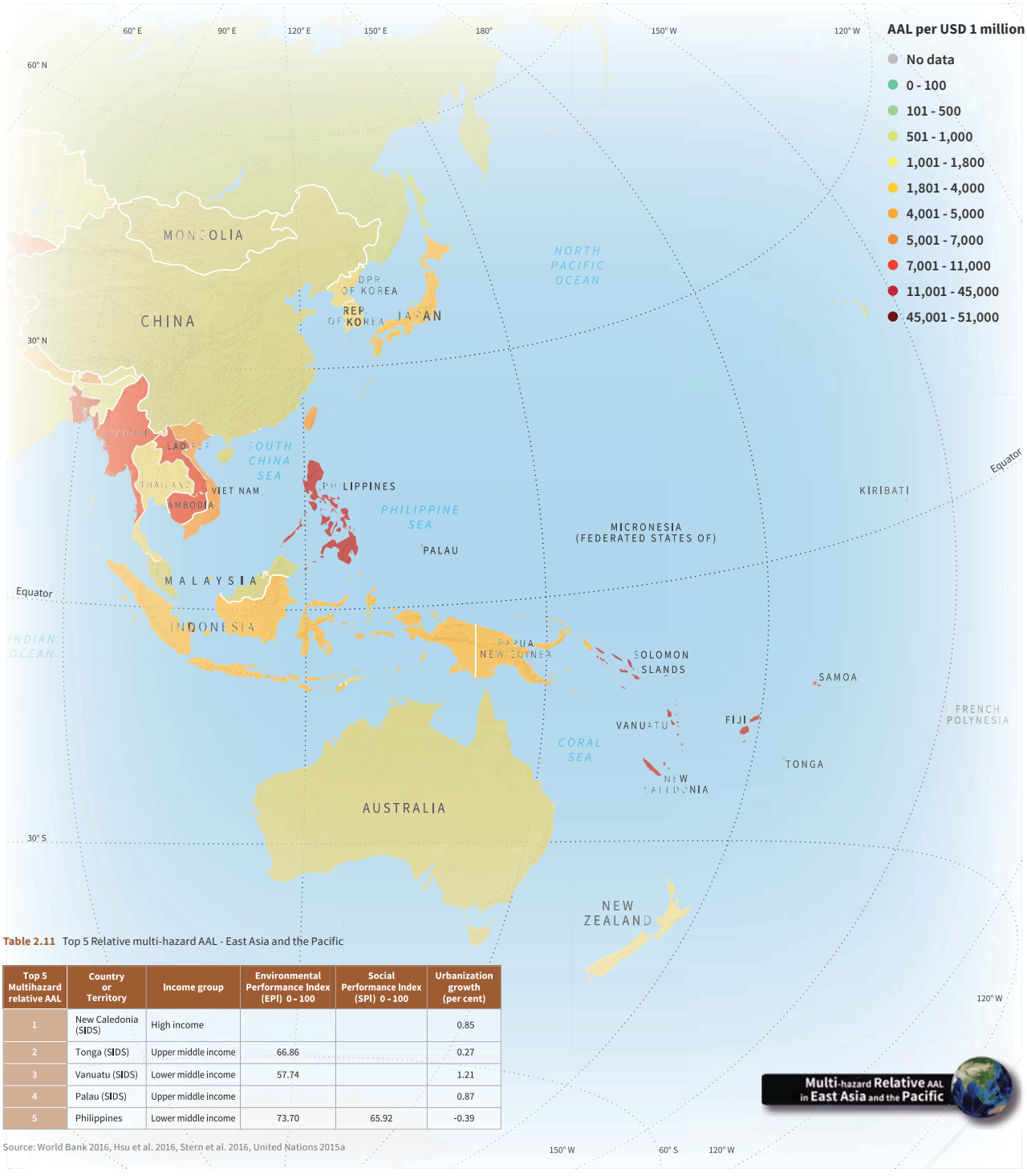

Table 2.11 Top 5 Relative multi-hazard AAL - East Asia and the Pacific

Top 5 Multihazard relative AAL	Country or Territory	Income group	Environmental Performance Index (EPI) 0 - 100	Social Performance Index (SPI) 0 - 100	Urbanization growth (per cent)
1	New Caledonia (SIDS)	High income			0.85
2	Tonga (SIDS)	Upper middle income	66.86		0.27
3	Vanuatu (SIDS)	Lower middle income	57.74		1.21
4	Palau (SIDS)	Upper middle income			0.87
5	Philippines	Lower middle income	73.70	65.92	-0.39

Source: World Bank 2016, Hsu et al. 2016, Stern et al. 2016, United Nations 2015a

Map 2.12 Multi-hazard AAL relative to capital stock - Europe and Central Asia

Table 2.12 Top 5 Relative multi-hazard AAL - Europe and Central Asia

Top 5 Multihazard relative AAL	Country or Territory	Income group	Environmental Performance Index (EPI) 0 - 100	Social Performance Index (SPI) 0 - 100	Urbanization growth (per cent)
1	Tajikistan	Low income	73.05	58.78	0.20
2	Kyrgyzstan	Lower middle income	73.13	62.91	0.23
3	Greece	High income	85.81	78.27	0.44
4	Georgia	Lower middle income	64.96	69.17	0.29
5	Serbia	Upper middle income	78.67	71.55	0.12

Source: World Bank 2016, Hsu et al. 2016, Stern et al. 2016, United Nations 2015a

Map 2.13 Multi-hazard AAL relative to capital stock - Latin America and the Caribbean

Table 2.13 Top 5 Relative multi-hazard AAL - Latin America and the Caribbean

Top 5 Multihazard relative AAL	Country or Territory	Income group	Environmental Performance Index (EPI) 0 - 100	Social Performance Index (SPI) 0 - 100	Urbanization growth (per cent)
1	Montserrat (SIDS)				-0.26
2	Bahamas (The) (SIDS)	High income	69.34		0.08
3	Cayman Islands (SIDS)	High income			
4	Antigua and Barbuda (SIDS)	High income	62.55		-1.97
5	Dominica (SIDS)	Upper middle income	73.25		0.42

Source: World Bank 2016, Hsu et al. 2016, Stern et al. 2016, United Nations 2015a

Map 2.14 Multi-hazard AAL relative to capital stock - Middle East and North Africa

Table 2.14 Top 5 Relative multi-hazard AAL - Middle East and North Africa

Top 5 Multihazard relative AAL	Country or Territory	Income group	Environmental Performance Index (EPI) 0 - 100	Social Performance Index (SPI) 0 - 100	Urbanization growth (per cent)
1	Iraq	Upper middle income	63.97	52.28	0.13
2	Iran (Islamic Republic of)	Upper middle income	66.32	59.45	0.76
3	Algeria	Upper middle income	70.28	61.18	0.93
4	Syrian Arab Republic	Lower middle income	66.91		0.70
5	Yemen	Lower middle income	49.79	41.76	1.73

Source: World Bank 2016, Hsu et al. 2016, Stern et al. 2016, United Nations 2015a

Map 2.15 Multi-hazard AAL relative to capital stock - North America

Table 2.15 Top 3 Relative multi-hazard AAL - North America

Top 3 Multihazard relative AAL	Country or Territory	Income group	Environmental Performance Index (EPI) 0 - 100	Social Performance Index (SPI) 0 - 100	Urbanization growth (per cent)
1	Bermuda (SIDS)	High income			
2	United States of America	High income	84.72	84.62	0.21
3	Canada	High income	85.06	89.49	0.22

Source: World Bank 2016, Hsu et al. 2016, Stern et al. 2016, United Nations 2015a

Map 2.16 Multi-hazard AAL relative to capital stock - South Asia

Table 2.16 Top 5 Relative multi-hazard AAL - South Asia

Top 5 Multihazard relative AAL	Country or Territory	Income group	Environmental Performance Index (EPI) 0 - 100	Social Performance Index (SPI) 0 - 100	Urbanization growth (per cent)
1	Bangladesh	Low income	41.77	52.73	2.36
2	Bhutan	Lower middle income	64.99		2.10
3	Afghanistan	Low income	37.50	35.89	1.57
4	Nepal	Low income	50.21	57.40	2.03
5	Pakistan	Lower middle income	51.42	49.13	1.15

Source: World Bank 2016, Hsu et al. 2016, Stern et al. 2016, United Nations 2015a

Map 2.17 Multi-hazard AAL relative to capital stock - Sub Saharan Africa

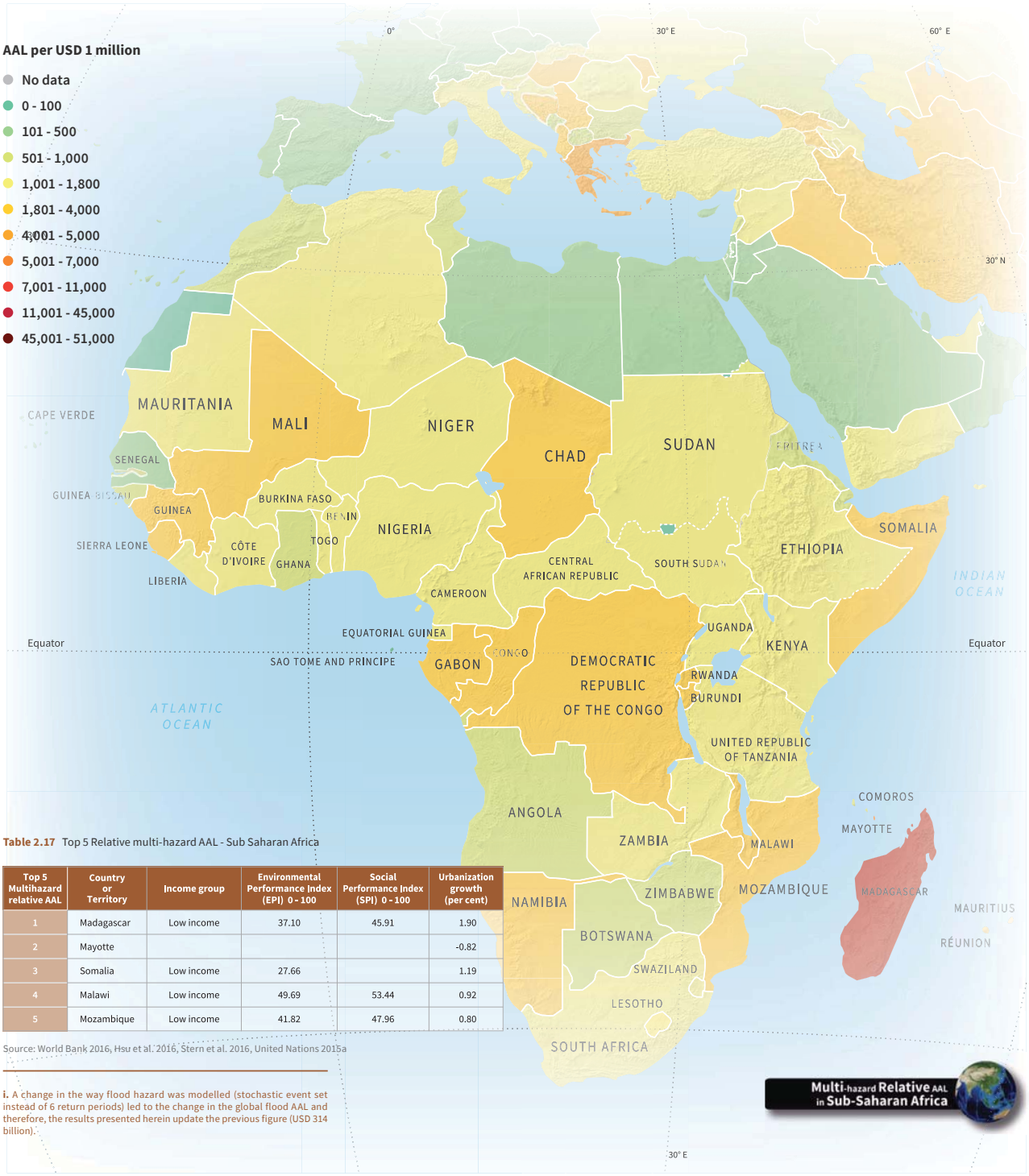

Table 2.17 Top 5 Relative multi-hazard AAL - Sub Saharan Africa

Top 5 Multihazard relative AAL	Country or Territory	Income group	Environmental Performance Index (EPI) 0 - 100	Social Performance Index (SPI) 0 - 100	Urbanization growth (per cent)
1	Madagascar	Low income	37.10	45.91	1.90
2	Mayotte				-0.82
3	Somalia	Low income	27.66		1.19
4	Malawi	Low income	49.69	53.44	0.92
5	Mozambique	Low income	41.82	47.96	0.80

Source: World Bank 2016, Hsu et al. 2016, Stern et al. 2016, United Nations 2015a

i. A change in the way flood hazard was modelled (stochastic event set instead of 6 return periods) led to the change in the global flood AAL and therefore, the results presented herein update the previous figure (USD 314 billion).

Section 3

Disaster risk implications for social and economic development

3.1 Fiscal resilience challenged

Governments do not have unlimited financial resources available to absorb disaster losses, recover and rebuild. Fiscal resilience can therefore be expressed as the ratio between the resources available for loss financing and the expected magnitude of direct disaster loss for any chosen return period. When the available resources exceed the expected loss, the country could be considered to be fiscally resilient, at least for loss events with certain return periods. If the expected loss exceeds the available resources, then a financing gap would exist. As such, while a country may be resilient to a 1-in-10-year loss event, it may experience a financing gap for any event above 1-in-20 years. Measuring fiscal resilience is therefore essential to understand how and under what circumstances disaster risk can extrapolate into broader risk for the financial stability of a country.

The Global Risk Model (GRM) facilitates a first order *stress test* of fiscal resilience by comparing the Probable Maximum Loss (PML) of different return periods with the financial resources available to deal with those losses. The financial resources in the analyses are those domestic and external resources that the country would have access to for response, recovery and relief, as of 2014. These resources are divided into ex-ante (reserve funds, sovereign insurance and catastrophe bonds) and ex-post (budget reallocation capacity, foreign reserves, domestic bonds and credit, multilateral borrowing, international borrowing and aid) disbursement of resources[i].

A first approach to stress testing fiscal resilience is to identify the return period for disaster loss beyond which a financing gap would exist. For example, the PML for a 20-year return period in the United States of America is estimated at USD 121 billion. However, the resources available for loss financing are around USD 391 billion. No resource gap, therefore, exists. In contrast, in Madagascar the PML for a 20-year return period is estimated at USD 900 million. However, the resources available for loss financing are only around USD 168 million, meaning that a significant financing gap would exist. In Madagascar, a financing gap exists for all losses with return periods higher than five years. This implies that Madagascar would experience a financing gap on average every five years[ii].

Map 3.1 analyses the fiscal resilience of 180 countries and territories and shows the return periods beyond which a financing gap would exist. Around half would experience a financing gap for losses below a 100-year return period. Fifty-six countries and territories would not experience a financing gap at all, while 32 could experience a financing gap for losses below a 10-year return period, thus highlighting extremely low fiscal resilience.

Given that fiscal resilience is calculated using direct disaster losses, these estimates are likely to be conservative, given the often considerable magnitude of indirect losses. It is not yet possible to estimate indirect losses with a global model such as the GRM. However, the analysis presented here offers a *first cut* estimate, which can stimulate the development of more detailed national-level studies that can account for indirect losses. At the same time, clearly the fiscal health of a country can change rapidly, meaning that the analysis should be updated on a regular basis.

A second approach to stress testing fiscal resilience is to examine the likely size of the financing gap for a loss with a 100-year return period. Map 3.2 shows that 93 countries and territories would have a financing gap for this level of loss. Twenty-seven would have a financing gap higher than USD 1 billion, while 10 would have a gap between USD 500 million and 1 billion. Forty-one countries and territories would have a gap between USD 100 – 500 million and the remaining 15 a gap smaller than USD 100 million[iii].

Map 3.1 Return period of PML beyond which countries and territories would experience a financing gap

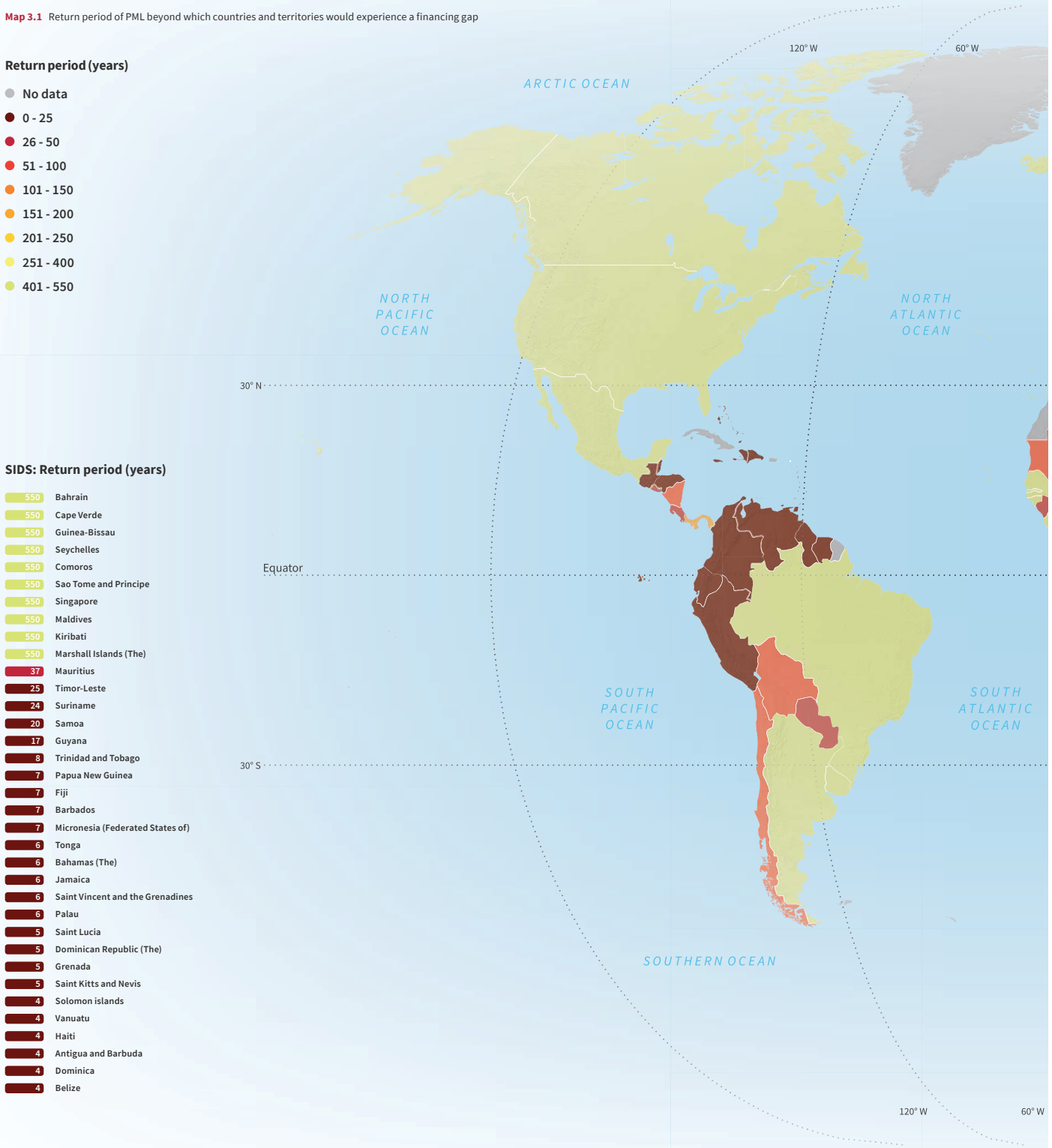

0°
60° E
120° E
180° E
ARCTIC OCEAN
ARCTIC OCEAN
NORTH PACIFIC OCEAN
30° N
INDIAN OCEAN
SOUTH PACIFIC OCEAN
30° S
SOUTHERN OCEAN
SOUTHERN OCEAN
0°
60° E
120° E
180° E
Financing gap

Map 3.2 Countries facing a financing gap for a 100 year return period loss

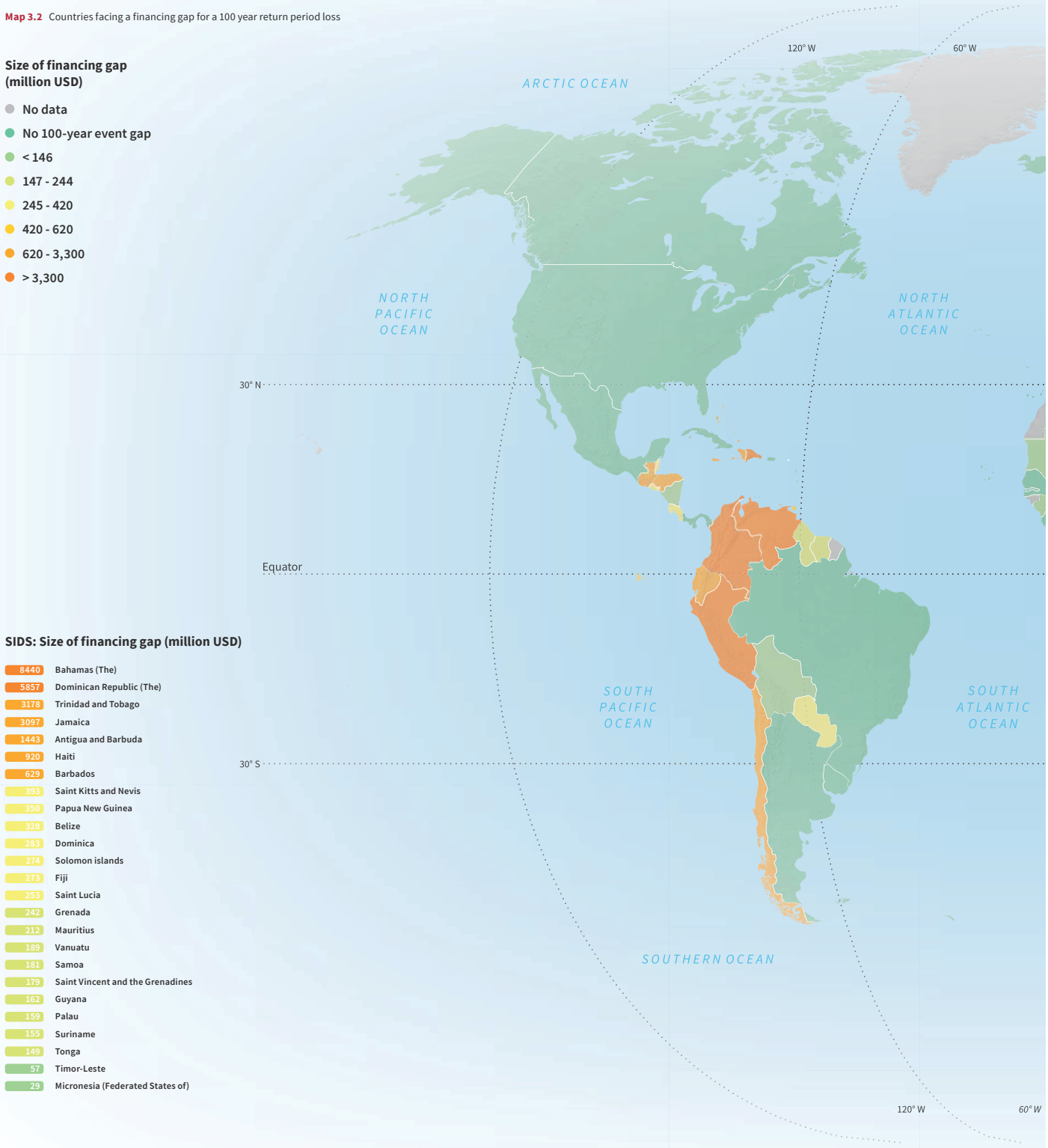

0°
60° E
120° E
180° E
ARCTIC OCEAN
ARCTIC OCEAN
NORTH PACIFIC OCEAN
30° N
INDIAN OCEAN
SOUTH PACIFIC OCEAN
30° S
SOUTHERN OCEAN
SOUTHERN OCEAN
0°
60° E
120° E
180° E
Financing gap
for 100 years of return period

3.2 Assessing the impact of disaster mortality

The GRM also allows the estimation of Annual Average Mortality (AAM) using the same probabilistic methods used to calculate economic loss. At present, AAM has been calculated globally for earthquakes[iv].

Global AAM for earthquakes is currently estimated to be around 13,000 deaths. Map 3.3 shows the distribution of global AAM, underscoring how high levels of mortality risk characterise not only middle-income countries like Colombia and Pakistan but also high-income countries like Italy and Japan.

Map 3.4 shows the distribution of earthquake AAM relative to the size of a country's population. Unsurprisingly, it highlights a very different distribution compared to the absolute AAM, with high levels of relative risk in small-countries, particularly in small island developing states (SIDS) and in middle-income countries, particularly in Latin America.

The concept of life years lost provides another metric to express how disaster risk affects social and economic development[v]. The concept of human life years provides a better representation of disaster impact, since it can be used as a metric that, combined with other macroeconomic indicators, provides an idea about the time required to produce economic development and social progress. The loss of human life years, be it through disasters, disease or accidents, is therefore a way of measuring setbacks to social and economic development[vi].

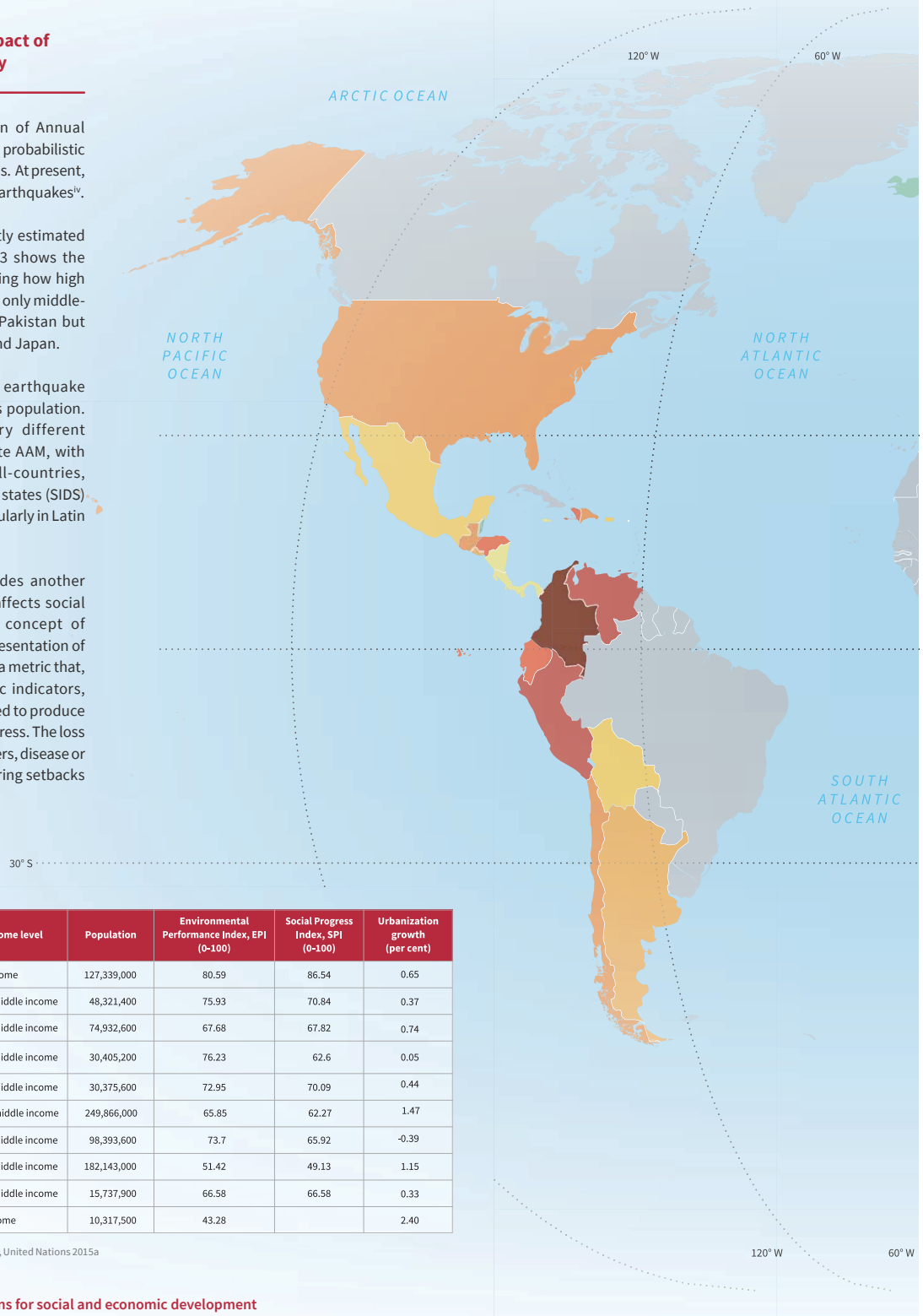

Table 3.1 Top 10 Average Annual Mortality

Top 10 AAM	Country or Territory	Income level	Population	Environmental Performance Index, EPI (0-100)	Social Progress Index, SPI (0-100)	Urbanization growth (per cent)
1	Japan	High income	127,339,000	80.59	86.54	0.65
2	Colombia	Upper middle income	48,321,400	75.93	70.84	0.37
3	Turkey	Upper middle income	74,932,600	67.68	67.82	0.74
4	Venezuela (Bolivarian Republic of)	Upper middle income	30,405,200	76.23	62.6	0.05
5	Peru	Upper middle income	30,375,600	72.95	70.09	0.44
6	Indonesia	Lower middle income	249,866,000	65.85	62.27	1.47
7	Philippines	Lower middle income	98,393,600	73.7	65.92	-0.39
8	Pakistan	Lower middle income	182,143,000	51.42	49.13	1.15
9	Ecuador	Upper middle income	15,737,900	66.58	66.58	0.33
10	Haiti	Low income	10,317,500	43.28		2.40

Source: World Bank 2016, Hsu et al. 2016, Stern et al. 2016, United Nations 2015a

Map 3.3 Average Annual Mortality (AAM) associated with earthquakes.

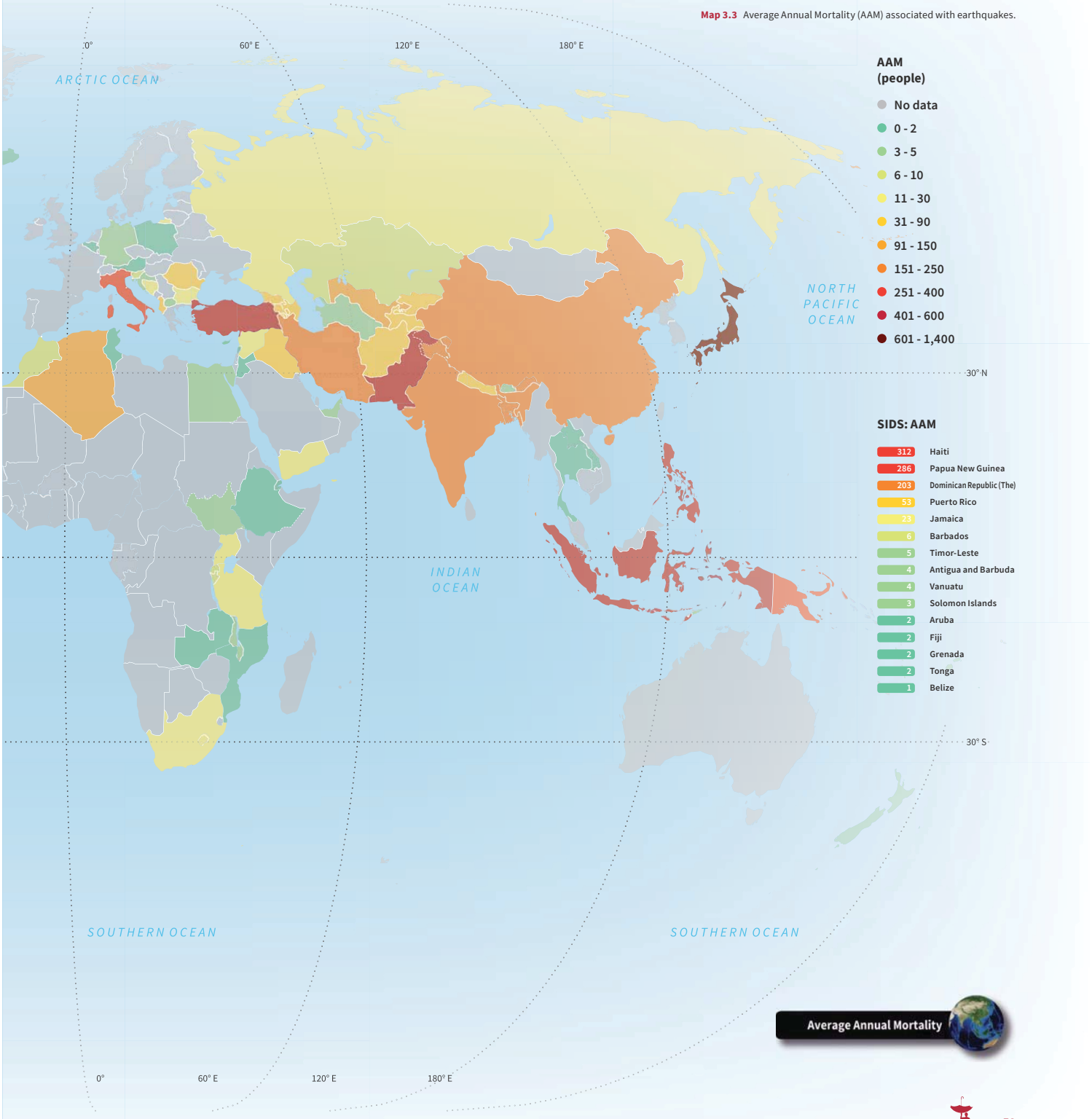

Map 3.4 Average Annual Mortality (AAM) associated with earthquakes relative to population size

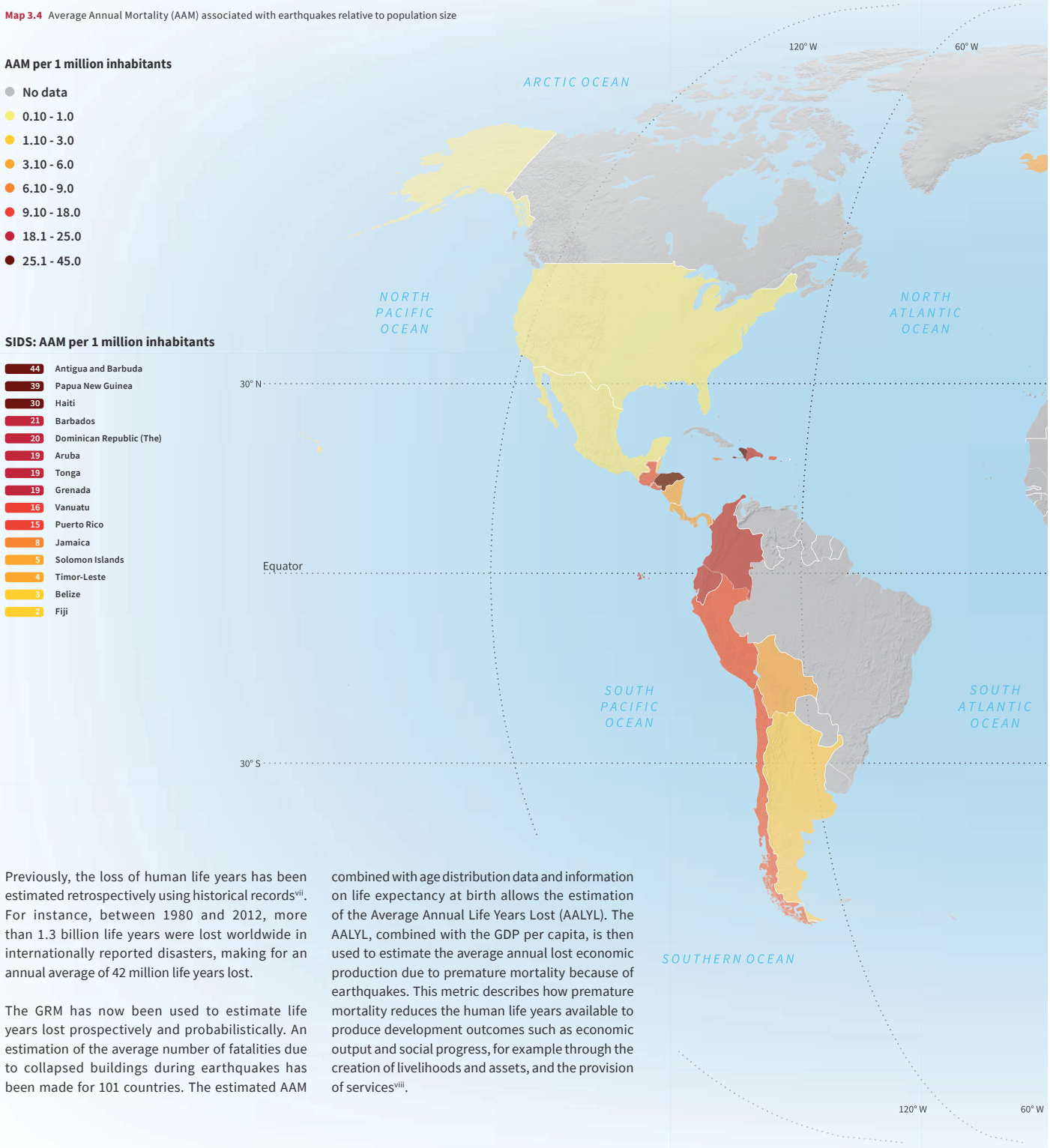

Previously, the loss of human life years has been estimated retrospectively using historical records[vii]. For instance, between 1980 and 2012, more than 1.3 billion life years were lost worldwide in internationally reported disasters, making for an annual average of 42 million life years lost.

The GRM has now been used to estimate life years lost prospectively and probabilistically. An estimation of the average number of fatalities due to collapsed buildings during earthquakes has been made for 101 countries. The estimated AAM combined with age distribution data and information on life expectancy at birth allows the estimation of the Average Annual Life Years Lost (AALYL). The AALYL, combined with the GDP per capita, is then used to estimate the average annual lost economic production due to premature mortality because of earthquakes. This metric describes how premature mortality reduces the human life years available to produce development outcomes such as economic output and social progress, for example through the creation of livelihoods and assets, and the provision of services[viii].

0°
60° E
120° E
180° E
ARCTIC OCEAN
ARCTIC OCEAN
NORTH PACIFIC OCEAN
30° N
INDIAN OCEAN
SOUTH PACIFIC OCEAN
30° S
SOUTHERN OCEAN
SOUTHERN OCEAN
0°
60° E
120° E
180° E
Average Annual
Mortality relative to country population

Map 3.5 Average annual number of life years lost (AALYL) associated with earthquake

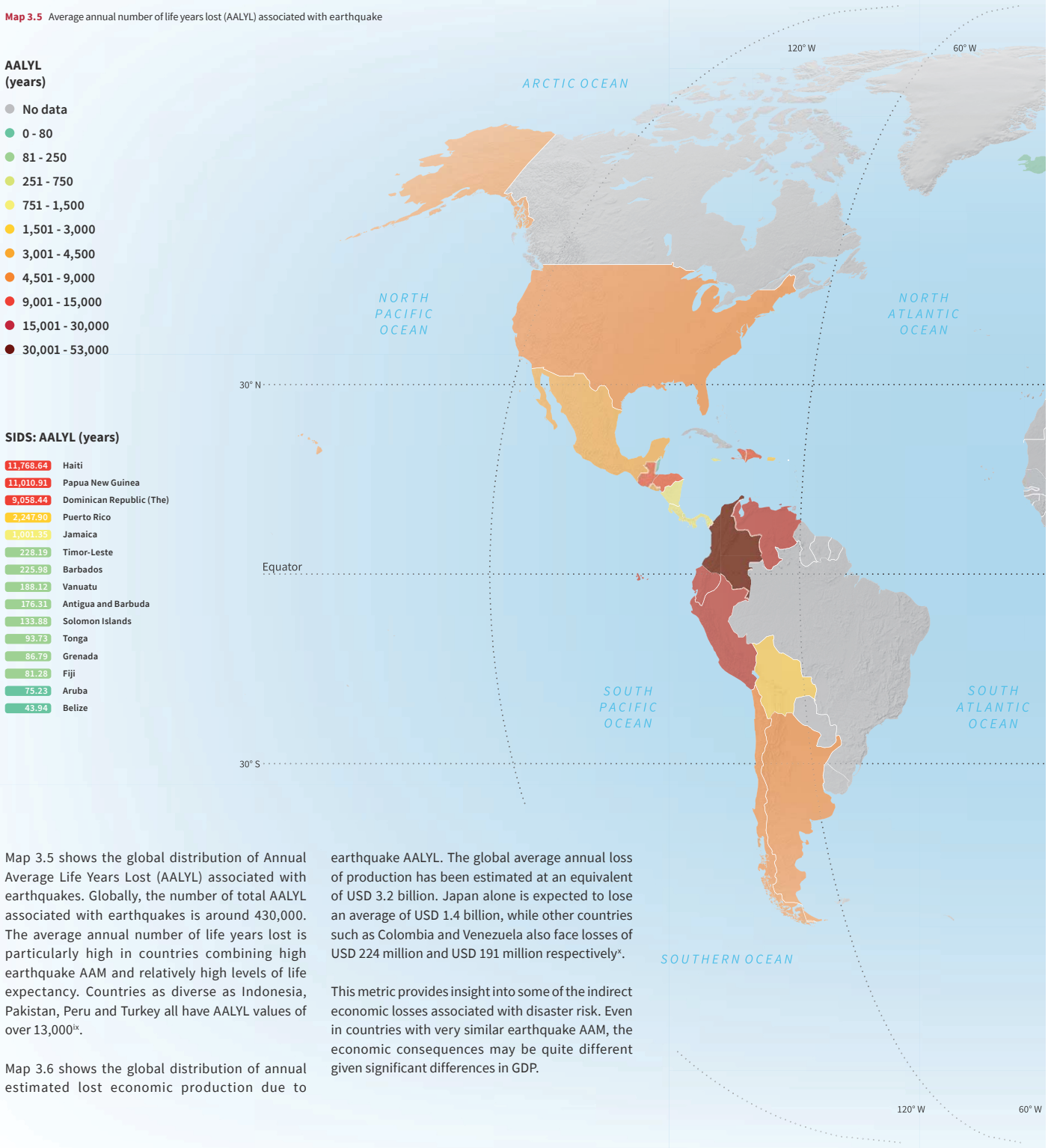

Map 3.5 shows the global distribution of Annual Average Life Years Lost (AALYL) associated with earthquakes. Globally, the number of total AALYL associated with earthquakes is around 430,000. The average annual number of life years lost is particularly high in countries combining high earthquake AAM and relatively high levels of life expectancy. Countries as diverse as Indonesia, Pakistan, Peru and Turkey all have AALYL values of over 13,000[ix].

Map 3.6 shows the global distribution of annual estimated lost economic production due to earthquake AALYL. The global average annual loss of production has been estimated at an equivalent of USD 3.2 billion. Japan alone is expected to lose an average of USD 1.4 billion, while other countries such as Colombia and Venezuela also face losses of USD 224 million and USD 191 million respectively[x].

This metric provides insight into some of the indirect economic losses associated with disaster risk. Even in countries with very similar earthquake AAM, the economic consequences may be quite different given significant differences in GDP.

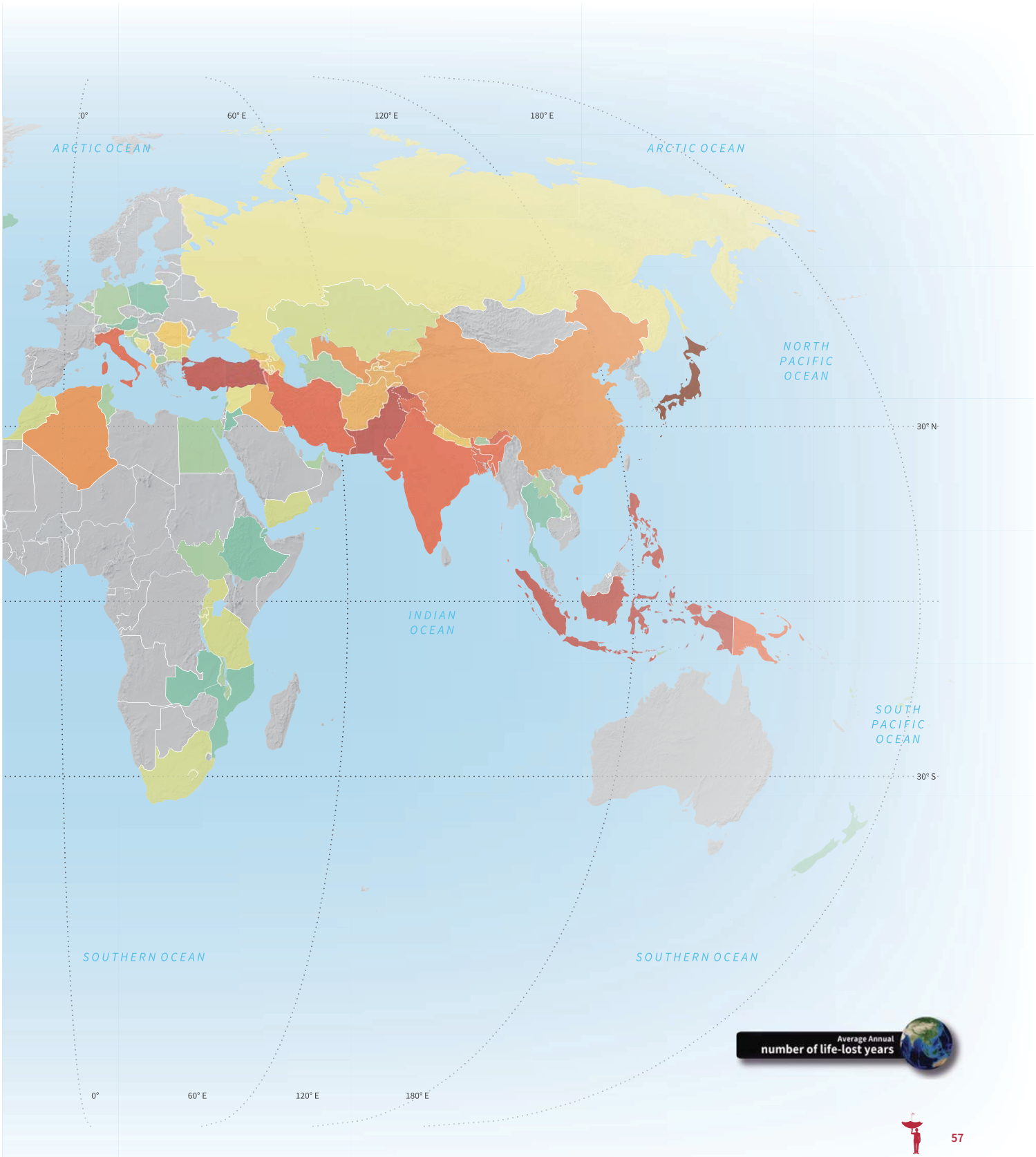
0°
60° E
120° E
180° E
ARCTIC OCEAN
ARCTIC OCEAN
NORTH PACIFIC OCEAN
30° N
INDIAN OCEAN
SOUTH PACIFIC OCEAN
30° S
SOUTHERN OCEAN
SOUTHERN OCEAN
0°
60° E
120° E
180° E
Average Annual
number of life-lost years

Map 3.6 Average annual loss in economic production due to life years lost in earthquakes

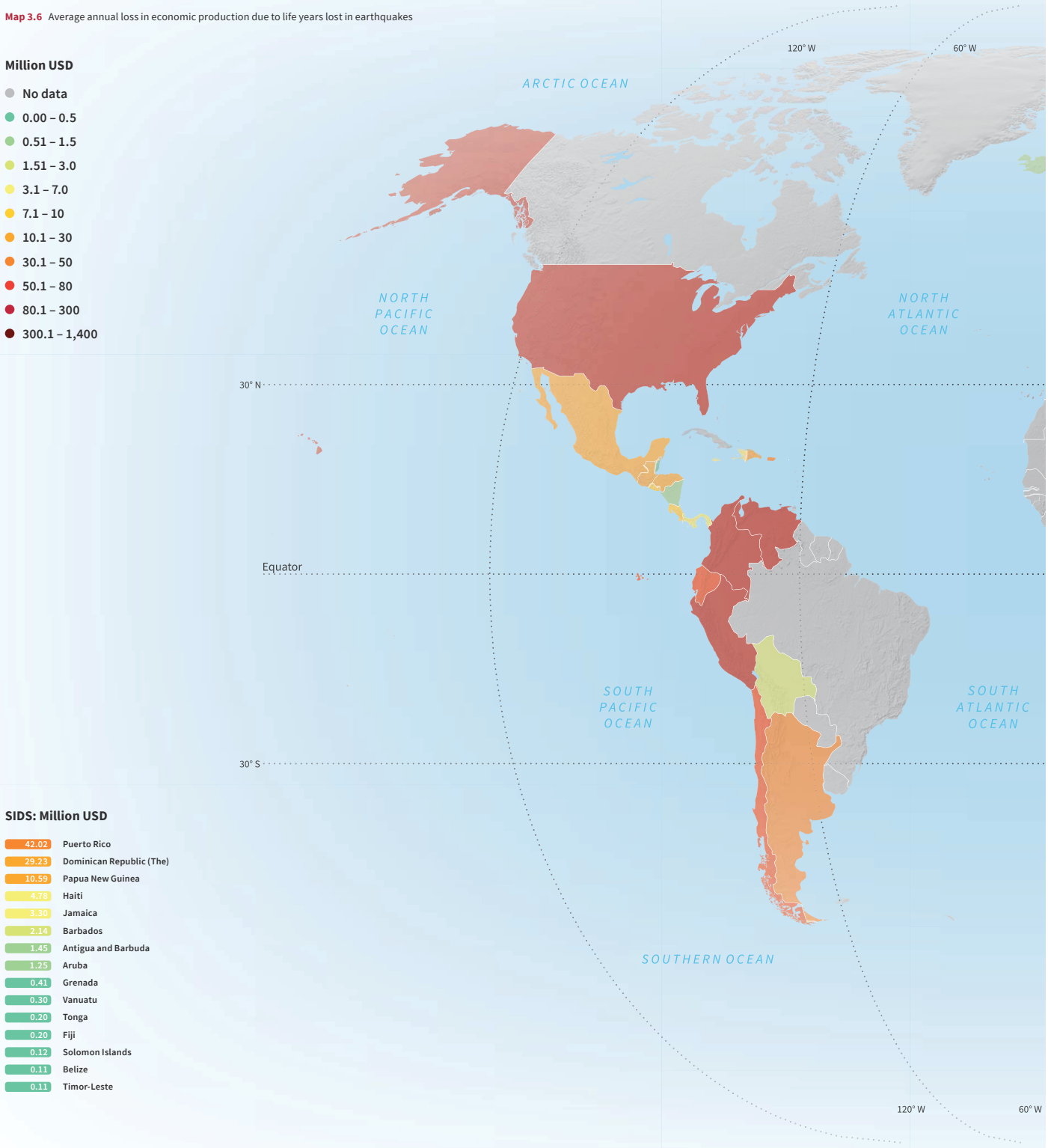

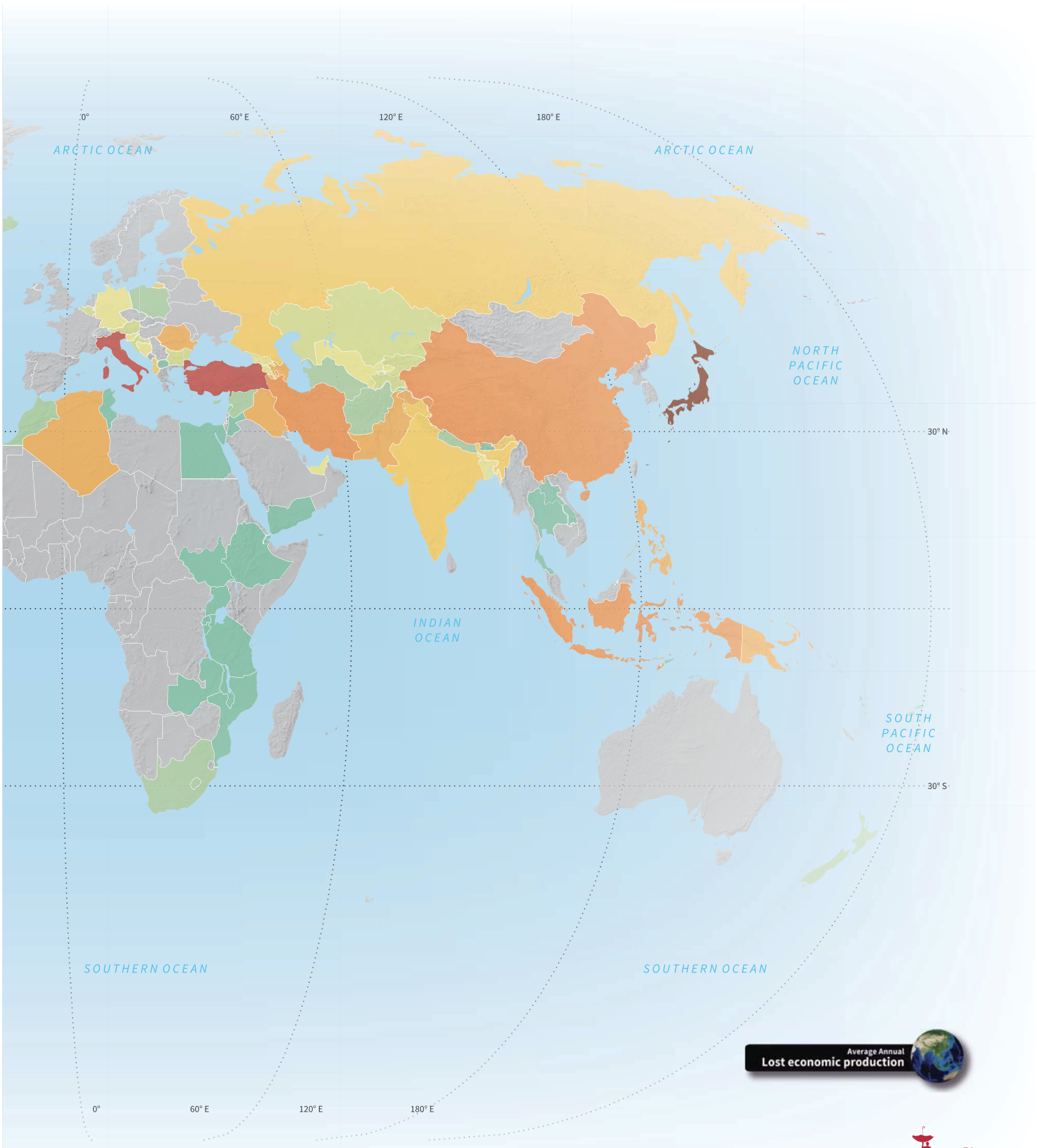
0°
60° E
120° E
180° E
ARCTIC OCEAN
ARCTIC OCEAN
NORTH PACIFIC OCEAN
30° N
INDIAN OCEAN
SOUTH PACIFIC OCEAN
30° S
SOUTHERN OCEAN
SOUTHERN OCEAN
0°
60° E
120° E
180° E
Average Annual
Lost economic production

Holistic approach concept

3.3 A holistic approach to understanding disaster risk and resilience

Disaster risk is socially constructed through a range of underlying drivers, including poverty and inequality, environmental degradation, badly planned and managed urban development, and weak governance[xi]. These drivers configure patterns of hazard, exposure and vulnerability over time. As outlined in Section 1 of the *GAR Atlas,* the AAL provides ways to condense the interdependence between a large variety of risk drivers into a single numerical value that represents disaster risk in a given country at a given time.

Current disaster risk is shaped by how a country has managed its risk drivers in the past. At the same time, how those drivers are managed in the present will influence not only future risk but also the impact that physical damage and direct economic loss have on societies and economies. As shown in the previous sections, mapping fiscal resilience and life years lost illustrate specific pathways through

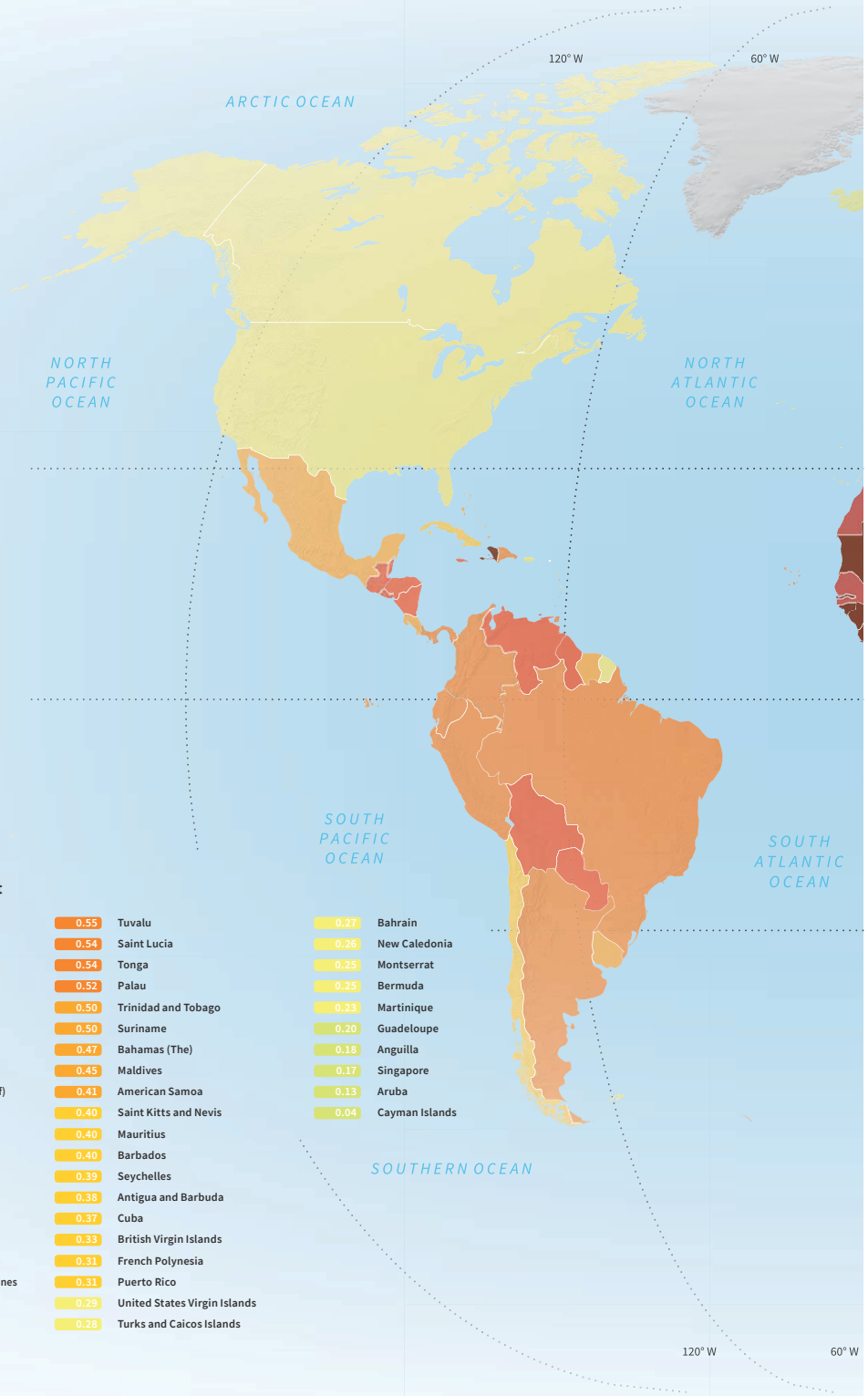

Map 3.7 Global distribution of risk-aggravating coefficient

Aggravating coefficient (Low:0 - High:1)

- No data
- 0 - 0.20
- 0.21 - 0.30
- 0.31 - 0.40
- 0.41 - 0.50
- 0.51 - 0.60
- 0.61 - 0.70
- 0.71 - 0.80
- 0.81 - 1.00

SIDS: Aggravating coefficient

0.83	Solomon Islands	0.55	Tuvalu	0.27	Bahrain
0.83	Haiti	0.54	Saint Lucia	0.26	New Caledonia
0.82	Guinea-Bissau	0.54	Tonga	0.25	Montserrat
0.77	Timor-Leste	0.52	Palau	0.25	Bermuda
0.74	Comoros	0.50	Trinidad and Tobago	0.23	Martinique
0.73	Sao Tome and Principe	0.50	Suriname	0.20	Guadeloupe
0.72	Kiribati	0.47	Bahamas (The)	0.18	Anguilla
0.72	Grenada	0.45	Maldives	0.17	Singapore
0.71	Micronesia (Federated States of)	0.41	American Samoa	0.13	Aruba
0.69	Vanuatu	0.40	Saint Kitts and Nevis	0.04	Cayman Islands
0.68	Papua New Guinea	0.40	Mauritius		
0.64	Guyana	0.40	Barbados		
0.61	Belize	0.39	Seychelles		
0.61	Jamaica	0.38	Antigua and Barbuda		
0.59	Dominican Republic (The)	0.37	Cuba		
0.59	Cabo Verde	0.33	British Virgin Islands		
0.59	Fiji	0.31	French Polynesia		
0.59	Saint Vincent and the Grenadines	0.31	Puerto Rico		
0.57	Dominica	0.29	United States Virgin Islands		
0.55	Marshall Islands (The)	0.28	Turks and Caicos Islands		

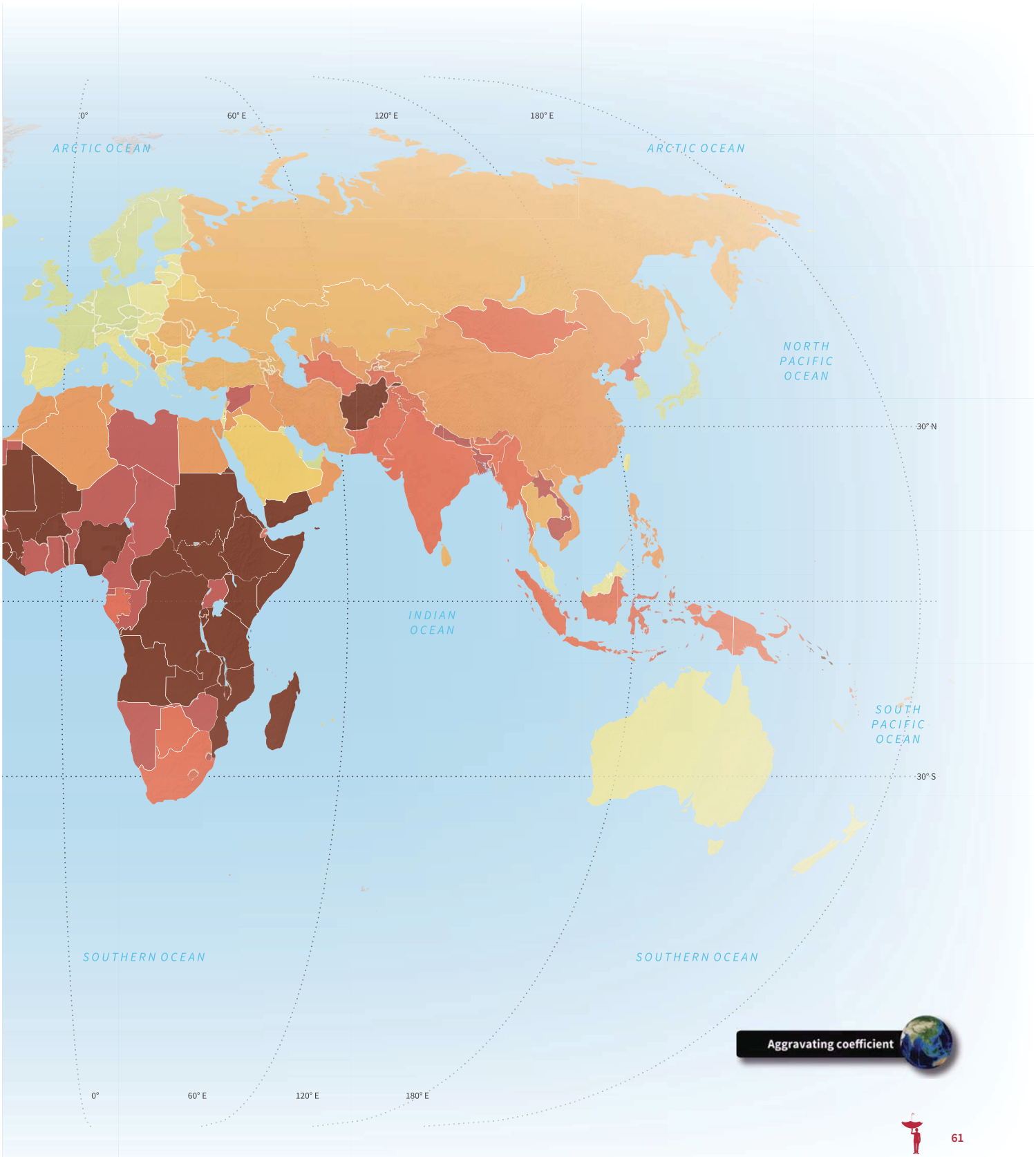
0°
60° E
120° E
180° E
ARCTIC OCEAN
ARCTIC OCEAN
NORTH PACIFIC OCEAN
30° N
INDIAN OCEAN
SOUTH PACIFIC OCEAN
30° S
SOUTHERN OCEAN
SOUTHERN OCEAN
0°
60° E
120° E
180° E
Aggravating coefficient

which probabilistic disaster risk metrics can be used to identify broader social and economic impact. Building on previous work at the city[xii] and country levels[xiii] this section of the *GAR Atlas* examines, from a more holistic perspective, how different risk drivers can magnify the impact of disaster loss and damage in different social and economic settings.

Fourteen variables were chosen as proxies for different risk drivers in the social, economic and environmental domains, and which together condition a society's resilience to disasters. These were transformed, combined and integrated as a coefficient that represents the likely magnification and aggravation of disaster impact, taking as a starting point the physical damage and direct economic loss as expressed through the multi-hazard AAL.

The global distribution of this *risk- aggravating* coefficient is shown in Map 3.7. Map 3.8 shows the distribution of total or holistic disaster resilience when the relative multi-hazard AAL is processed with the *risk- aggravating* coefficient[xiv].

This vision represents a broader picture of disaster resilience, highlighting in particular the likely impact of disaster risk in contexts with high social, economic and environmental fragility. It also provides guidance on which risk drivers will need to be addressed if disaster risk is to be managed and reduced by 2030, as per the Goal of the Sendai Framework.

Map 3.8 Global distribution of total or holistic disaster risk

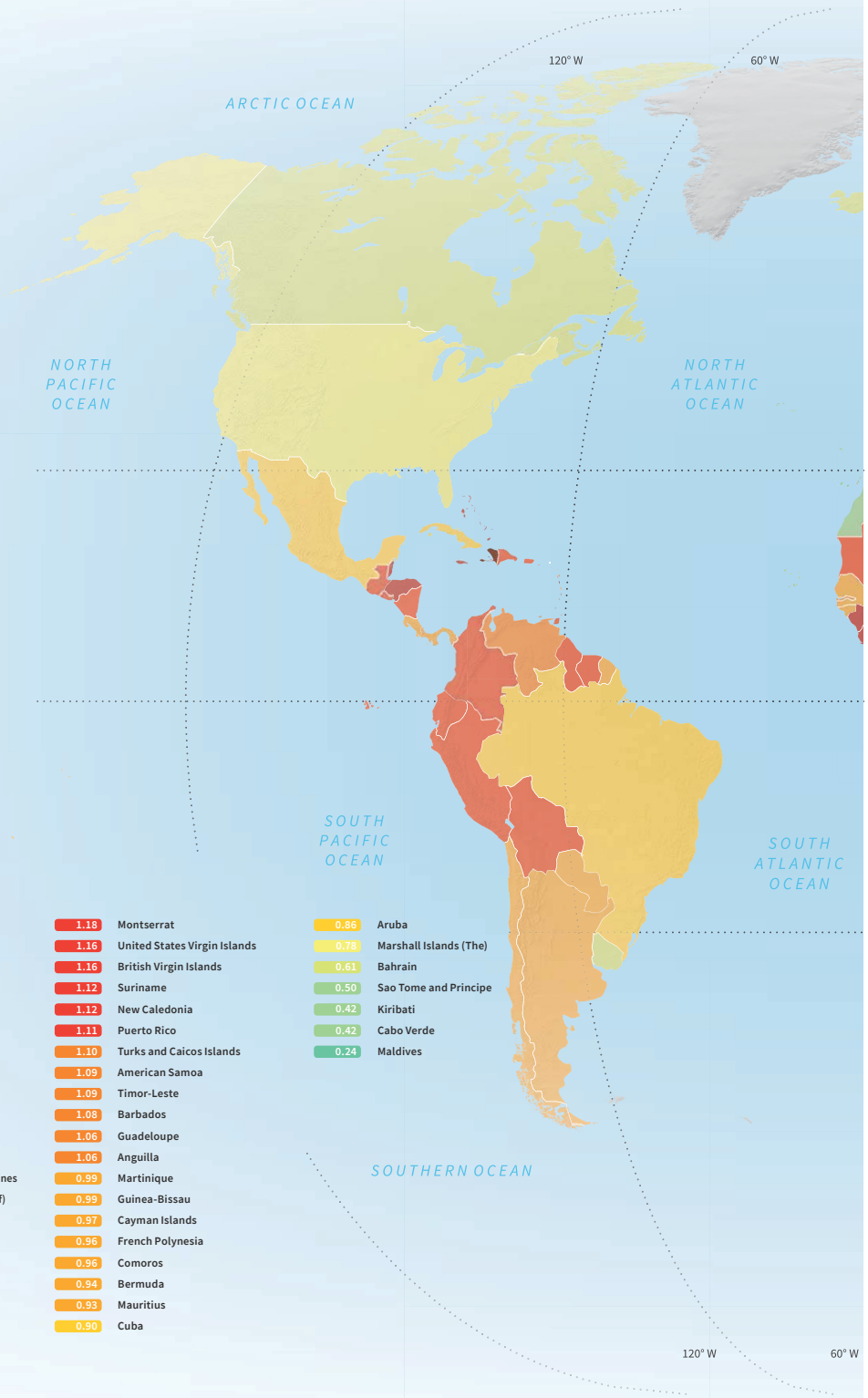

Total Risk (Low: 0 - High: 2)

- No data
- 0 - 0.40
- 0.41 - 0.60
- 0.61 - 0.70
- 0.71 - 0.80
- 0.81 - 0.90
- 0.91 - 1.00
- 1.01 - 1.10
- 1.11 - 1.20
- 1.21 - 1.40
- 1.41 - 2.00

SIDS: Total risk

1.49	Solomon Islands	1.18	Montserrat	0.86	Aruba
1.47	Vanuatu	1.16	United States Virgin Islands	0.78	Marshall Islands (The)
1.42	Dominica	1.16	British Virgin Islands	0.61	Bahrain
1.40	Haiti	1.12	Suriname	0.50	Sao Tome and Principe
1.38	Bahamas (The)	1.12	New Caledonia	0.42	Kiribati
1.35	Tonga	1.11	Puerto Rico	0.42	Cabo Verde
1.34	Belize	1.10	Turks and Caicos Islands	0.24	Maldives
1.31	Grenada	1.09	American Samoa		
1.29	Fiji	1.09	Timor-Leste		
1.28	Palau	1.08	Barbados		
1.28	Antigua and Barbuda	1.06	Guadeloupe		
1.28	Saint Lucia	1.06	Anguilla		
1.26	Saint Vincent and the Grenadines	0.99	Martinique		
1.26	Micronesia (Federated States of)	0.99	Guinea-Bissau		
1.22	Jamaica	0.97	Cayman Islands		
1.20	Saint Kitts and Nevis	0.96	French Polynesia		
1.19	Papua New Guinea	0.96	Comoros		
1.19	Guyana	0.94	Bermuda		
1.19	Trinidad and Tobago	0.93	Mauritius		
1.18	Dominican Republic (The)	0.90	Cuba		

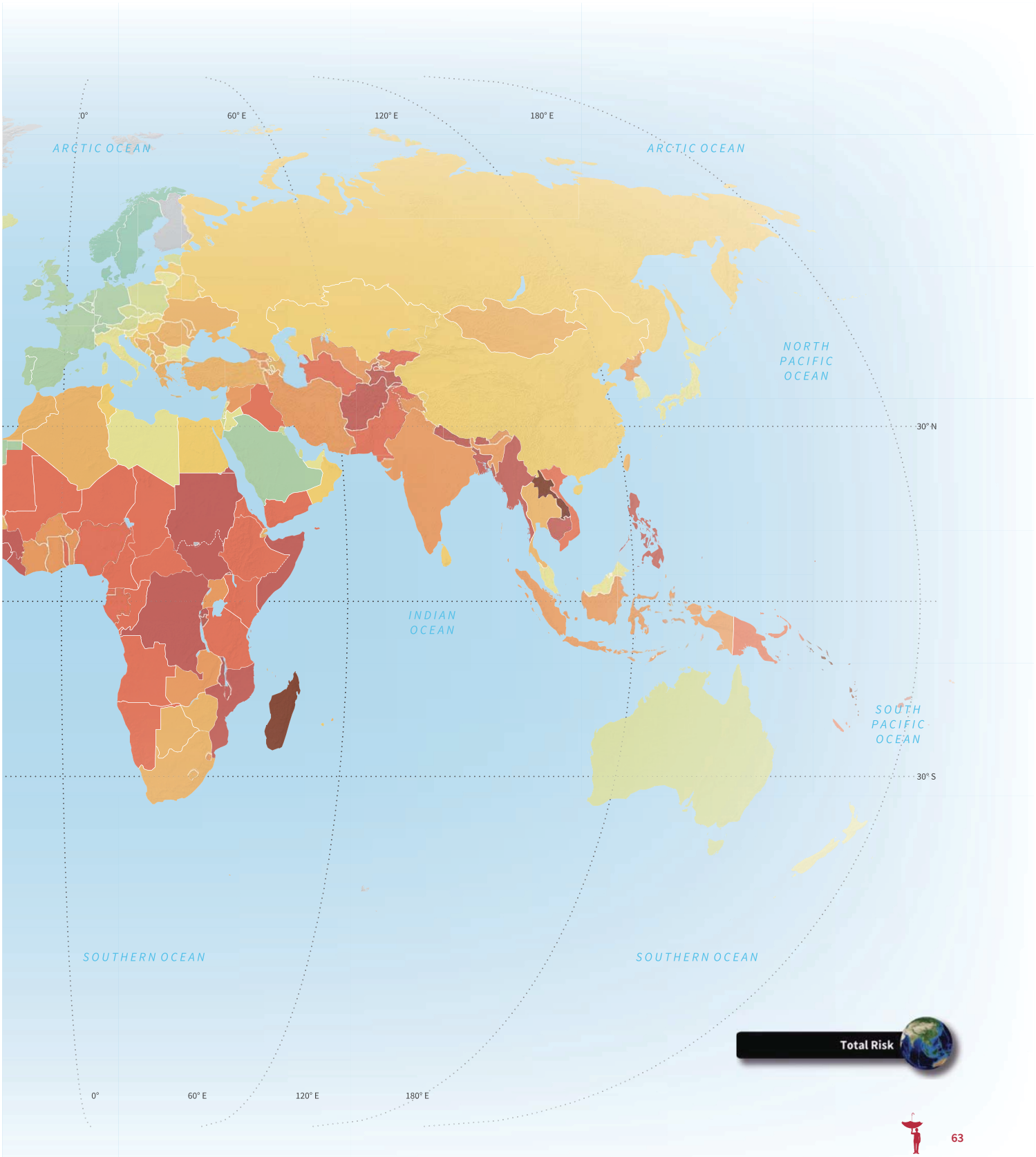
0°
60° E
120° E
180° E
ARCTIC OCEAN
ARCTIC OCEAN
NORTH PACIFIC OCEAN
30° N
INDIAN OCEAN
SOUTH PACIFIC OCEAN
30° S
SOUTHERN OCEAN
SOUTHERN OCEAN
0°
60° E
120° E
180° E
Total Risk

3.4 The implications for sustainable development

In order to achieve the promise of the 2030 Agenda for Sustainable Development, and more specifically the Sustainable Development Goals (SDGs)[xv], significant investment will be required across all income and geographic regions. At the same time, the capacity to make those investments will be constrained by potential disaster losses. Unfortunately, many countries have not identified the *hidden veins* of disaster risk that flow through their economies. Even fewer have measured that risk by using probabilistic techniques. And only a handful have successfully integrated risk metrics into social and economic planning.

In particular, in order to make progress across a range of SDGs, many countries will have to strengthen capital investment in infrastructure with proper building standards and in social expenditure that improves access to health, education and social

Map 3.9 Multi-hazard AAL as a percentage of Gross Fixed Capital Formation (GFCF)

AAL/GFCF (per cent)

- No data
- 0 - 0.7
- 0.8 - 1.4
- 1.5 - 2.1
- 2.2 - 3.5
- 3.6 - 5.0
- 5.1 - 7.0
- 7.1 - 11.0
- 11.1 - 30.0
- 30.1 - 50.0
- 50.1 - 93.0

SIDS: AAL/GFCF (per cent)

92.97	Bahamas (The)	8.03	Aruba
87.68	Dominica	7.59	Dominican Republic (The)
86.08	Antigua and Barbuda	7.32	Haiti
48.12	Puerto Rico	5.65	Guyana
44.52	Anguilla	4.94	Cuba
39.59	British Virgin Islands	4.71	Papua New Guinea
32.56	Solomon Islands	3.87	Mauritius
32.00	Saint Kitts and Nevis	3.04	Timor-Leste
31.52	Vanuatu	1.88	Suriname
30.39	Belize	1.51	Guinea-Bissau
21.54	Palau	0.64	Comoros
21.25	Tonga	0.50	Bahrain
19.32	Bermuda	0.07	Sao Tome and Principe
19.24	Grenada	0.02	Cabo Verde
18.63	Barbados	0.01	Maldives
17.77	Saint Lucia		
16.66	Fiji		
15.55	Trinidad and Tobago		
15.12	Jamaica		
15.07	Saint Vincent and the Grenadines		

protection. When the AAL represents a significant proportion of current capital investment and social expenditure, it is likely that a country will face severe constraints to increase its capacity to invest, as that capacity will periodically be eroded by disaster loss. At the same time, of course, if the investment is made without taking disaster risk into account, the investment itself can lead to increasing future risk.

Map 3.9 shows the global distribution of multi-hazard AAL as a proportion of 2014 capital investment in infrastructure and housing (represented by Gross Fixed Capital Formation). It highlights how a number of countries will be challenged to make the capital investments necessary to achieve the SDGs unless disaster risk is reduced. These countries include low-income countries like Madagascar and Myanmar, middle-income countries like Honduras and the Philippines as well as a high-income country like Greece. In the case of countries with sluggish or contracting economies and with low capacity to make new capital investments, disaster risk poses a serious threat to future development.

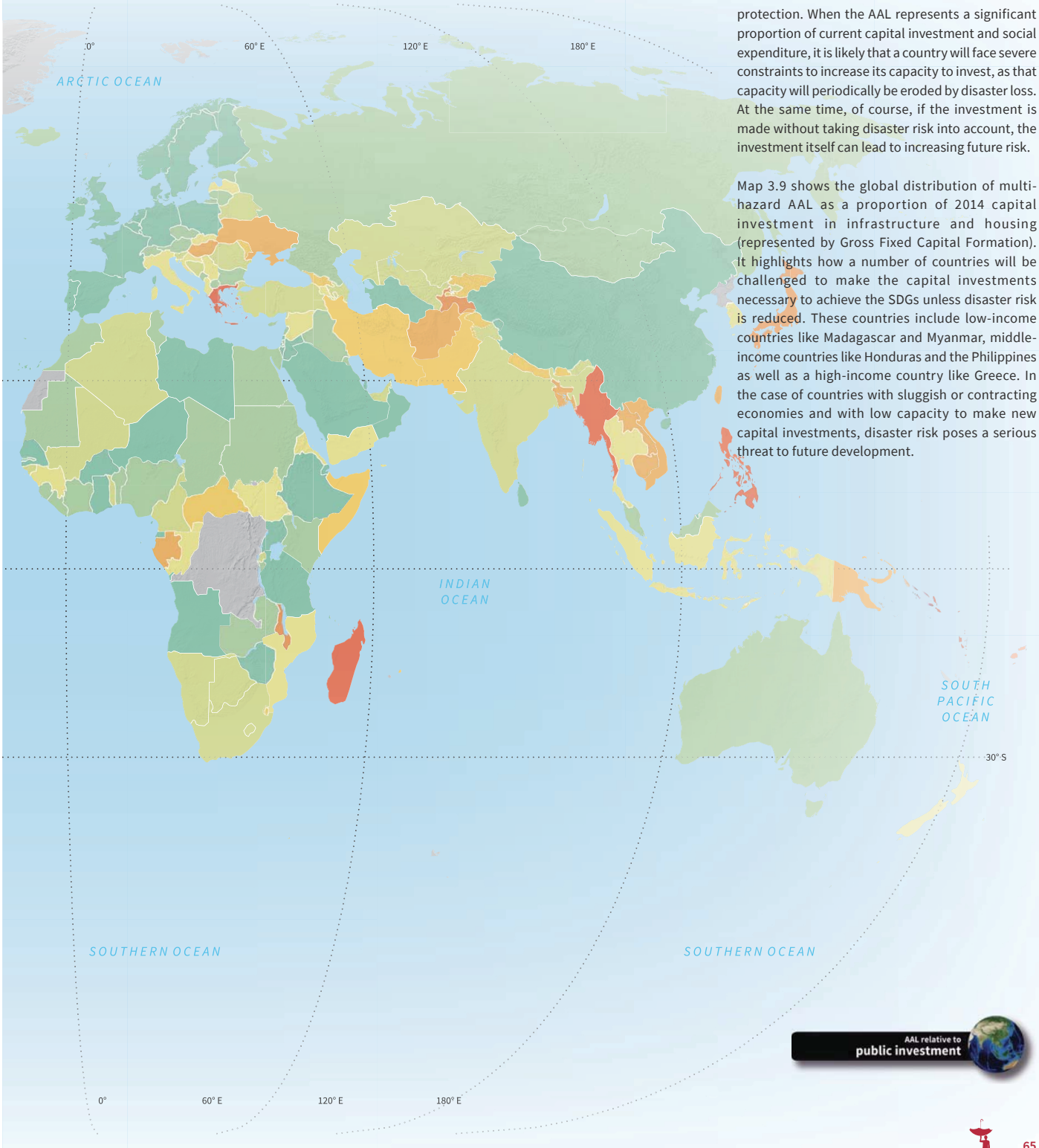

AAL relative to **public investment**

Map 3.10 Multi-hazard AAL as a percentage of social expenditure (SE)

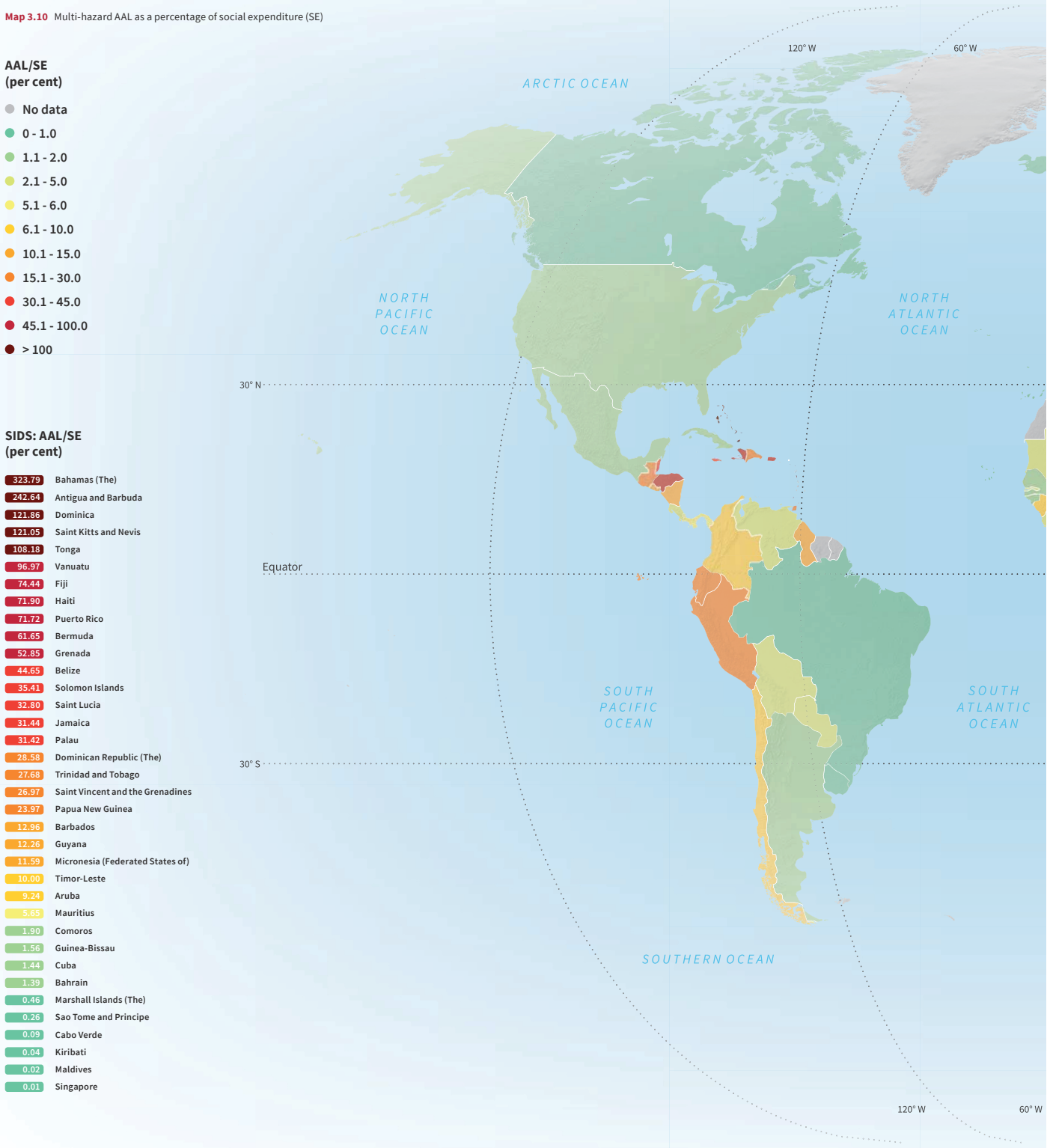

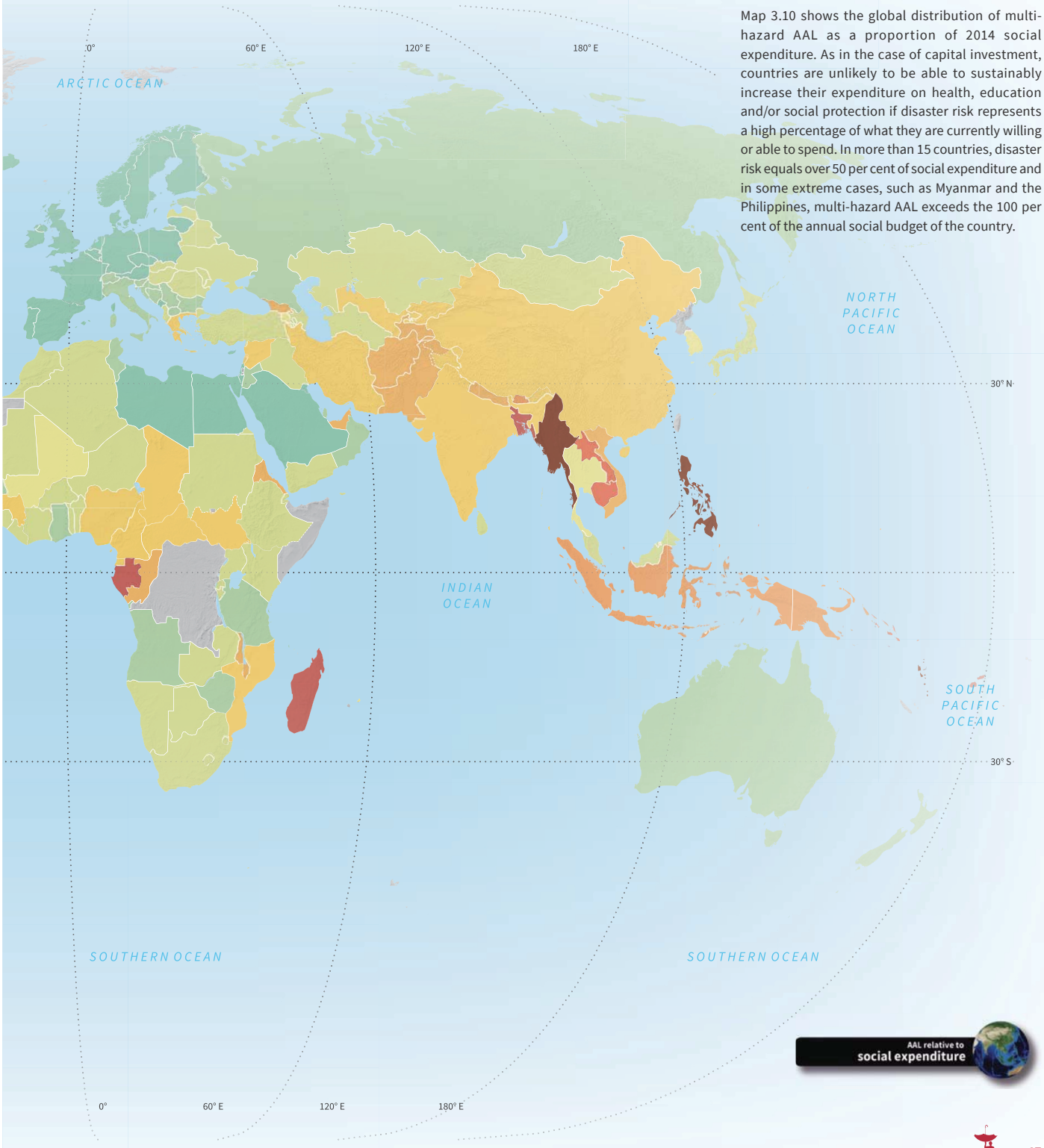

Map 3.10 shows the global distribution of multi-hazard AAL as a proportion of 2014 social expenditure. As in the case of capital investment, countries are unlikely to be able to sustainably increase their expenditure on health, education and/or social protection if disaster risk represents a high percentage of what they are currently willing or able to spend. In more than 15 countries, disaster risk equals over 50 per cent of social expenditure and in some extreme cases, such as Myanmar and the Philippines, multi-hazard AAL exceeds the 100 per cent of the annual social budget of the country.

Map 3.11 Global distribution of disaster risk constraints on the potential for sustainable development

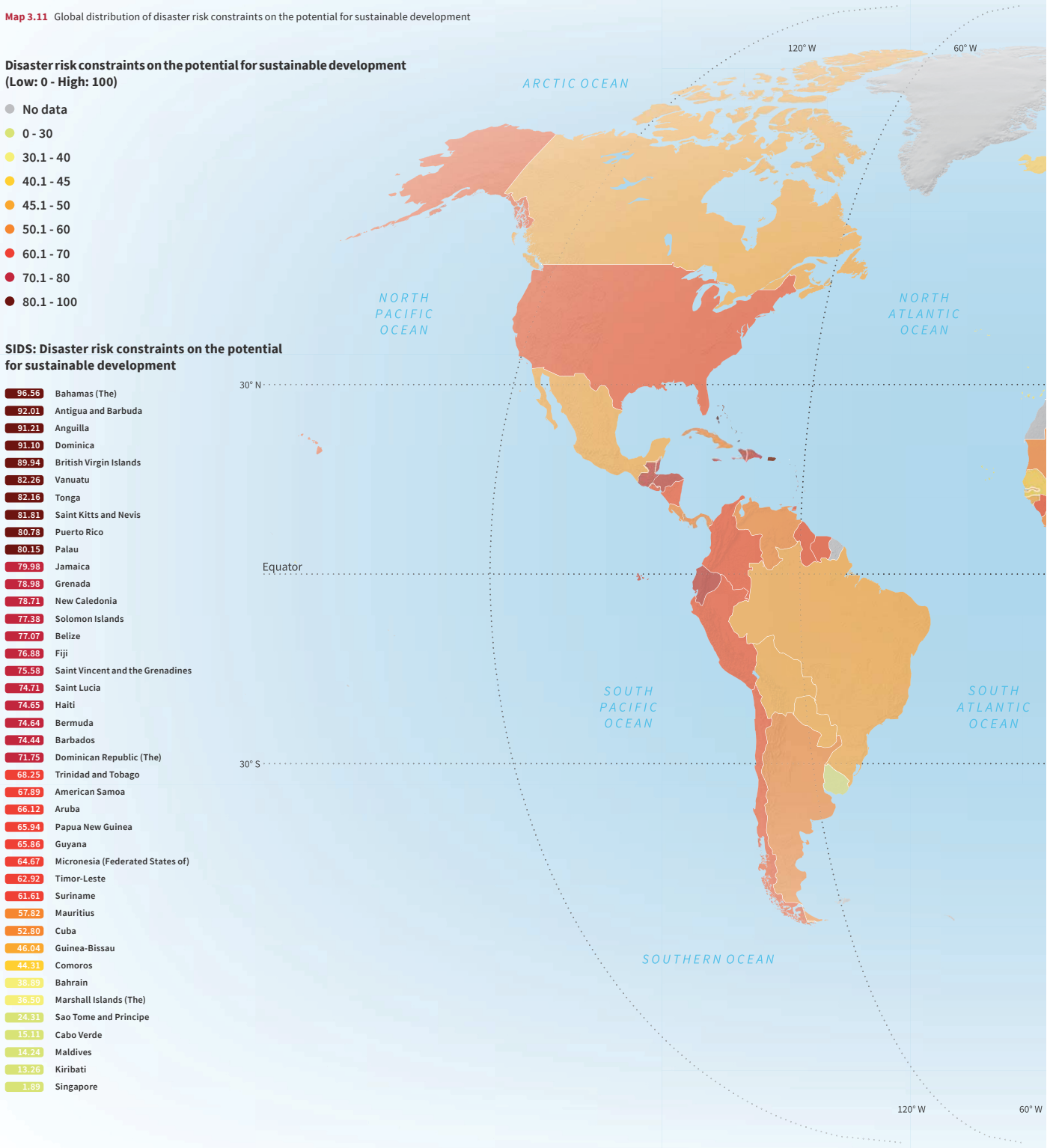

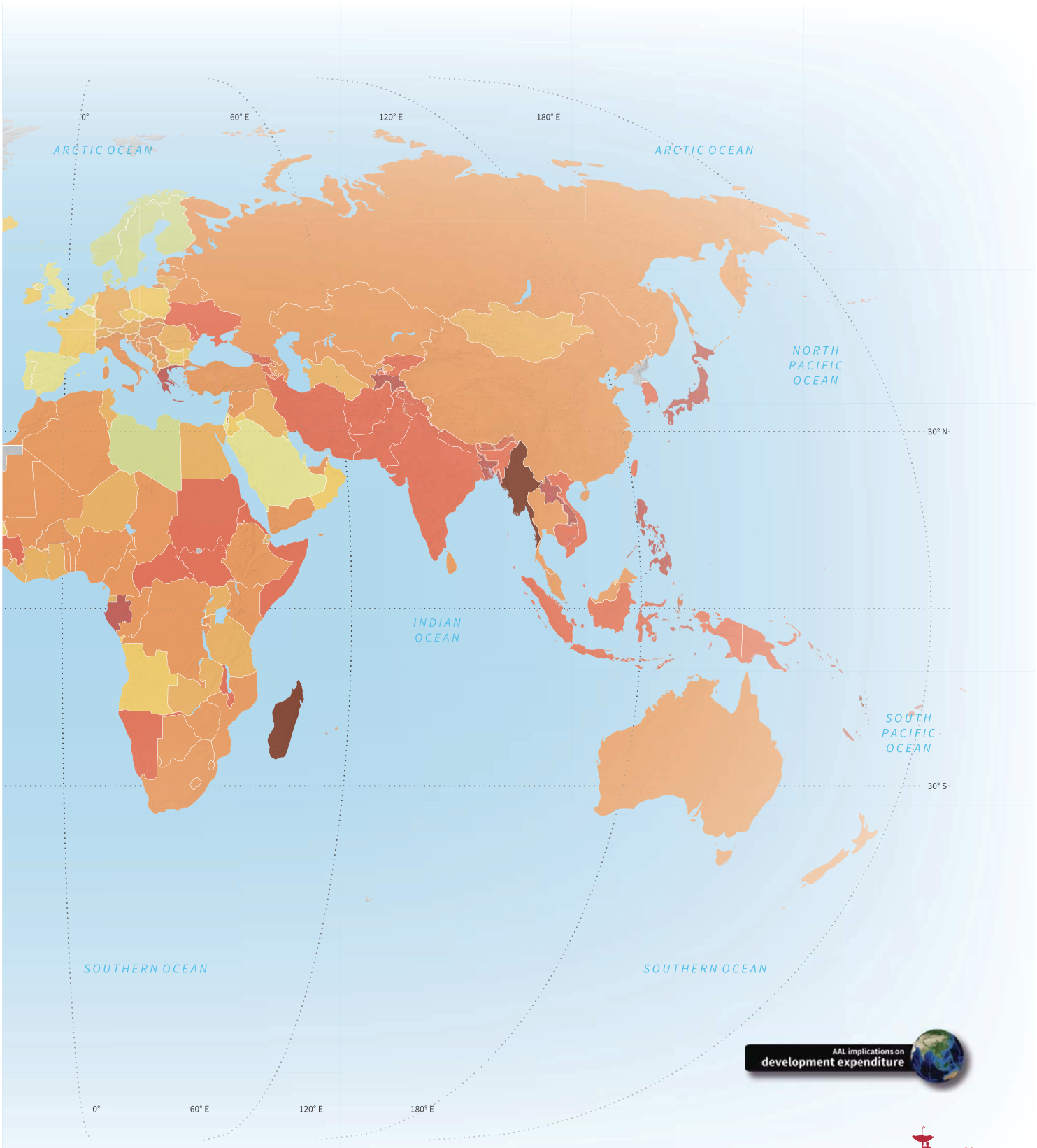

AAL implications on
development expenditure

Small island developing states (SIDS) are disproportionately at risk[xvi], given that disasters may affect 100per cent of their economies, populations and physical assets. Figure 3.1 highlights that disaster risk in many SIDS represents a significant proportion of their capital stock, capital investment and social expenditure, meaning that risk becomes an existential threat to their future development.

Map 3.11 shows the global distribution of a coefficient that integrates the relative weight of disaster risk with respect to four development metrics: capital stock, capital investment, social expenditure and national savings. This coefficient represents the overall constraint posed by disaster risk on their potential for sustainable development. Where risk represents a high proportion of these metrics, the country is likely to be more constrained in achieving the SDGs. These figures show that countries with very different levels of multi-hazard AAL have similar constraints on their potential for sustainable development.

i. IDEA 2005 Williges et al. 2015
ii. Williges et al. 2015
iii. Williges et al. 2015
iv. Cardona et al. 2015
v. Noy 2014, 2015, UNISDR 2015b
vi. UNISDR 2015b
vii. UNISDR 2015b, Noy 2014, 2015
viii. Salgado-Galvez et al. 2016a
ix. Salgado-Gálvez 2016b
x. Salgado-Gálvez 2016b
xi. UNISDR 2009, 2011, 2013, 2015b
xii. Carreño et al. 2007, Marulanda et al. 2013, Salgado-Gálvez et al. 2016b
xiii. IDEA 2005
xiv. Cardona 2001
xv. United Nations 2015b
xvi. UNISDR 2013, 2015b

Figure 3.1 Disaster risk implications on Small Islands Development States, SIDS

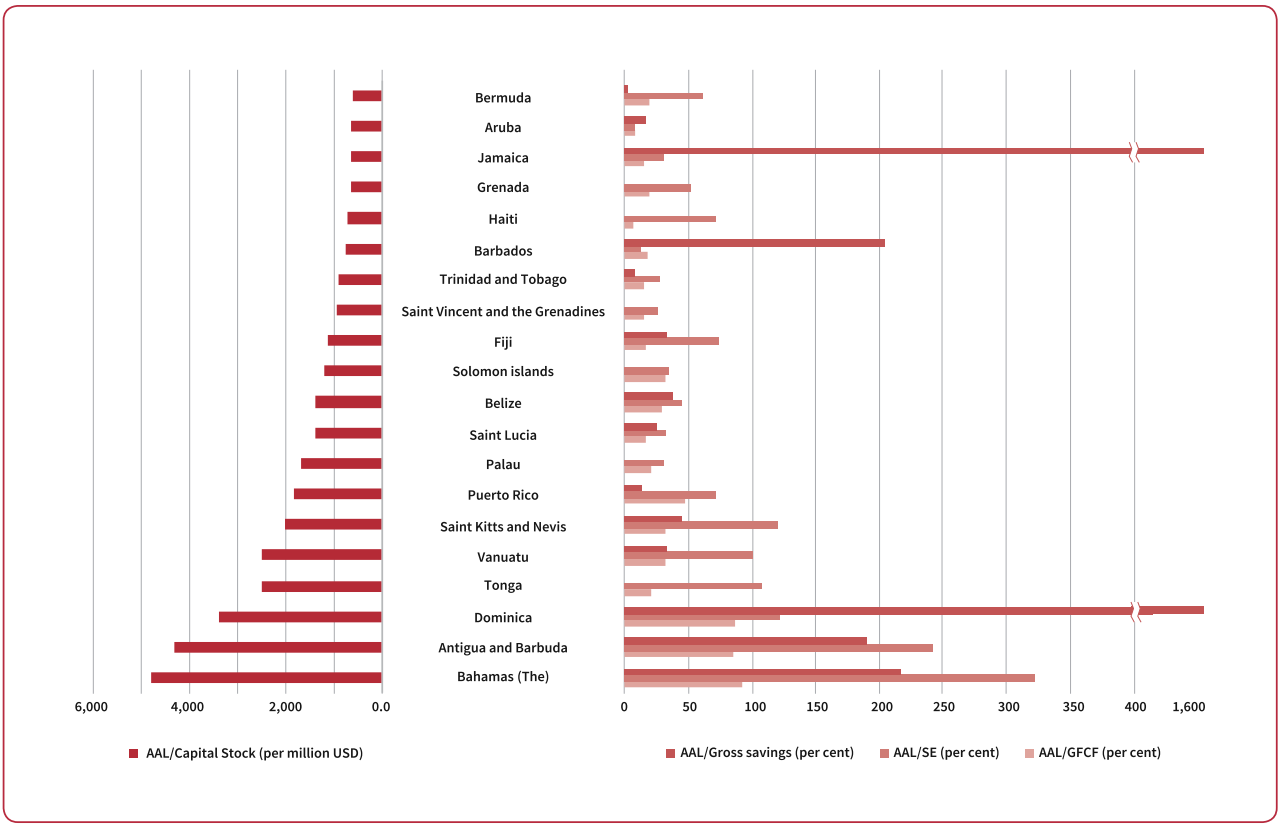

Source: UNISDR

Section 4

Applications of the Global Risk Model

Figure 4.1 Hazard intensity with and without climate change in selected cities of Central America and the Caribbean

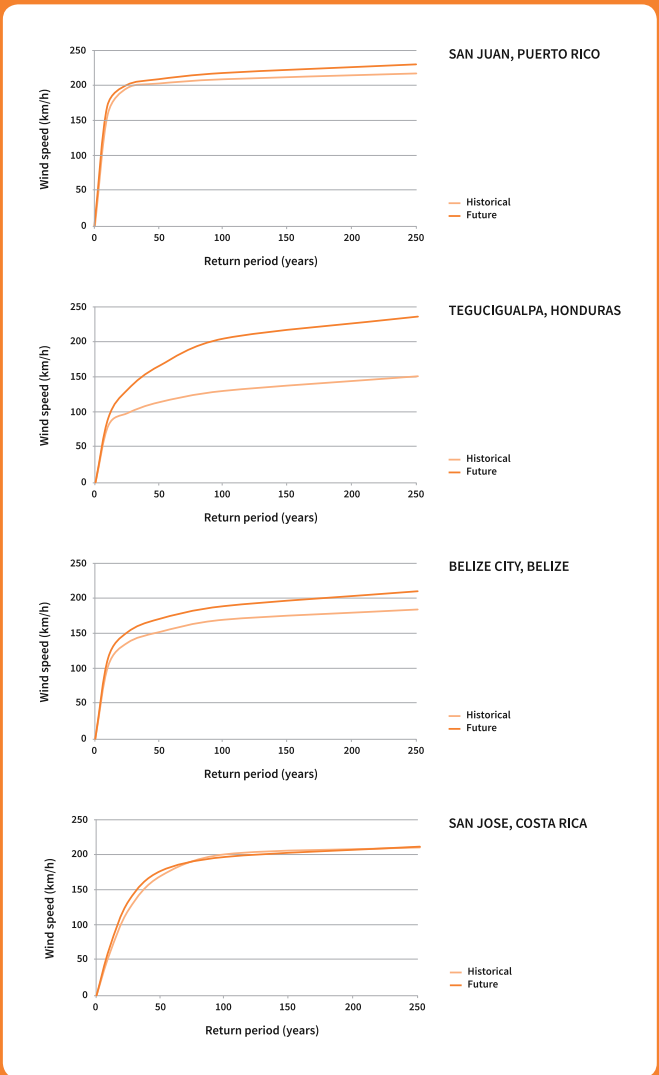

Source: Cardona et al. 2015

4.1 How climate change modifies disaster risk

Climate change is already modifying the frequency, intensity and regularity of hazards such as flood, cyclonic wind and storm surge and droughts. Long-term trends, however, can often only be inferred with a low level of confidence at this stage[i]. Changing hazard patterns can also lead to increasing exposure in some areas as well as increases in vulnerability, all of which generate new risk.

While it is impossible to predict exactly how climate change will modify disaster risk in the future, it is possible to calculate risk scenarios on the basis of climate models for specific regions. In other words, instead of calculating risk with today's hazards, a future scenario is calculated with new hazard parameters derived from a climate change model. By maintaining the exposure and vulnerability constant in the risk model, it is therefore possible to identify by how much climate change could increase risk levels under a given scenario.

Using the Global Risk Model, disaster risk associated with cyclonic wind was calculated for the North Atlantic basin. This involved comparing current risk levels with the ones obtained after considering the climate change scenario using the Nested Regional Climate Model (NRCM) developed by the National Center for Atmospheric Research of the United States (NCAR).

Figure 4.1 illustrates how, under this climate change scenario, hazard intensity associated with wind velocity increase in selected capital cities, though not in the same way[ii].

Figure 4.2 shows that under this scenario climate change would add around USD 1.4 billion to the cyclonic wind AAL in the North Atlantic basin. This increase in risk, however, is not evenly distributed. Mexico, for example, would experience reduced wind -related risk due to Caribbean hurricanes.

Figure 4.2 Comparison of cyclonic wind AAL with and without climate change

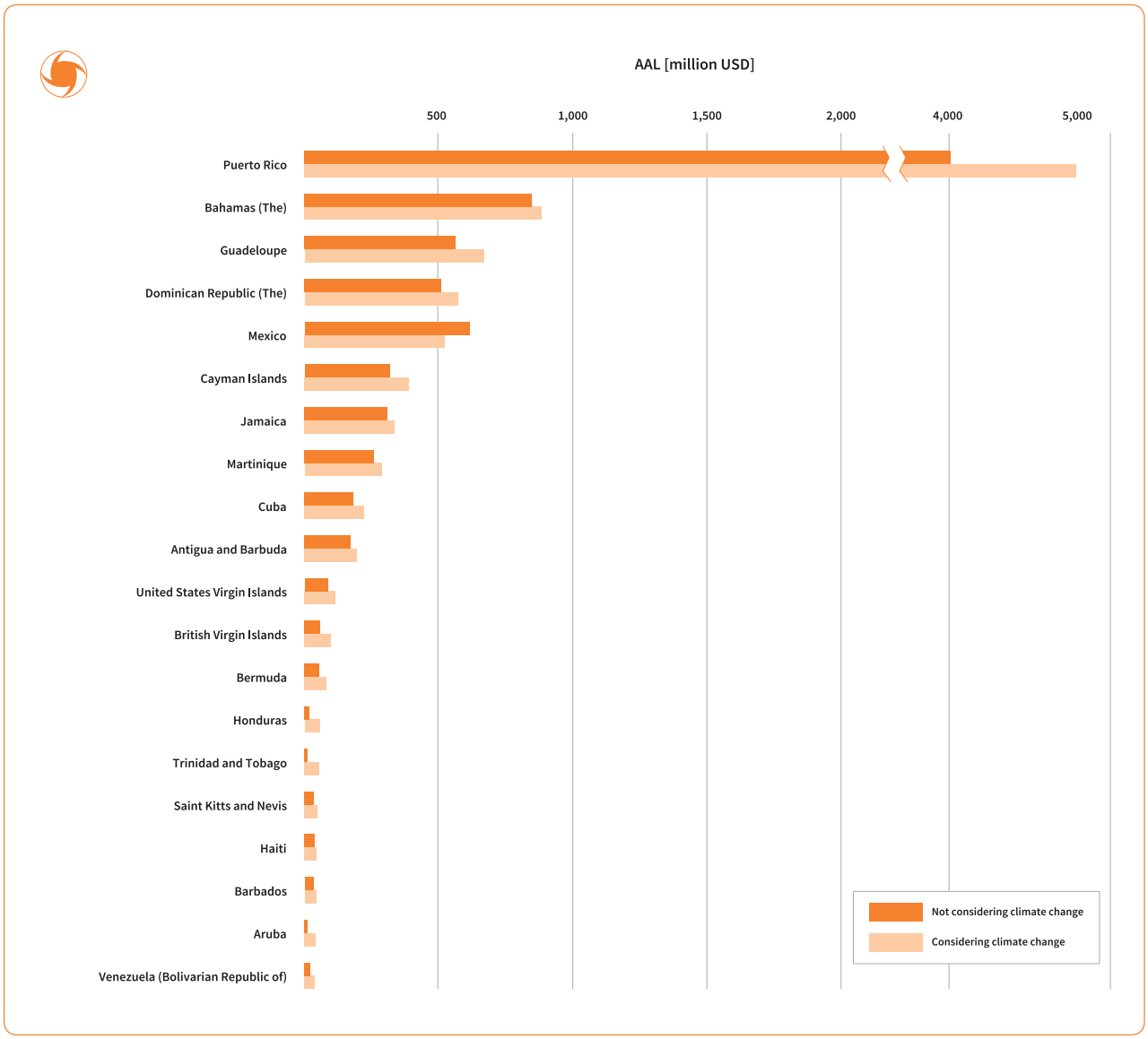

Source: Cardona et al. 2015

4.2 Estimating the risk from volcanic ash

Most active volcanoes are located along the boundaries between tectonic plates[iii]. Figure 4.3 shows the location of known active and inactive volcanoes on land. Overall, there are 1,551 volcanoes that have been active in the last 10,000 years.

Volcanoes are associated with a range of hazards, including pyroclastic flows and surges, volcanic ash and tephra, ballistics, lahars and floods, debris avalanches, landslides and tsunamis, volcanic gases and aerosols, lava flows, earthquakes and lightning. Each of these hazards can affect people, the built environment, agriculture, transportation and other sectors in very different ways.

The Global Risk Model has been used to estimate the risk associated with volcanic ash fall in the Asia-Pacific region as a proof of concept[iv]. By using the same approach as for other hazards calculated globally, it enables volcanic ash risk to be included in national risk metrics such as AAL and PML. The results show that, given the infrequency of volcanic eruptions, the volcanic ash AAL is generally lower than that associated with other hazards. However, in some countries the PML can be very significant.

Map 4.1 and Map 4.2 show the AAL from volcanic ash fall in absolute values and as a share of the capital stock for the Asia-Pacific region. The combined AAL for the 16 countries studied is USD 18 billion, mainly concentrated in Japan, Indonesia and the Philippines as shown in Table 4.1. However, in some countries, such as Indonesia and Vanuatu, the relative AAL represents 0.2 per cent and 0.1 per cent of the value of capital stock, which is not insignificant. Similarly, it represents 12 per cent of the value of social expenditure in Indonesia and 7 per cent in the Philippines.

Figure 4.3 Location of active and inactive volcanoes in the world

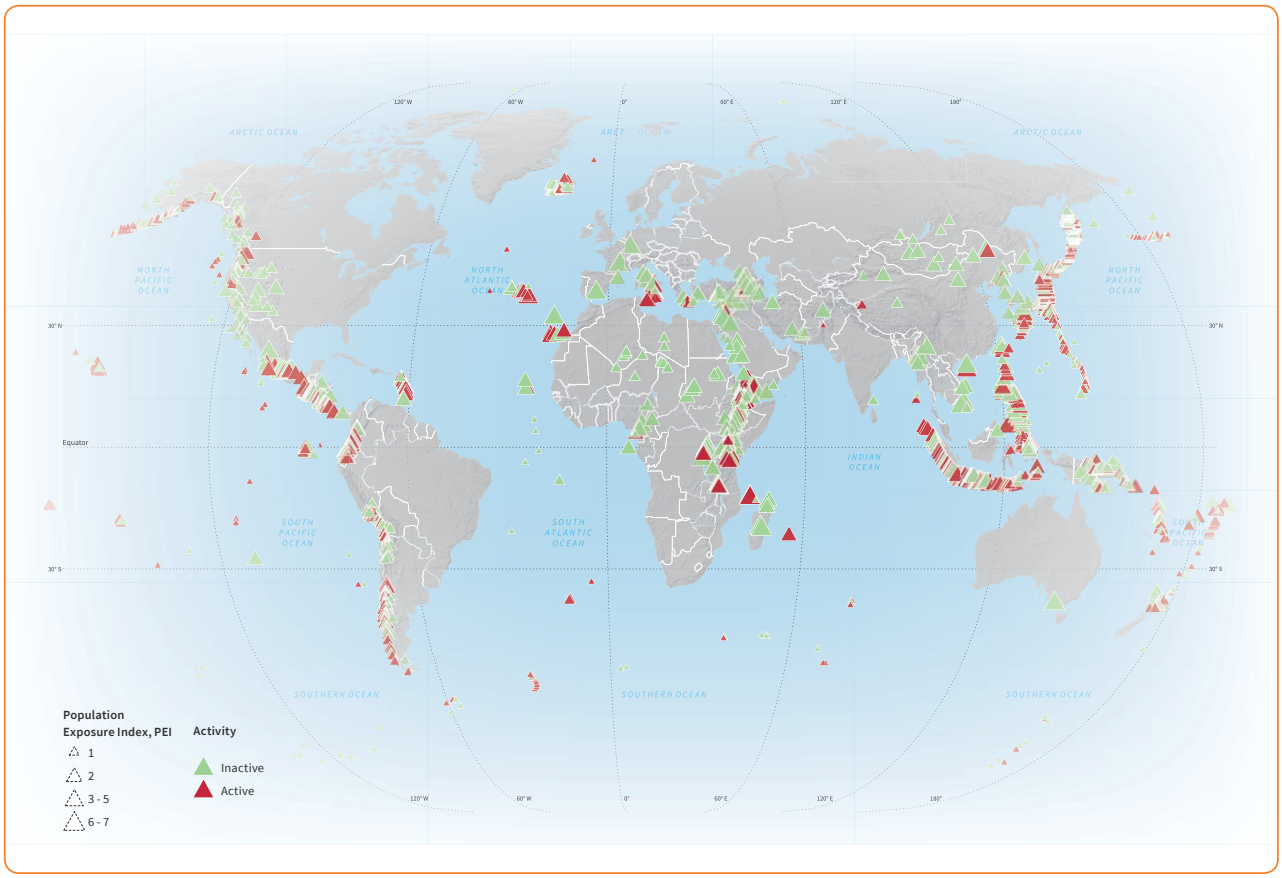

Source: Bear Crozier et al. 2014

Map 4.1 Absolute AAL associated with volcanic ash fall - Asia Pacific Region

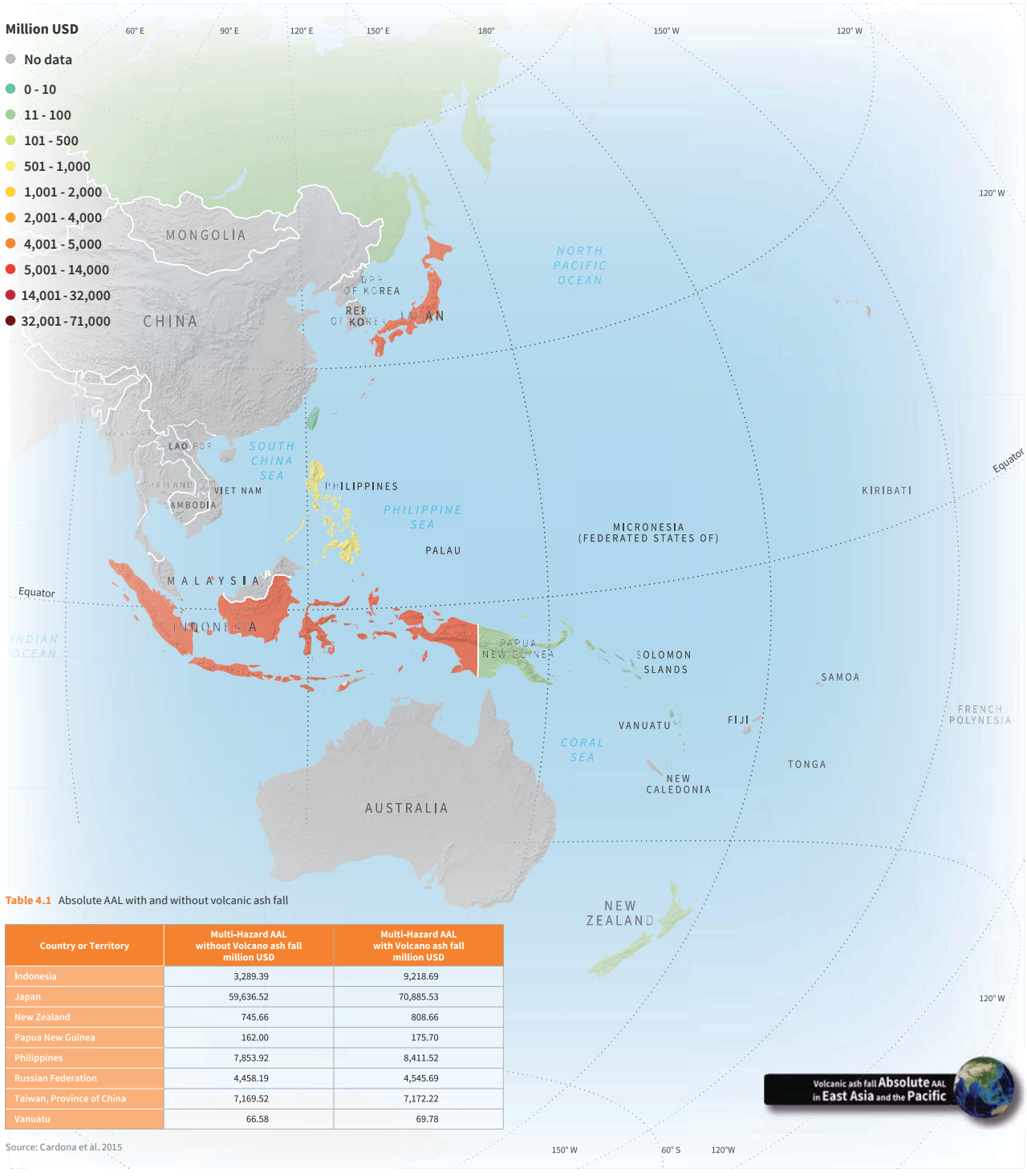

Table 4.1 Absolute AAL with and without volcanic ash fall

Country or Territory	Multi-Hazard AAL without Volcano ash fall million USD	Multi-Hazard AAL with Volcano ash fall million USD
Indonesia	3,289.39	9,218.69
Japan	59,636.52	70,885.53
New Zealand	745.66	808.66
Papua New Guinea	162.00	175.70
Philippines	7,853.92	8,411.52
Russian Federation	4,458.19	4,545.69
Taiwan, Province of China	7,169.52	7,172.22
Vanuatu	66.58	69.78

Source: Cardona et al. 2015

Map 4.2 AAL associated with volcanic ash fall relative to capital stock - Asia Pacific Region

Table 4.2 Relative AAL with and without volcanic ash fall

Country or Territory	Multi-Hazard AAL without Volcano ash fall per million USD	Multi-Hazard AAL with Volcano ash fall per million USD
Indonesia	1,163.22	3,259.99
Japan	1,519.20	1,805.76
New Zealand	1,097.03	1,189.72
Papua New Guinea	3,445.50	3,736.87
Philippines	13,852.96	14,836.47
Russian Federation	704.76	718.60
Solomon Islands	11,750.47	11,777.54
Taiwan, Province of China	4,266.56	4,268.16
Vanuatu	23,697.24	24,836.19

Source: Cardona et al. 2015

4.3 Modelling extensive risk

The GRM models the risk associated with major hazards such as earthquakes, tsunamis, tropical cyclones and riverine floods. As discussed in Section 1, probabilistic models enable the estimation of the intensive risk associated with low frequency, high severity loss events in a way that cannot be adequately captured from historical data.

However, in many countries a significant proportion of disaster risk is associated with high frequency, low severity loss events, associated with localised hazards such as flash floods, landslides, storms and wildfires. This extensive risk cannot be captured at the global scale using probabilistic models, given the highly idiosyncratic nature of the hazards involved.

There has been little interest in modelling extensive risk given that it poses little threat to the insolvency of insurance companies. And for many governments it is a largely *invisible* risk, given that it mainly affects the lives and livelihoods of low-income rural and urban households[v] and small and medium enterprises[vi] rather than strategic infrastructure and large businesses. However, making extensive risk visible is critical to the achievement of the SDGs.

Given the high frequency of losses, extensive risk can be modeled using historical records from national disaster loss databases to generate an empirical loss exceedance curve (LEC)[vii].

The historical LEC for extensive risk can then be combined with an analytical LEC for intensive risk produced by the GRM to create a hybrid LEC that covers the full spectrum of risk. In general, the historical LEC tends to better represent small and frequent losses at one end of the curve while the analytical LEC better represents the extreme and infrequent economic losses at the other end[viii].

The hybrid LEC therefore provides AAL and PML metrics that offer a more complete risk profile, enabling governments to adopt appropriate disaster risk management strategies for all risk layers.

Figure 4.4 highlights two hybrid LEC for Venezuela and Lao PDR respectively. As of March 2017 around ninety countries have developed national disaster loss databases[ix]. With the adoption by the UN General Assembly of the indicators to measure progress towards the Global Targets of the Sendai

Box 4.1 Intensive and extensive disaster risk definitions

Intensive disaster risk
The risk of high-severity, mid- to low-frequency disasters, mainly associated with major hazards.

Extensive disaster risk
The risk of low-severity, high-frequency hazardous events and disasters, mainly but not exclusively associated with highly localised hazards.

Source: United Nations, 2016
It is recommended that these definitions are read together with their annotations in the report.
United Nations, 2016

Figure 4.4 Hybrid loss exceedance curves (LEC) for Venezuela (top) and Lao PDR (bottom)

Empirical Loss Exceedance Curve construction for Venezuela

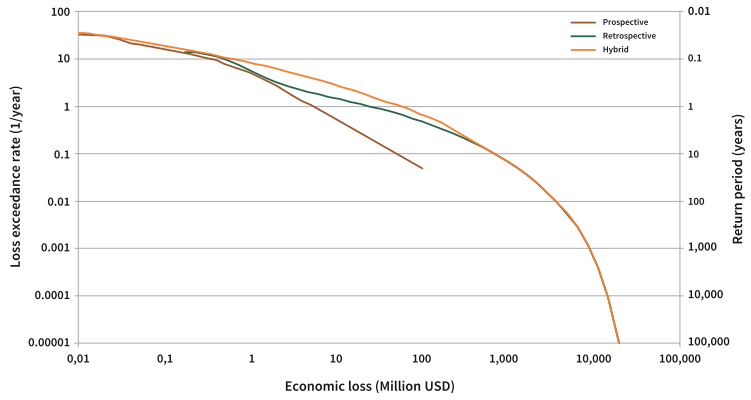

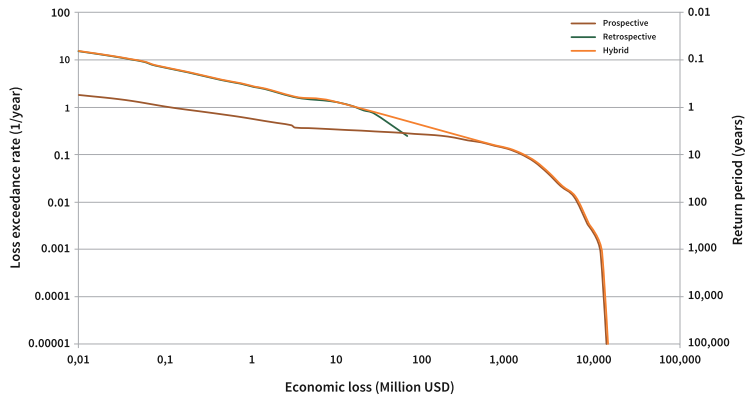

Empirical Loss Exceedance Curve construction for Lao PDR

Source: Cardona et al. 2014 and UNISDR

Framework, it is expected that most countries will have this data in place by 2020. This would enable the development of hybrid LEC at the global scale and a more complete representation of risk in the GRM.

4.4 Local level applications

The Global Risk Model calculates a first level order of magnitude of disaster risk in different countries and regions. However, the same methodology can be used at the local level to provide higher resolution risk metrics, which in turn can be used to inform appropriate disaster risk management measures.

4.4.1 Volcanic risk in Nariño, Colombia

A local assessment of disaster risk associated with the *Galeras* volcano, located approximately 10 kilometres west of the city of Pasto in the Department of Nariño, Colombia revealed an AAL of USD 130,000 in the area surrounding the volcano[x].

Volcanic hazard was calculated in relation to the intensity of ash fall, pyroclastic and lava flows[xi]. Figure 4.5 highlights the hazard associated with pyroclastic flows around the volcano.

Figure 4.5 Pyroclastic flows hazard map for Galeras Volcano

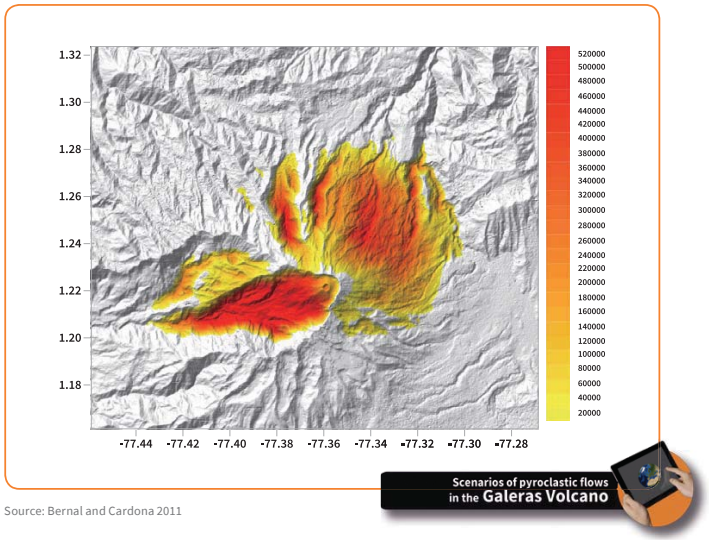

Source: Bernal and Cardona 2011

In the case of pyroclastic and lava flows, building vulnerability can be described as binary, given that if the building is affected it is likely to suffer complete loss. In contrast, the loss associated with volcanic ash fall depends on the structure of the building and the strength of the roof.

The risk assessment was performed for the municipalities close to the volcano. Figure 4.6 shows the volcanic ash AAL in absolute terms and relative to the exposed value.

Figure 4.6 Average annual loss associated with ash fall in Galeras volcano region: absolute value (left) and relative to the exposed value (right)

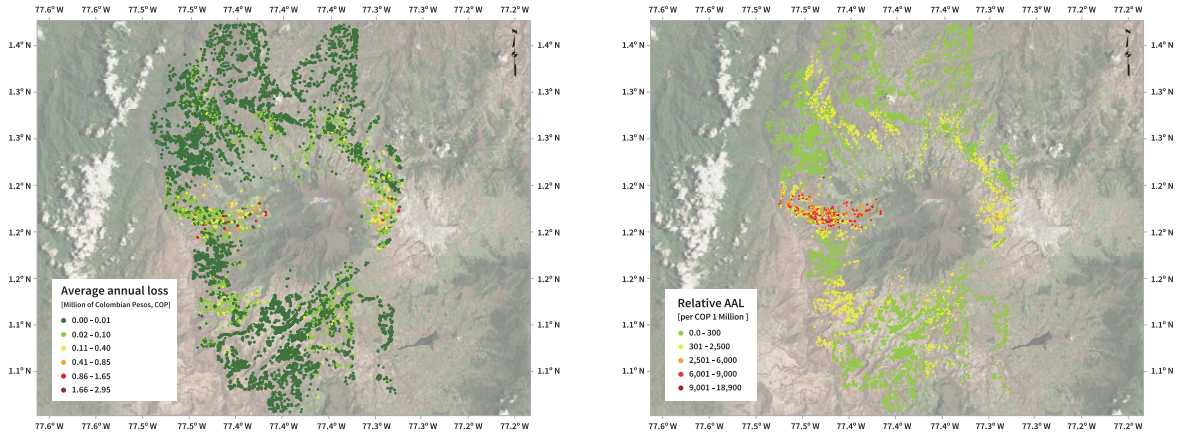

Source: Bernal and Cardona 2011

4.4.2 Earthquake risk in Lorca, Spain

On 11 May 2011, a moderate earthquake hit the Murcia region of Spain, causing significant damage in Lorca, a city of around 60,000 inhabitants.

After the earthquake, a risk assessment for Lorca compared observed losses with those modelled using a similar event in terms of magnitude, location, depth and ground acceleration[xii]. Figure 4.7 highlights the distribution of the modeled losses, which totalled EUR 615 million. This was of the same order of magnitude as the observed insured losses. which totalled EUR 490 million.

The example of Lorca highlights that local-level risk models can provide robust estimations of expected losses associated with specific scenarios. Even though the timing and location of future hazardous events cannot be determined, this can enable local planners and decision-makers to estimate the likely damages and assess the costs and benefits of disaster risk management strategies, including insurance or retrofitting buildings.[xiii]

4.5 Estimating risk scenarios using the Global Risk Model

As highlighted in section 4.2, local-level risk assessments provide the granularity required to inform disaster risk management strategies in cities and in other local administrative areas. However, in many parts of the world, particularly in low- and middle-income countries, the data infrastructure necessary to produce high-resolution models may not exist.

Simulations developed with the GRM show that despite its coarse grain resolution, it is possible to generate credible risk scenarios in these *blank areas* on the world map of risk and where modelled losses are within the order of magnitude of observed losses. Naturally there are always differences between the observed and modelled losses of particular events, given the idiosyncrasy of each disaster. However, as the following case studies show, in regions where local-level risk assessment is not possible, the GRM can be used to provide a robust first-level vision of risk.

Figure 4.7 Modeled distribution of damage in Lorca

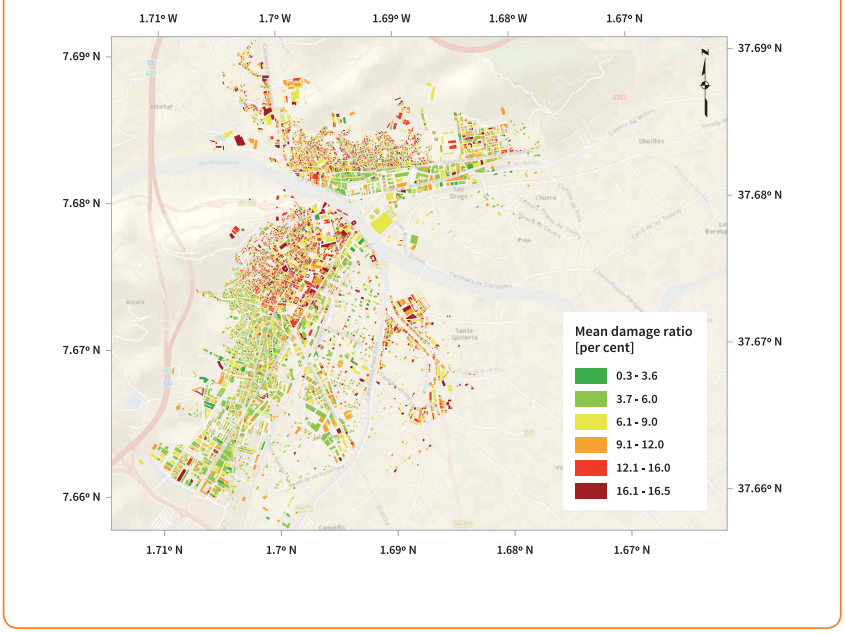

Source: Salgado-Gálvez et al. 2016c

The 2015 Nepal Earthquake

4.5.1 The April 2015 Nepal earthquake

The GRM was used to estimate direct economic losses and fatalities following the April 2015 Nepal earthquake[xiv]. Taking the characteristics of the earthquake[xv], five different hazard scenarios[xvi] based on previous seismic and risk assessments in Nepal[xvii] and the GRM vulnerability functions and exposure model (see Figure 4.8), estimates of both direct economic loss and mortality were generated. The results are not statistically significant given that the modelled estimates are being compared with a single observation. However, while mortality levels were overestimated, direct economic loss was in the same order of magnitude as the observed losses.

Mortality (limited to people inside buildings) was estimated by the GRM to be between 17,397 and 80,084, depending on the hazard scenario chosen and assuming a 60 per cent occupancy rate of buildings. This represented an overestimation, given that the observed mortality was reported as 8,857. Given that the earthquake occurred at 11:56 AM on a Saturday, many people, particularly in rural areas, would have been outside their homes and schools were closed. The 60 per cent occupancy rate, therefore, is likely to have been an overestimation.

The direct economic loss was estimated at between USD 2.2 and 6.8 billion, a figure that does not take into account the value of the cultural heritage damaged in the earthquake. This figure is much closer to the observed direct economic losses estimated at USD 10 billion by the Nepal Economic Forum[xviii], a figure that includes the value of infrastructure such as hydroelectric power stations, which is not considered in the modelled estimates.

The August 2016 Amatrice, Italy Earthquake

4.5.2 The August 2016 Amatrice, Italy Earthquake

On 24 August 2016 at approximately 3:36 AM, a magnitude 6.2 earthquake occurred in Italy. Following the earthquake, the GRM was used to model both mortality and economic loss, based on a similar procedure to that employed in Nepal but with only one hazard scenario[xix].

Figure 4.8 Exposed value in million USD in Nepal calculated using the exposure model of the GRM

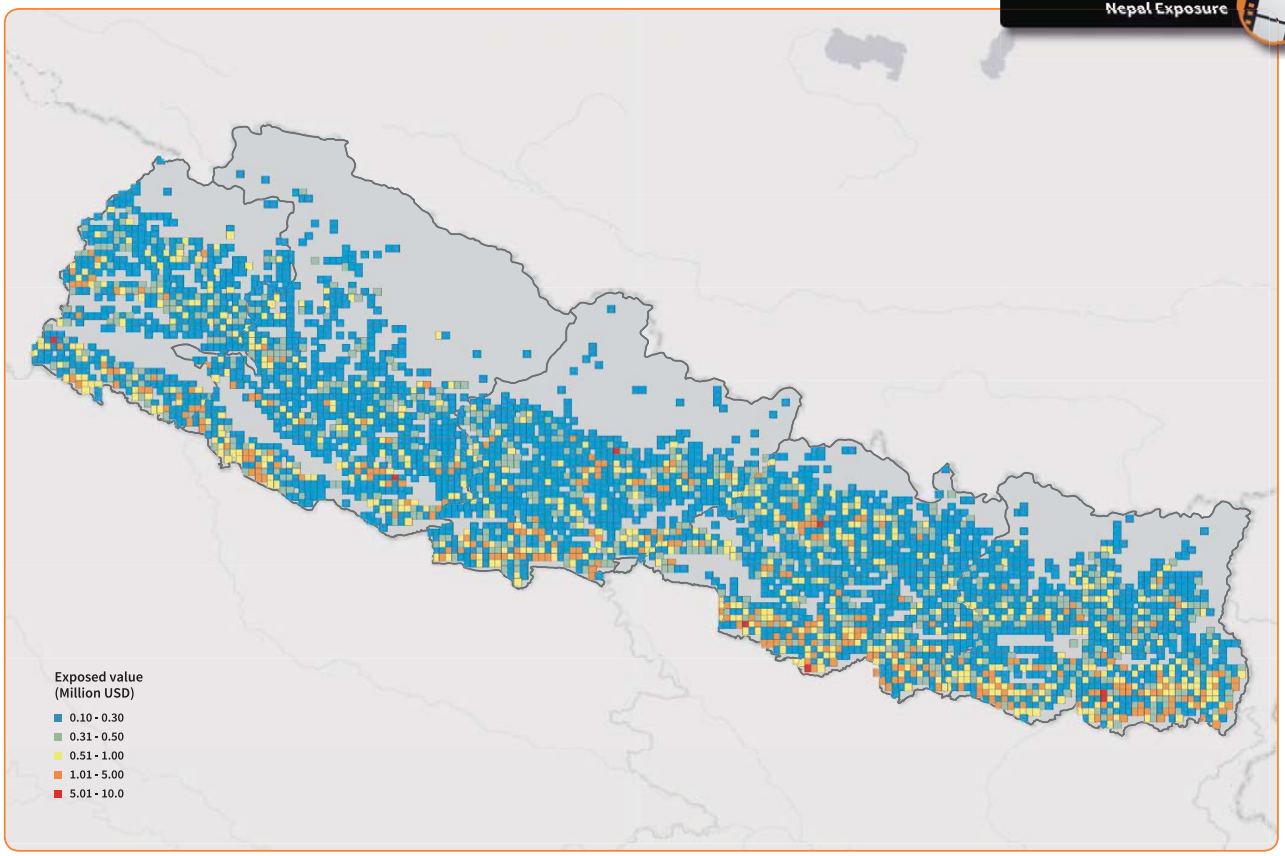

Source De Bono and Chatenoux 2014

The modelled direct economic losses were estimated at USD 3.3 billion, taking into account residential and non-residential buildings, while the mortality inside buildings was estimated at 241 people[xx].

The observed mortality was of 298 people, which is in the same order of magnitude as the modelled mortality. In the case of economic losses, those in the property insurance market have been estimated at around EUR 66 million[xxi]. However, the affected region had earthquake insurance penetration as low as 1 per cent by some estimates[xxii]. This implies that the real direct economic loss, including uninsured losses, may be in the same order of magnitude as the modelled estimates.

Hurricane Matthew

4.5.3
Estimating risk during an unfolding event: Hurricane Matthew, October 2016

Hurricane Matthew formed on 28 September 2016 as a tropical storm over the island of St. Lucia in the Caribbean. On 29 September it developed into a hurricane of Category 1 on the Saffir-Simpson scale, with a maximum wind speed of 92.6 km/h. On 1 October it reached Category 5 approximately 100 kilometers north of the Guajira Peninsula in Colombia, with a maximum wind speed of 260 km/h. It affected Haiti, Jamaica, Cuba, the Dominican Republic and the Bahamas as well as Florida, Georgia, South and North Carolina in the United States of America.

During the build-up of the hurricane the GRM was used to forecast where potential losses could occur as it moved forward[xxiii]. Five different loss estimations were produced at different points in time.

The first two estimations were produced on 4 October, when Matthew was approaching the east coast of Cuba as a Category 4 hurricane. They were based on two scenarios of the hurricane track recorded to date and the forecast for the next five days by the National Hurricane Center. Subsequent estimations were produced on 7 October, when Matthew was moving along the east coast of Florida as a Category 3 hurricane, again based on National Hurricane Center real and forecast tracks. The last estimation was performed on 10 October for Matthew's real total track.

Figure 4.9 Modelled direct loss associated with Hurricane Matthew computed on a) 4 October, b) 7 October and c) 10 October

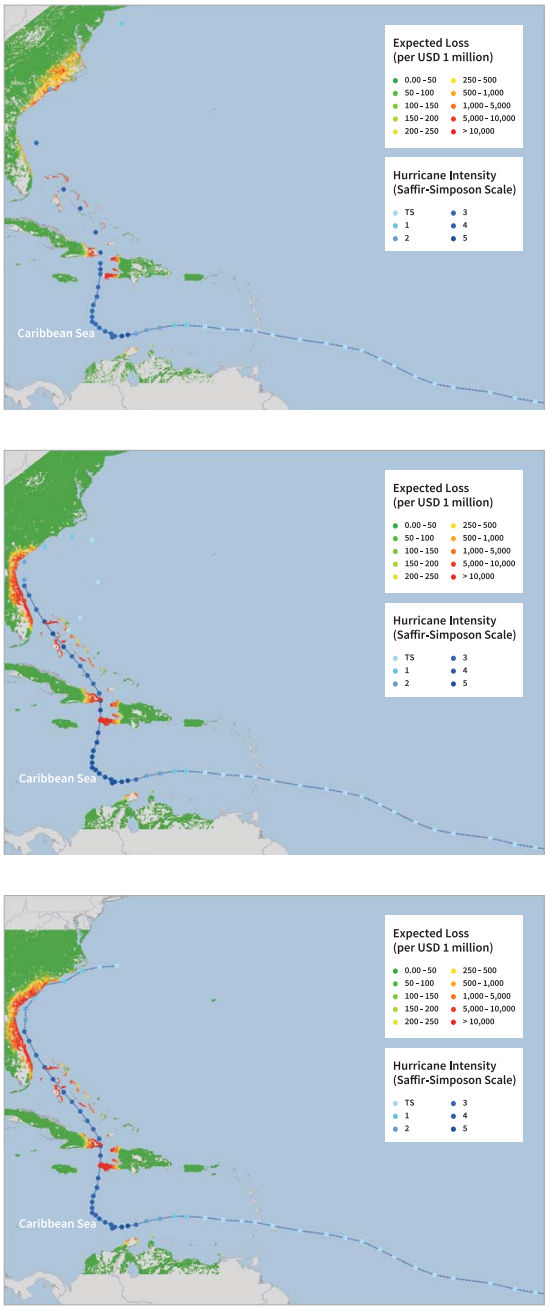

Source: Ingeniar Ltda 2016

Figure 4.9 shows that economic losses along the hurricane's path and forecast were modelled at USD 17 billion in the first estimate, USD 20 billion in the second and USD 26 billion in the final estimate. This compared with insured losses estimated at between USD 1.5 and 5 billion in the United States of America and between USD 1 and 3 billion in the Caribbean[xxiv]. These differences are significant. However, if uninsured losses are accounted for, particularly in the Caribbean, the total losses may be closer to the modelled figures.

i. IPCC 2014

ii. Cardona et al. 2015

iii. Brown et al. 2015

iv. Bear Crozier. et al. 2014, Cardona, et al. 2015

v. UNISDR 2015b

vi. UNISDR 2013

vii. For example, a loss with an exceedance rate of 0,1 means there is a 10per cent probability of that loss being exceeded in a year (or 10-year return period). A loss with an exceedance rate of 10 means there is probability of it being exceeded 10 times in a year.

viii. Velásquez et al. 2014

ix. DesInventar, disaster loss databases (UNISDR)

x. Bernal and Cardona 2011

xi. Bernal 2010

xii. Salgado-Gálvez et al. 2016c and Cardona et al. 2015

xiii. It is important to note that a mapping of the results from the model by building is misleading as the simulated results represent mean values and do not provide an exact prediction of expected losses for each building. Results should always be grouped in categories such as building classes, neighbourhoods, districts etc.

xiv. Salgado-Gálvez 2015

xv. http://earthquake.usgs.gov/earthquakes/eqarchives/poster/2015/20150425.pdf

xvi. Using different Ground Motion Prediction Equations

xvii. Chaulagain et al. 2015

xviii. http://www.nepaleconomicforum.org/news/news.php?n=99

xix. Ground Motion Prediction Model: Cauzzi and Faccioli 2008

xx. Salgado-Gálvez et al. 2016d

xxi. http://www.artemis.bm/blog/2016/11/24/perils-almost-doubles-italy-quake-loss-estimate-to-eur66m/

xxii. http://www.royalgazette.com/re-insurance/article/20160901/reinsurers-face-up-to-166m-italy-quake-loss

xxiii. Ingeniar Ltda 2016

xxiv. https://www.rms.com/newsroom/press-releases/press-detail/2016-10-21/rms-estimates-hurricane-matthew-insured-losses-for-the-us-will-be-between-15-billion-and-5-billion

Section 5

Probabilistic hazard and risk assessment methodology

Given its global scale and coarse grain resolution, the GRM uses simplified hazard and exposure models, developed and tested using a robust methodology in the context of a fully probabilistic risk assessment. The risk assessment process can be divided into four steps: probabilistic hazard assessment, development of exposure databases, development of damage and loss (vulnerability) functions, and loss assessment.

Each specific hazard was represented by a set of simulated events that provide information about all the possible ways in which the hazard may manifest in the region under analysis. This allowed for a probabilistic representation of the hazard where not only the expected value and the dispersion are provided for the geographical distribution for each hazard intensity (e.g. wind speed, acceleration, water depth) but also the frequency of occurrence.

The development of the exposure databases required two complementary stages: identification, followed by characterisation of the exposed assets. The first refers to the selection of the assets to be included and their location, whereas the second refers to the assigning of relevant parameters to these assets, such as structural characteristics and economic value. The structural characteristics assigned to each asset included in the exposure database determined the physical vulnerability.

Physical vulnerability relates the hazard intensities with the expected damages and, therefore, losses of the exposed elements. Vulnerability functions were selected for each region, allowing for a quantitative, continuous and probabilistic representation of physical vulnerability by characterising the capacity of each asset during the occurrence of hazardous events. A unique vulnerability function was assigned to each structural class and for each hazard.

A convolution between hazard and vulnerability (note that exposure is implicitly associated to the latter) was performed. It was then expressed in terms of the potential damages and losses on a set of exposed elements in a given period, resulting from hazardous events with different intensities and origin and the level of susceptibility to damage of those elements to the hazard intensities (vulnerability).

5.1 Probabilistic hazard analysis

5.1.1 Probabilistic seismic hazard analysis

Firstly, the earth was divided in more than 400 seismic provinces (see Figure 5.1). Seismicity patterns within each region are assumed to be uniform. The recurrence frequencies were obtained for each of those provinces by using instrumental data from openly available databases (NEIC-USGS and ISC-GEM), later classified as a function of their location and depth. Seismicity parameters were estimated using a smoothed seismicity approach[i]. Finally, a strong ground motion attenuation relationship and a maximum magnitude were assigned to each province.

The seismic hazard was calculated using the CRISIS2014 programme[ii], a module of the CAPRA Platform, which is a well-known, globally-accepted tool for the seismic hazard calculation. The output was a set of more than 1.1 million simulated earthquakes. Results were obtained for a range of different heights of buildings in order to take into account the seismic performance of buildings with different characteristics in the risk assessment stage. The probabilistic integration of the hazard intensities associated with these simulated events, together with their frequency of occurrence, then allowed the development of seismic hazard maps (Maps 5.1 – 5.7)[iii].

A more detailed description on the seismic hazard modelling methodology can be found in Cardona et al. (2014, 2015).

Figure 5.1 Seismic provinces

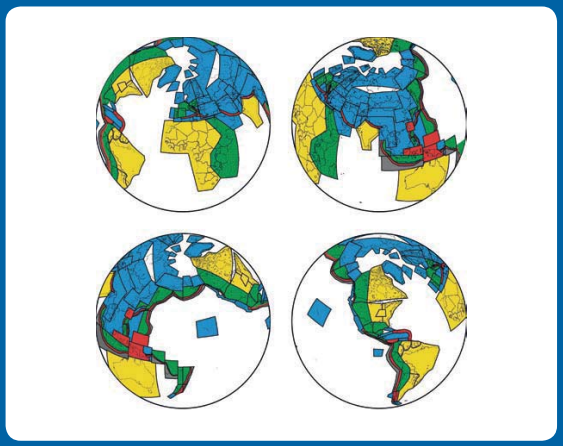

Source: Cardona et al. 2013, Ordaz et al. 2014b

Map 5.1 Global seismic hazard (0.5s 475 years return period)

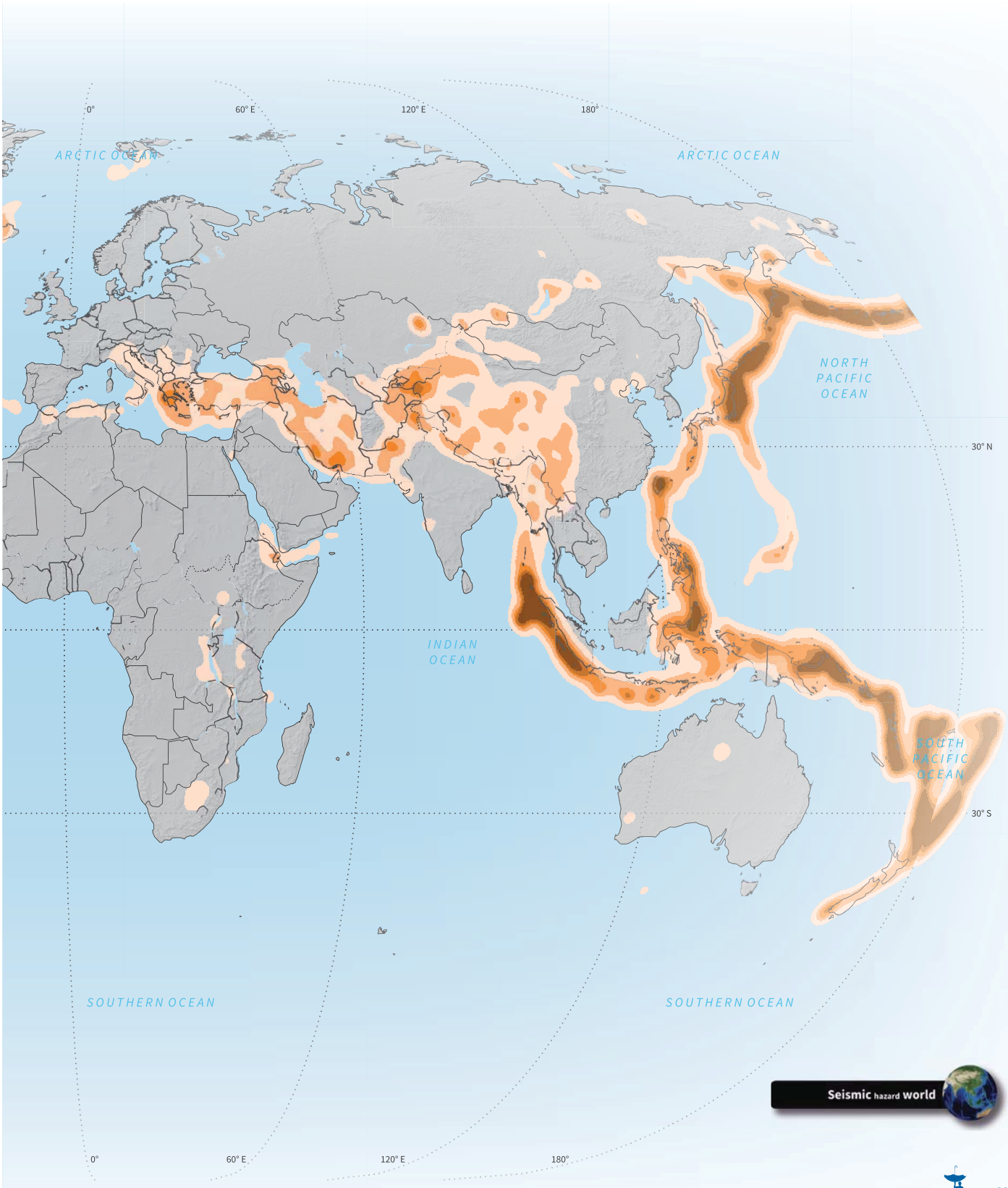

Seismic hazard world

Map 5.2 Seismic hazard-East Asia and the Pacific (0.5s 475 years Return period)

Map 5.3 Seismic hazard-Europe and Central Asia (0.5s 475 years Return period)

Map 5.4 Seismic hazard-Latin America and the Caribbean (0.5s 475 years Return period)

Map 5.5 Seismic hazard-Middle East and North Africa (0.5s 475 years Return period)

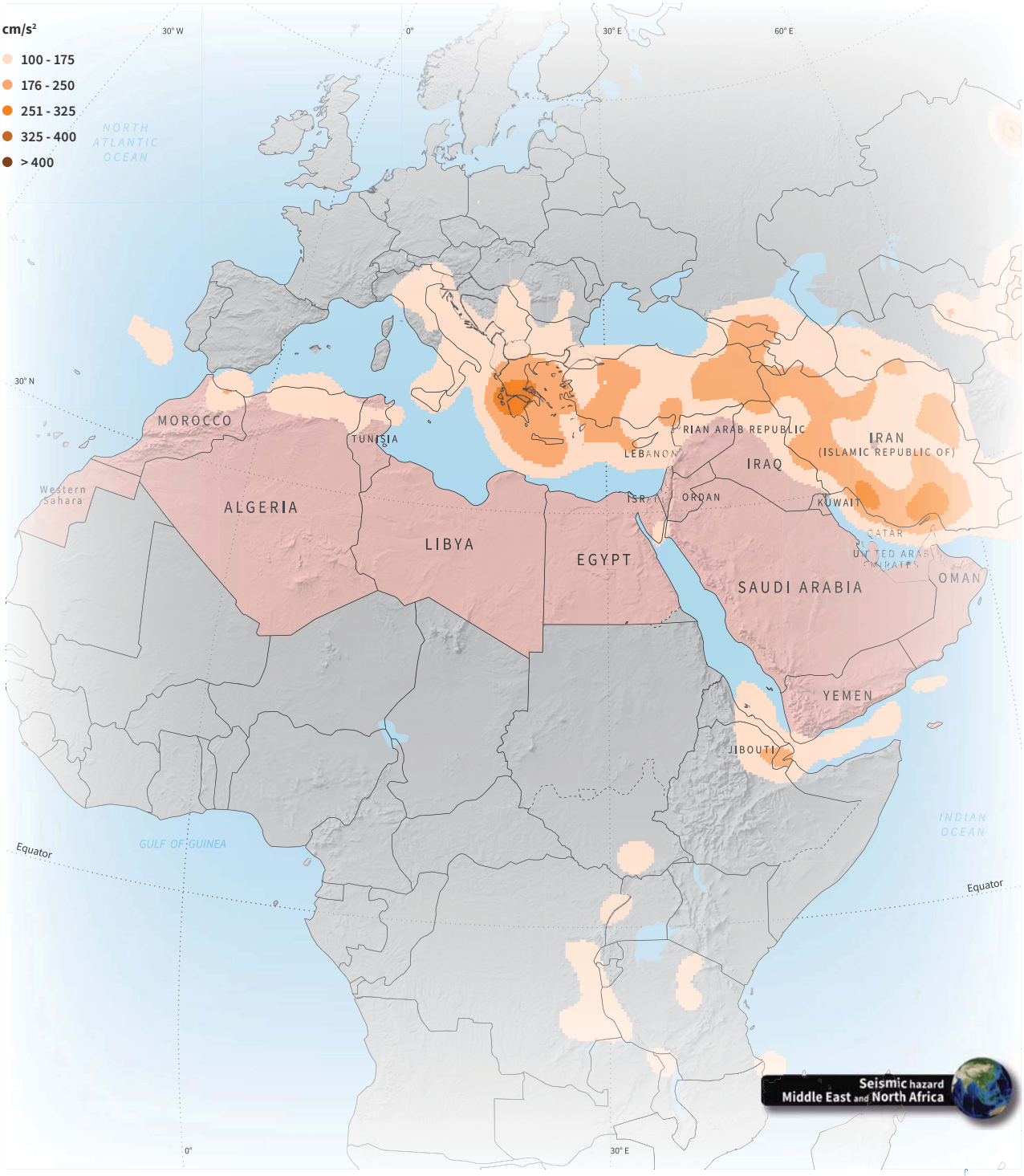

Map 5.6 Seismic hazard- North America (0.5s 475 years Return period)

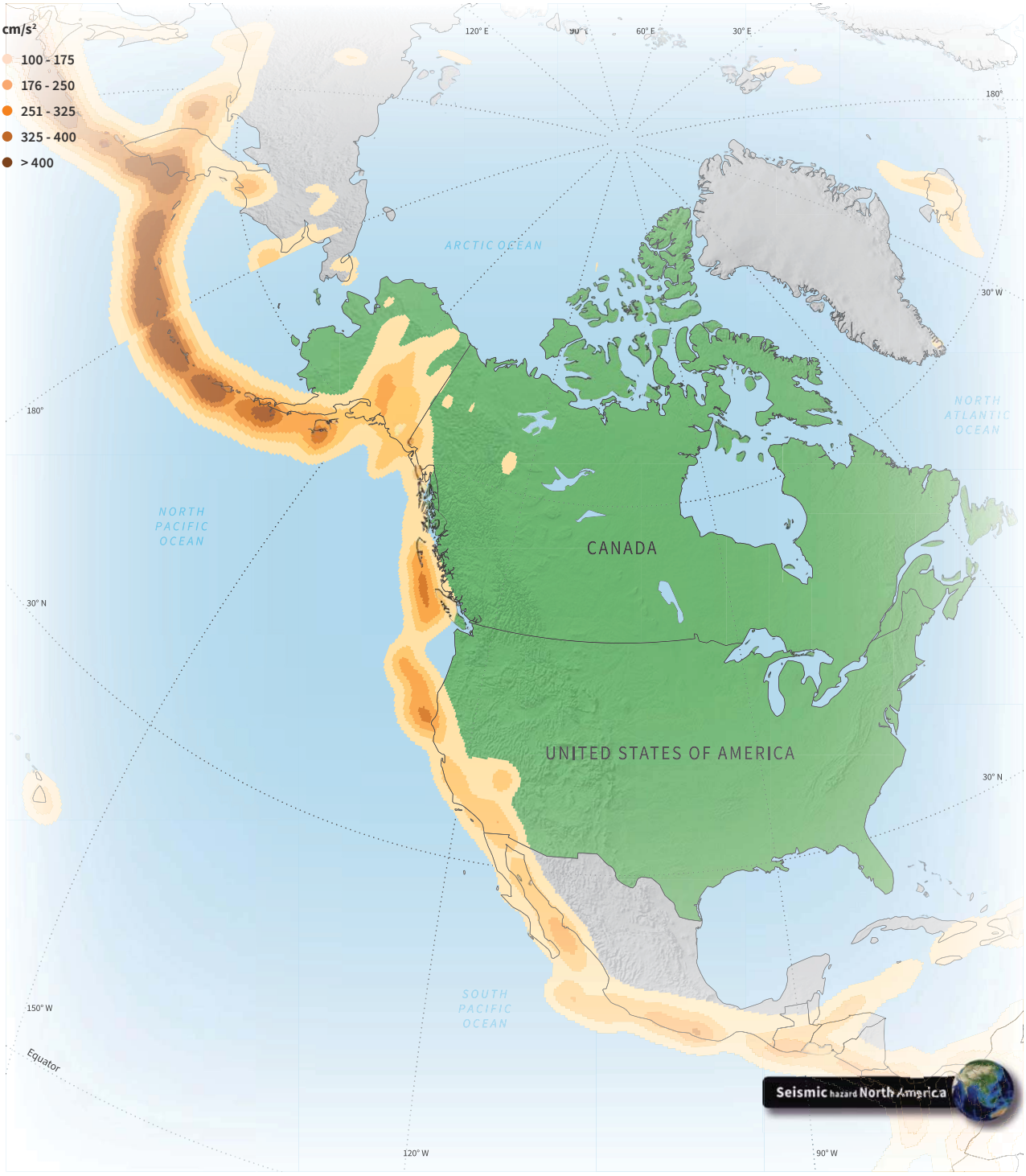

Map 5.7 Seismic hazard- South Asia (0.5s 475 years Return period)

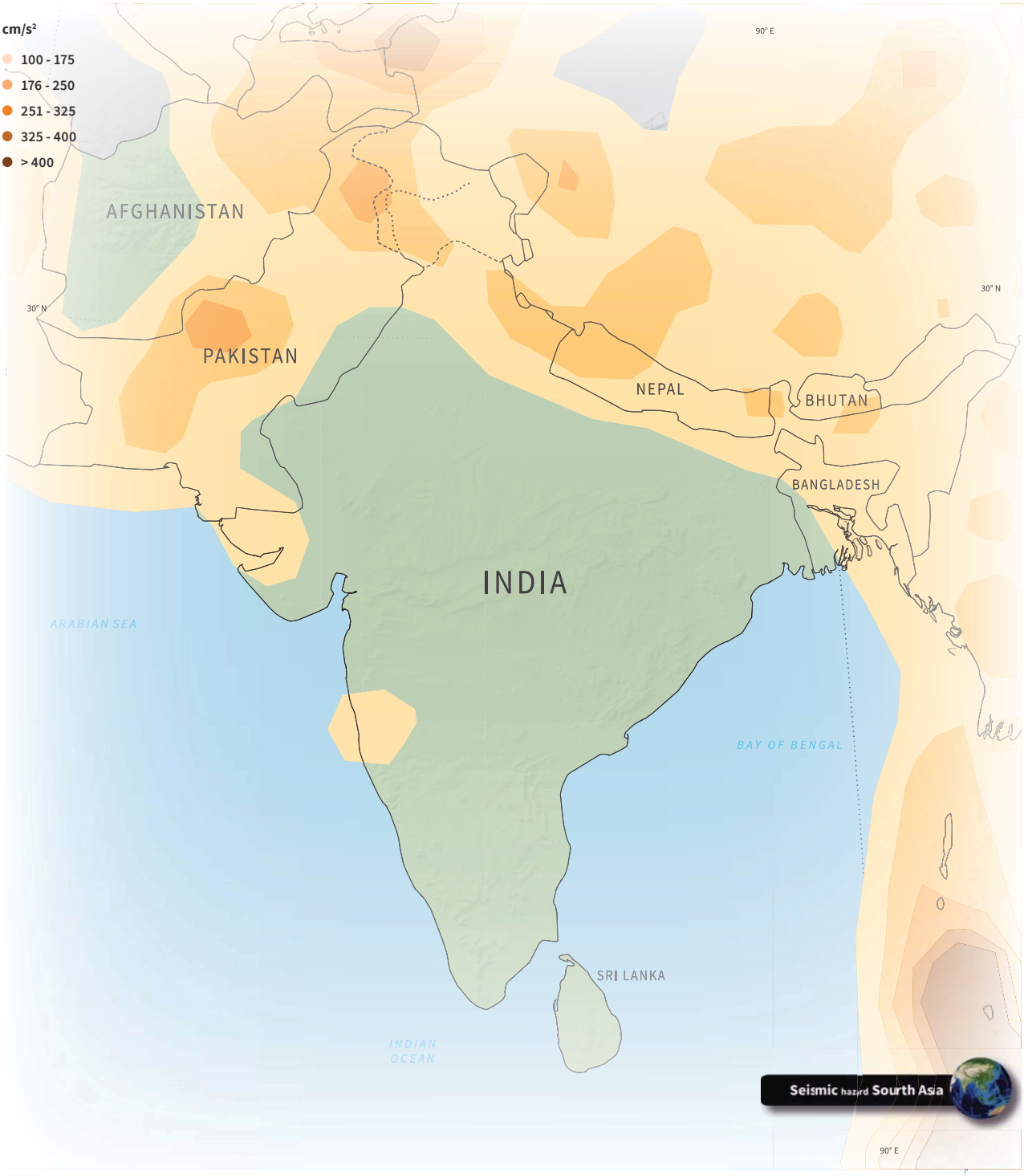

Map 5.8 Seismic hazard- Sub-Saharan Africa (0.5s 475 years Return period)

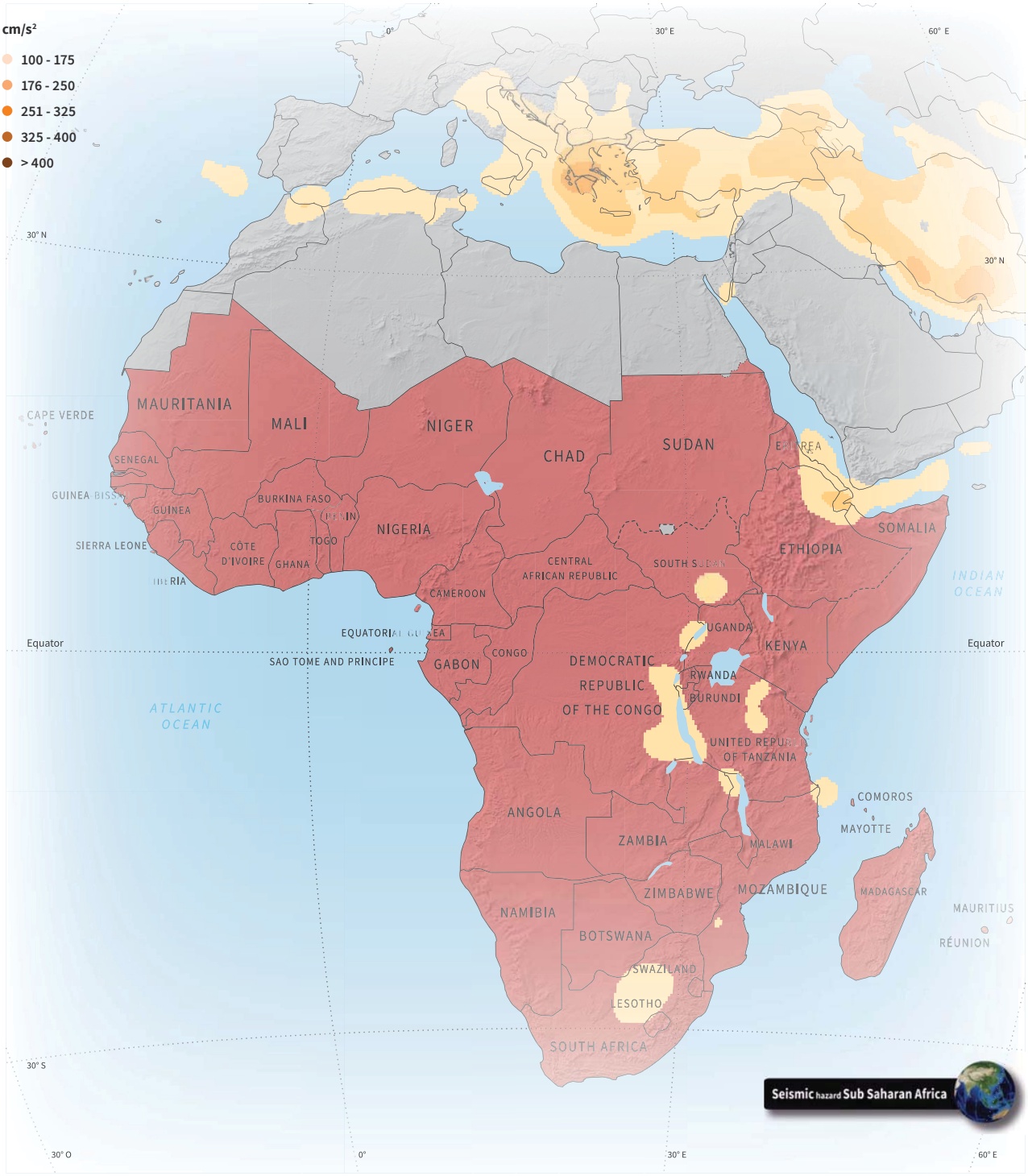

5.1.2 Probabilistic tsunami hazard analysis

For the probabilistic tsunami hazard analysis, different tsunami sources were defined as shown in Figure 5.2 based on the definition of openly-available subduction zones. Each source was divided into smaller sub-faults for which seafloor deformations were calculated. For each source, a synthetic earthquake catalogue of events was generated for magnitudes higher than 7.85. For each earthquake event in the catalogue, the tsunami was propagated from the source to each entry of the exposure database, estimating the maximum water level. The maximum water level was defined based on the sum of the waves from all the individual sub-faults involved in the event. Finally, the tsunami waveforms were synthesized for any slip distribution by summing the individual sub-fault tsunami waveforms (weighted by their slip).

The probabilistic integration of the hazard intensities (run-up height) associated with these events together with their occurrence frequency enabled the development of tsunami hazard maps.

More details about the tsunami hazard analysis methodology can be found in NGI – Norwegian Geotechnical Institute and GA – Geoscience Australia (2014) and Løvholt et al. 2015.

Figure 5.2 Subduction zones considered in the probabilistic tsunami hazard analysis

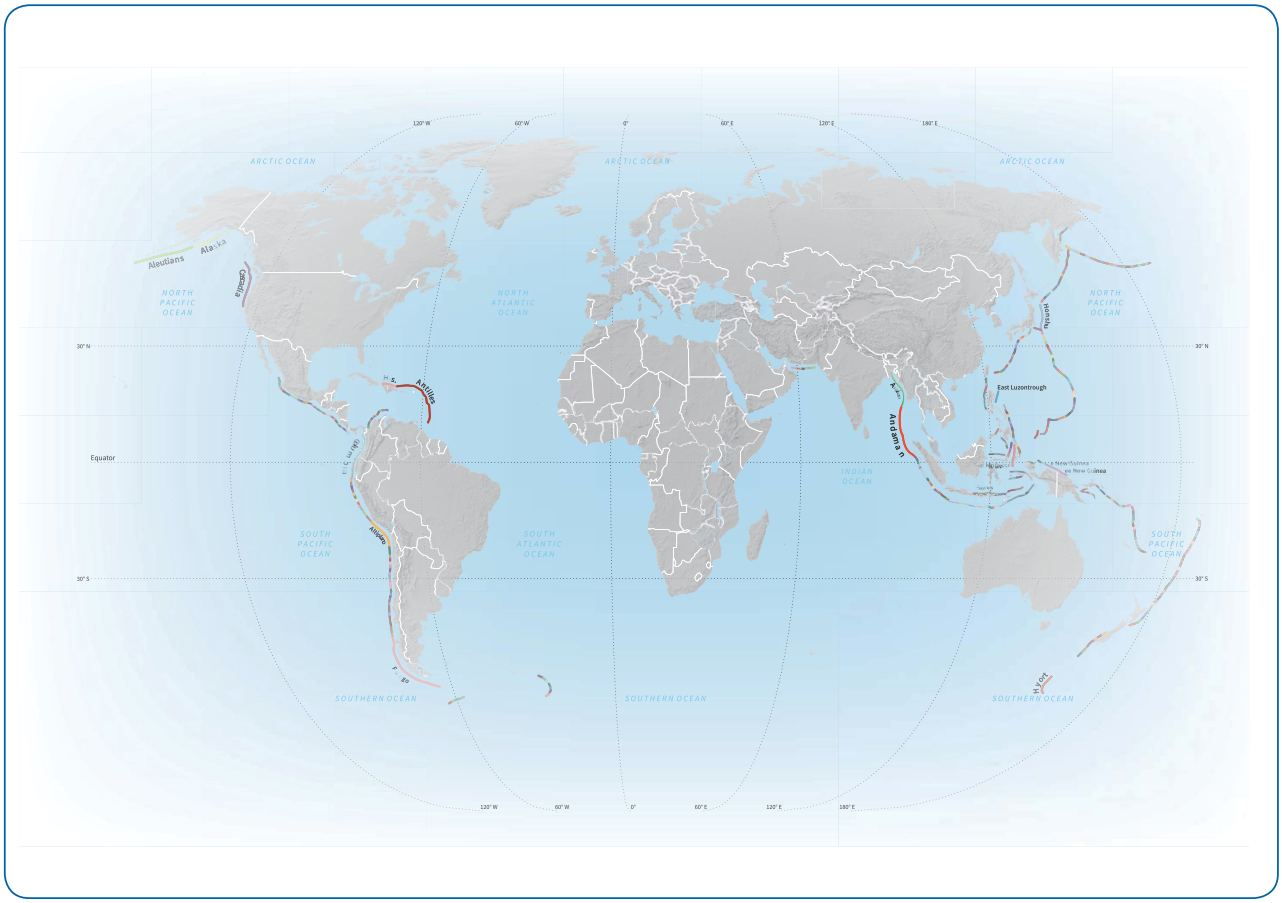

Source: NGI – Norwegian Geotechnical Institute and GA – Geoscience Australia (2014)

Map 5.9 Global tsunami hazard (Run-up height 475 years return period)

Tsunami hazard world

Map 5.10 Tsunami hazard-East Asia and the Pacific (Run-up height 475 years return period)

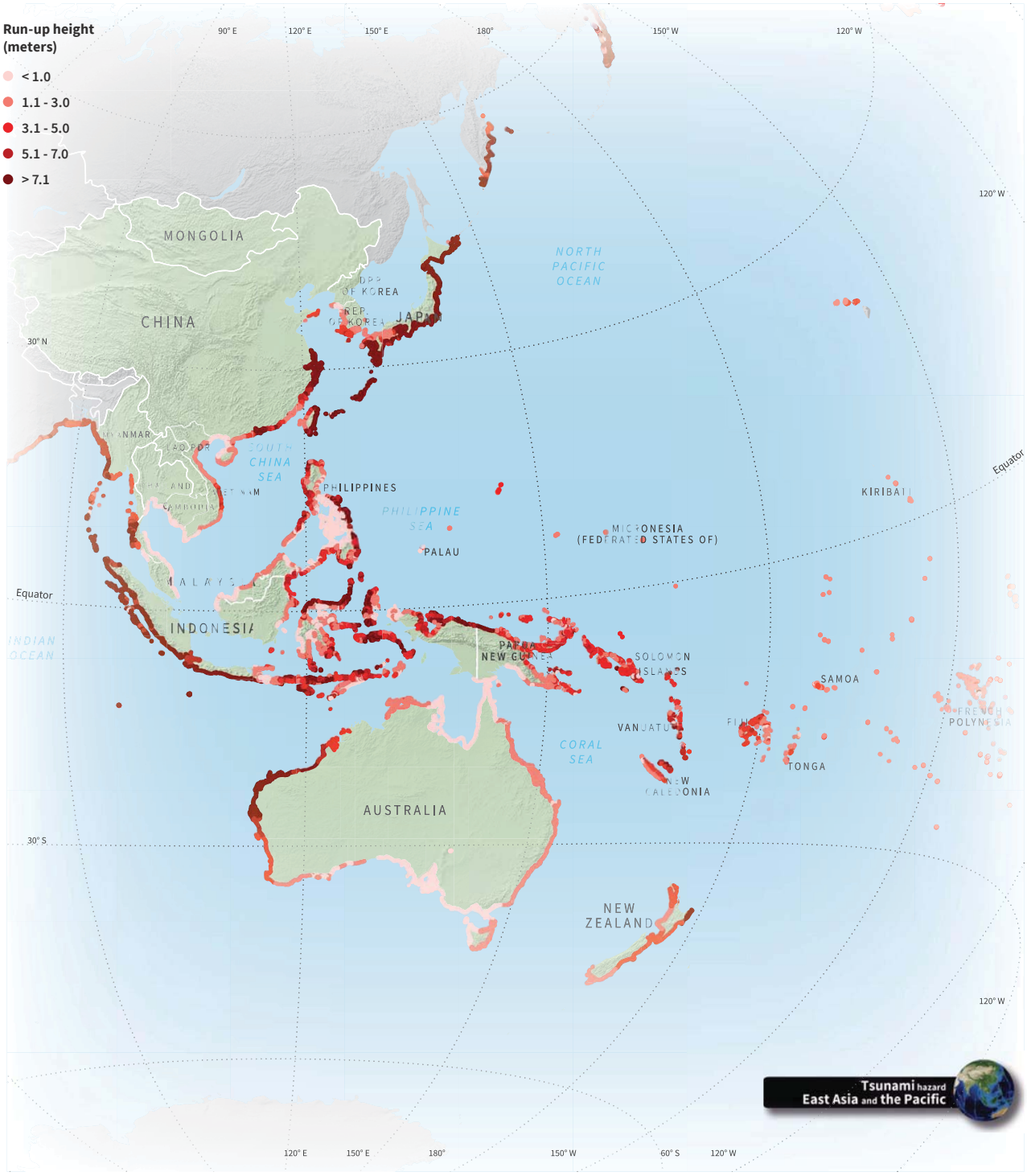

Map 5.11 Tsunami hazard-Europe and Central Asia (Run-up height 475 years return period)

Map 5.12 Tsunami hazard-Latin America and The Caribbean (Run-up height 475 years return period)

Map 5.13 Tsunami hazard-Middle East and North Africa (Run-up height 475 years return period)

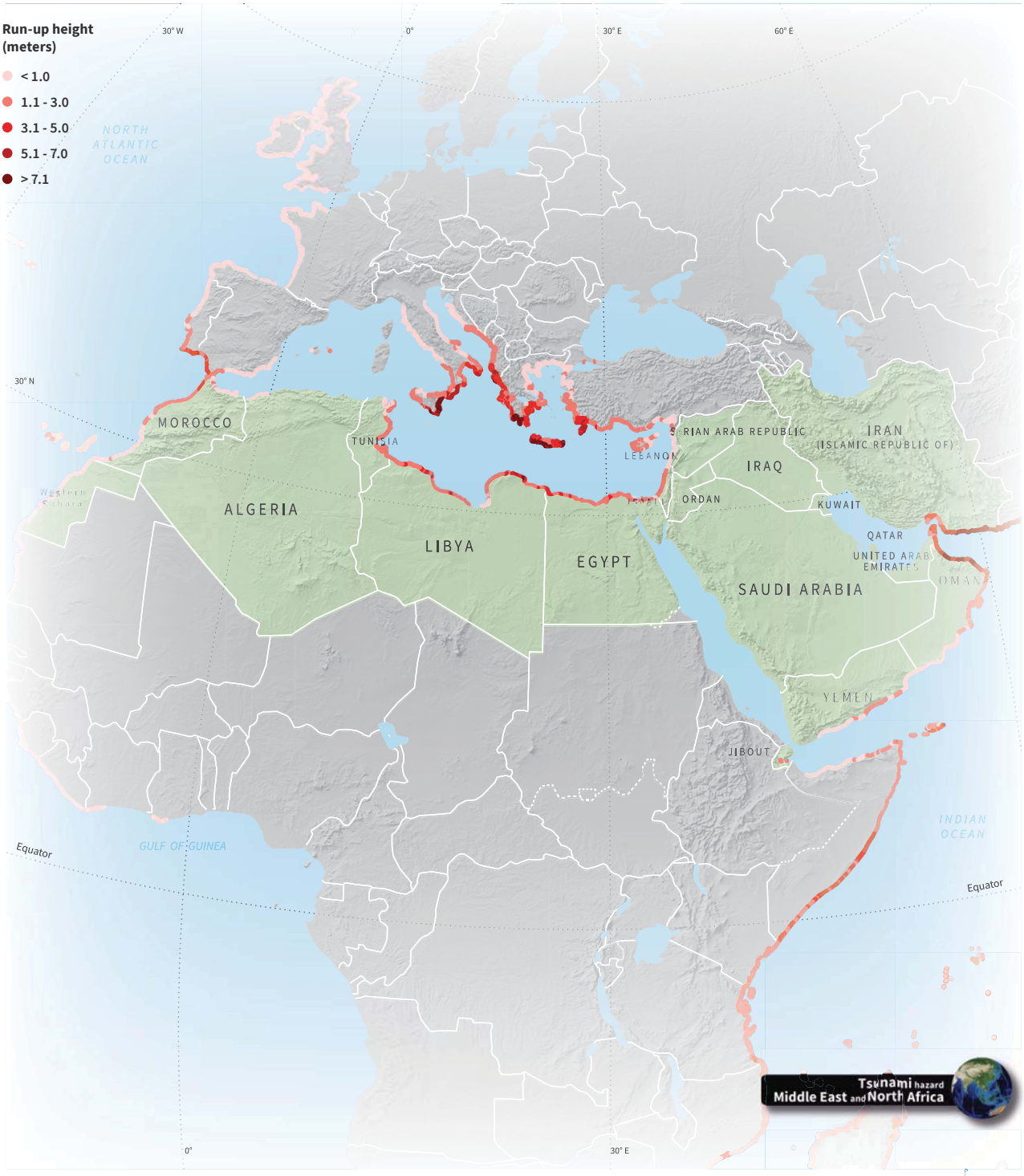

Map 5.14 Tsunami hazard-North America (Run-up height 475 years return period)

Map 5.15 Tsunami hazard-South Asia (Run-up height 475 years return period)

Map 5.16 Tsunami hazard-Sub-Saharan Africa(Run-up height 475 years return period)

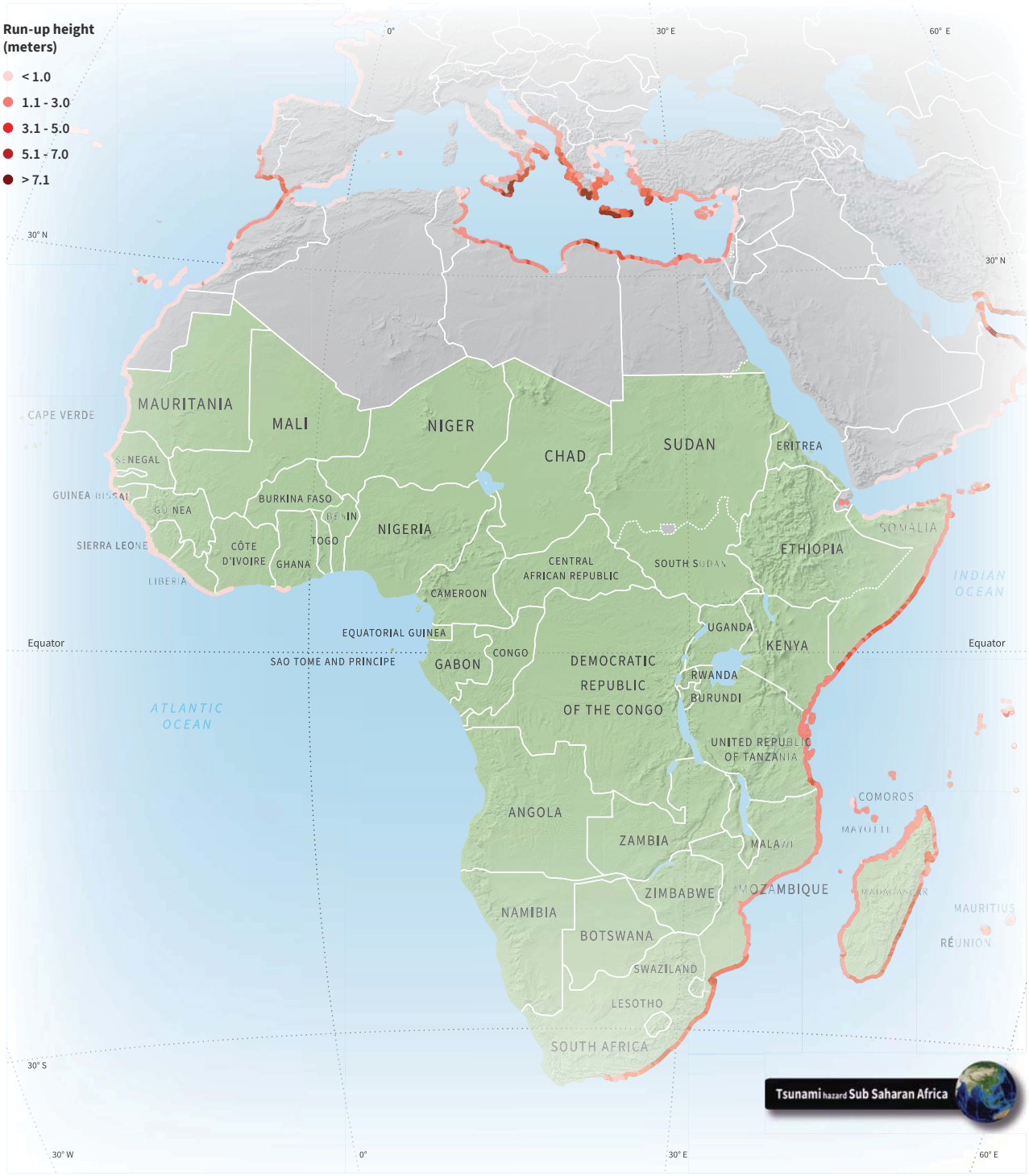

5.1.3 Probabilistic tropical cyclonic wind and storm surge hazard analysis

The probabilistic cyclonic wind and storm surge hazards analysis is based on the historical frequency of occurrence and intensity of tropical cyclones in different oceanic basins. This data was obtained from the IBTrACS database[iv], whereas parameters such as the surface roughness, topographic effects and bathymetry, also considered in the hazard modelling, were obtained from the most complete and openly available international databases[v]. For wind hazard modelling, the first two parameters are considered given that they significantly modify the wind speed at local level, while for storm surge hazard modelling, the parameters were topographic effects and bathymetry.

From each historical cyclone track, artificial disturbances were generated to create 100 "child tracks". Each point on the child track has the same central pressure and sustained wind speed as its original historical track, assuming that the cyclone's main characteristics remain unaltered. Using the hazard intensities for each of the child tracks, the expected value and the dispersion for the geographical distribution of the wind speed are obtained for each simulated event.

In the case of storm surge modelling, a mean sea level was assumed for each shore location for all the child tracks. The total run-up height at each shore location as a consequence of strong winds and lower atmospheric pressure was modelled by considering the wind-forced run-up height and the barometric run-up. Astronomic tides were not considered in the analysis, given the global nature of the assessment. The wind and storm surge hazard was calculated using the Tropical Cyclones Hazard Model programme[vi], the cyclonic hazard module of the CAPRA Platform, which uses a widely-accepted approach. The output of the assessment was a set of 2,594 simulated events for five different oceanic basins (Northeast Pacific, Northwest Pacific, South Pacific, North Indian, South Indian and North Atlantic) which were later used for the probabilistic wind and storm surge risk assessment.

The probabilistic integration of the hazard intensities associated with these events, together with their occurrence frequency, was used to develop cyclonic hazard maps. The results are expressed in terms of the geographical distribution of the sustained wind speed of three-second gusts (the average wind speed measured over an interval of three seconds), for strong winds, and for storm surge, as the distribution along the shorelines of the maximum surge run-up and its associated flooding. Tropical cyclone hazard maps for Middle East and North Africa, and Europe and Central Asia regions are not included since hazard intensities are very low at those locations

Complete details on the probabilistic wind and storm surge hazard methodology can be found in Cardona et al. (2014, 2015).

Map 5.17 Global tropical cyclonic wind hazard (wind speed 100 years return period)

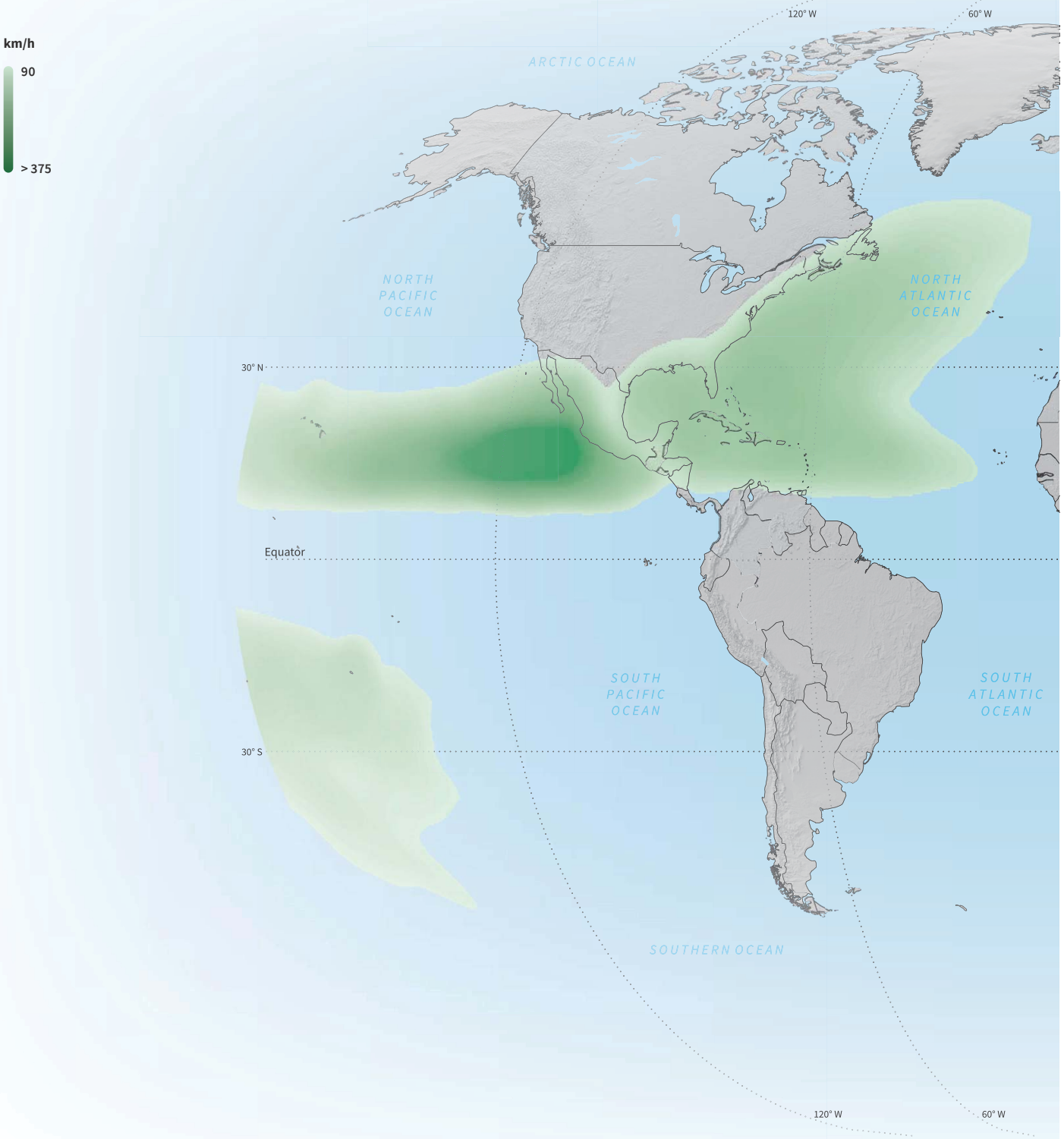

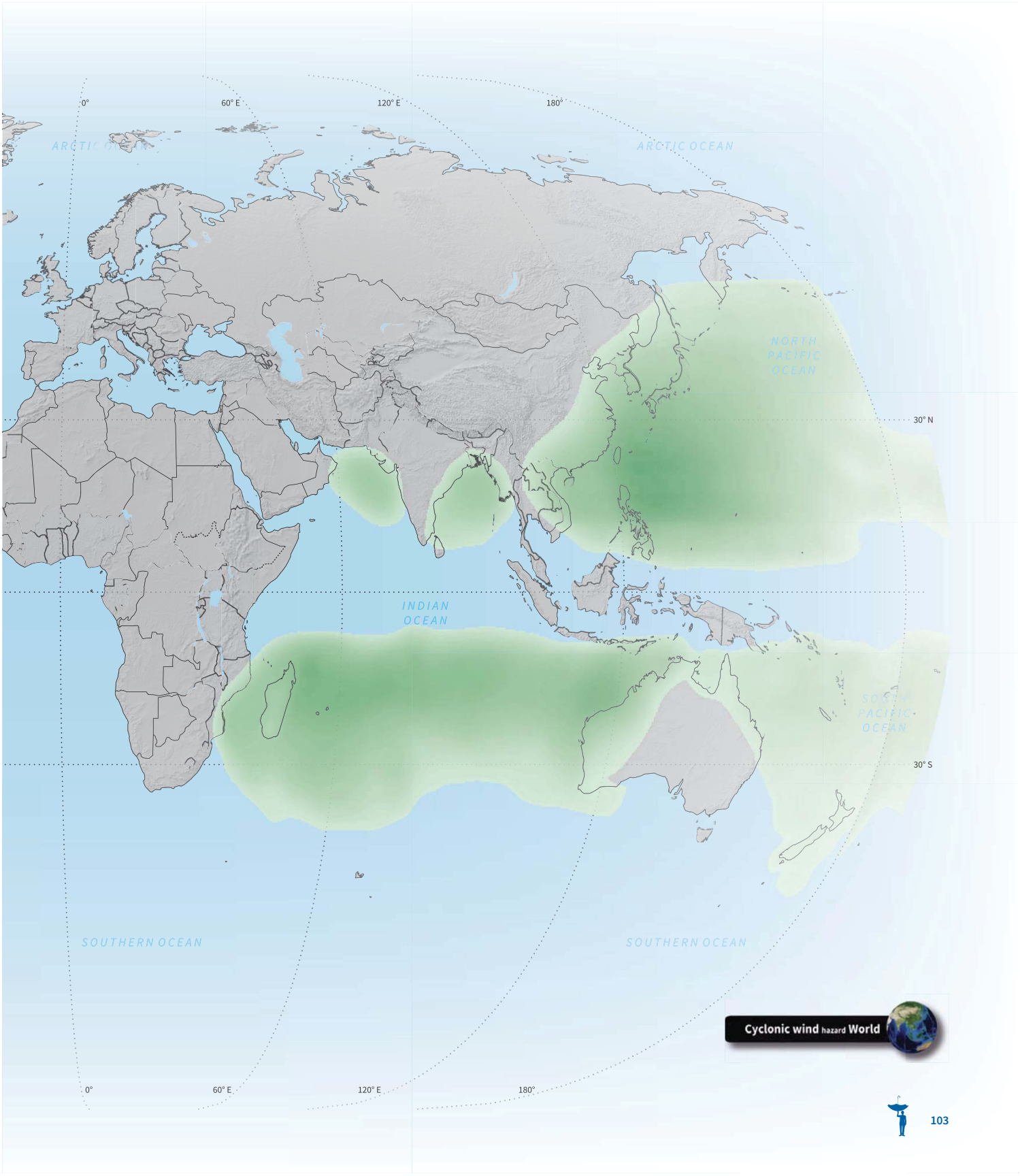

Cyclonic wind hazard World

Map 5.18 Global tropical cyclones - storm surge hazard (Run-up height 100 years return period)

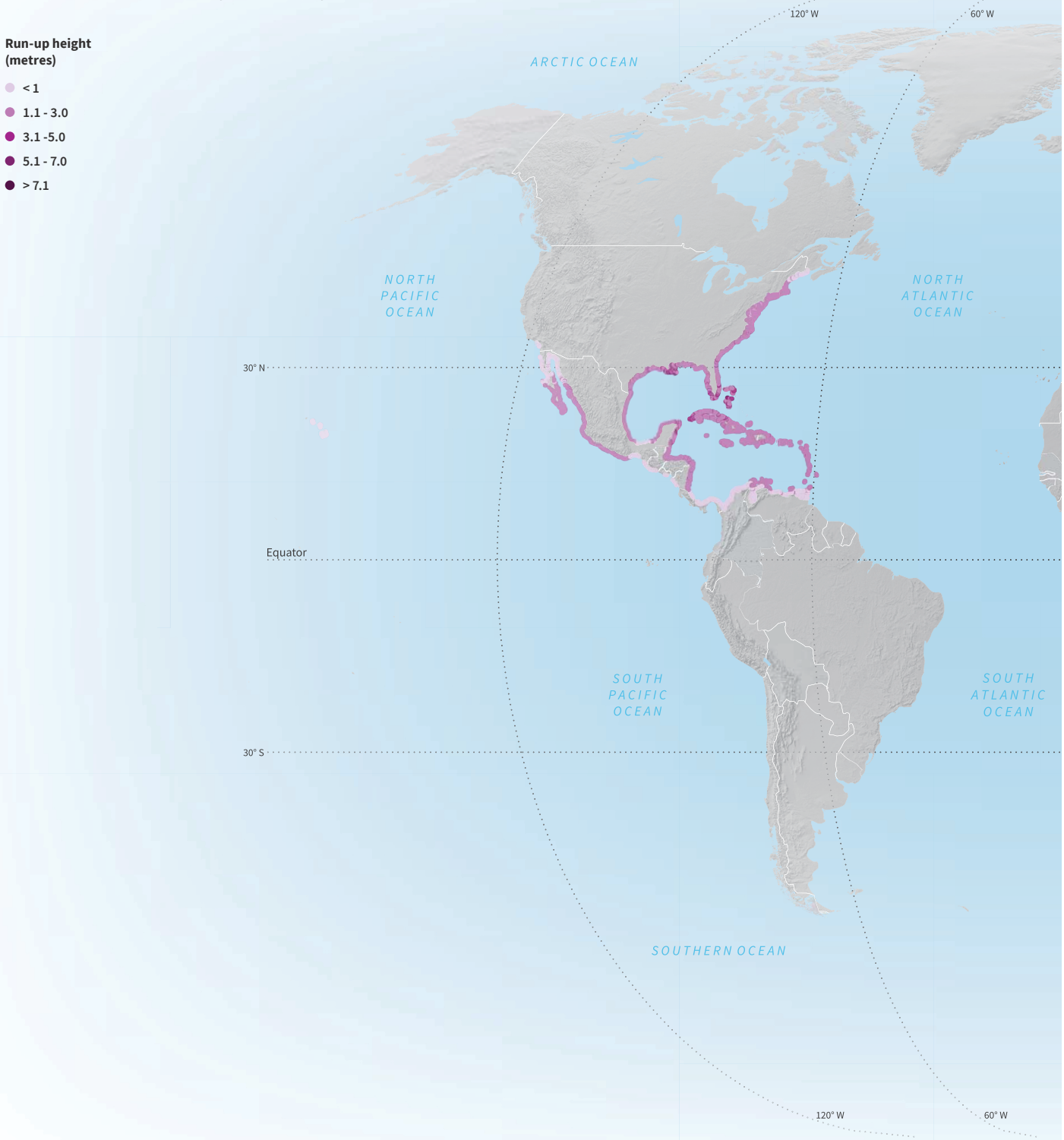

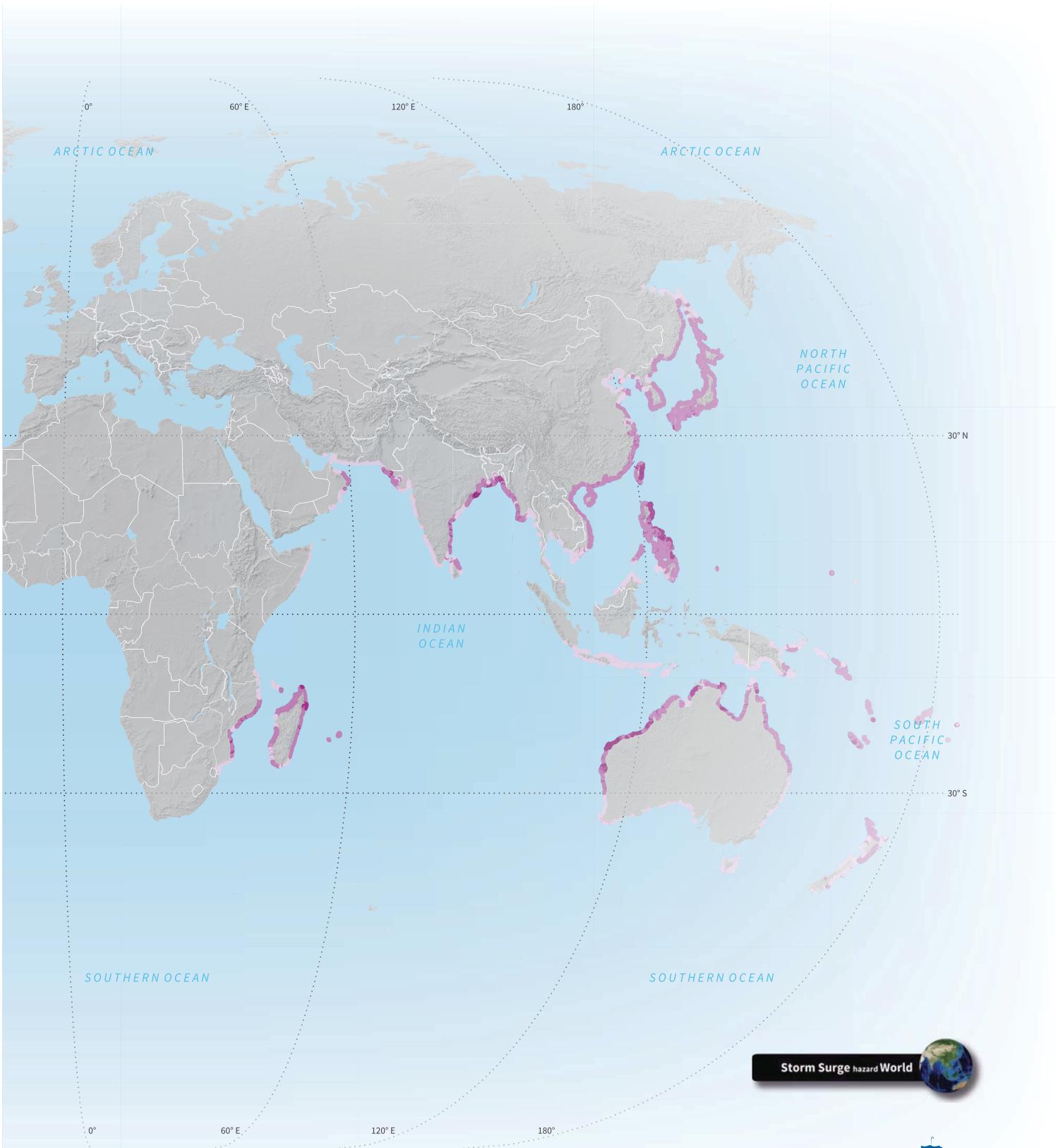

Storm Surge hazard World

Map 5.19 Cyclonic wind hazard East Asia and the Pacific (wind speed 100 years return period)

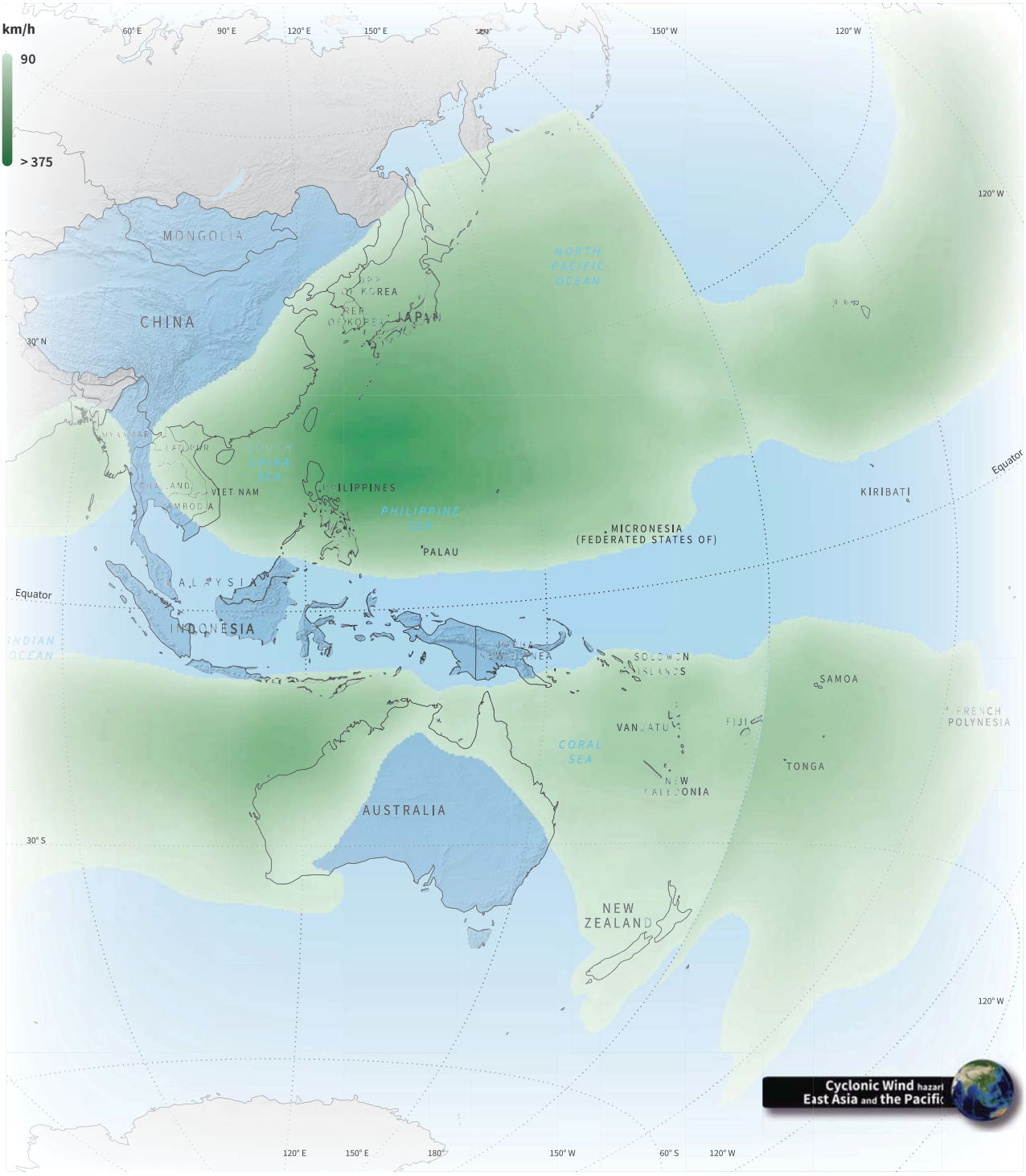

Map 5.20 Tropical cyclones (Storm surge) hazard-East Asia and the Pacific (Run-up height 100 years return period)

Map 5.21 Cyclonic wind hazard Latin America and the Caribbean (wind speed 100 years return period)

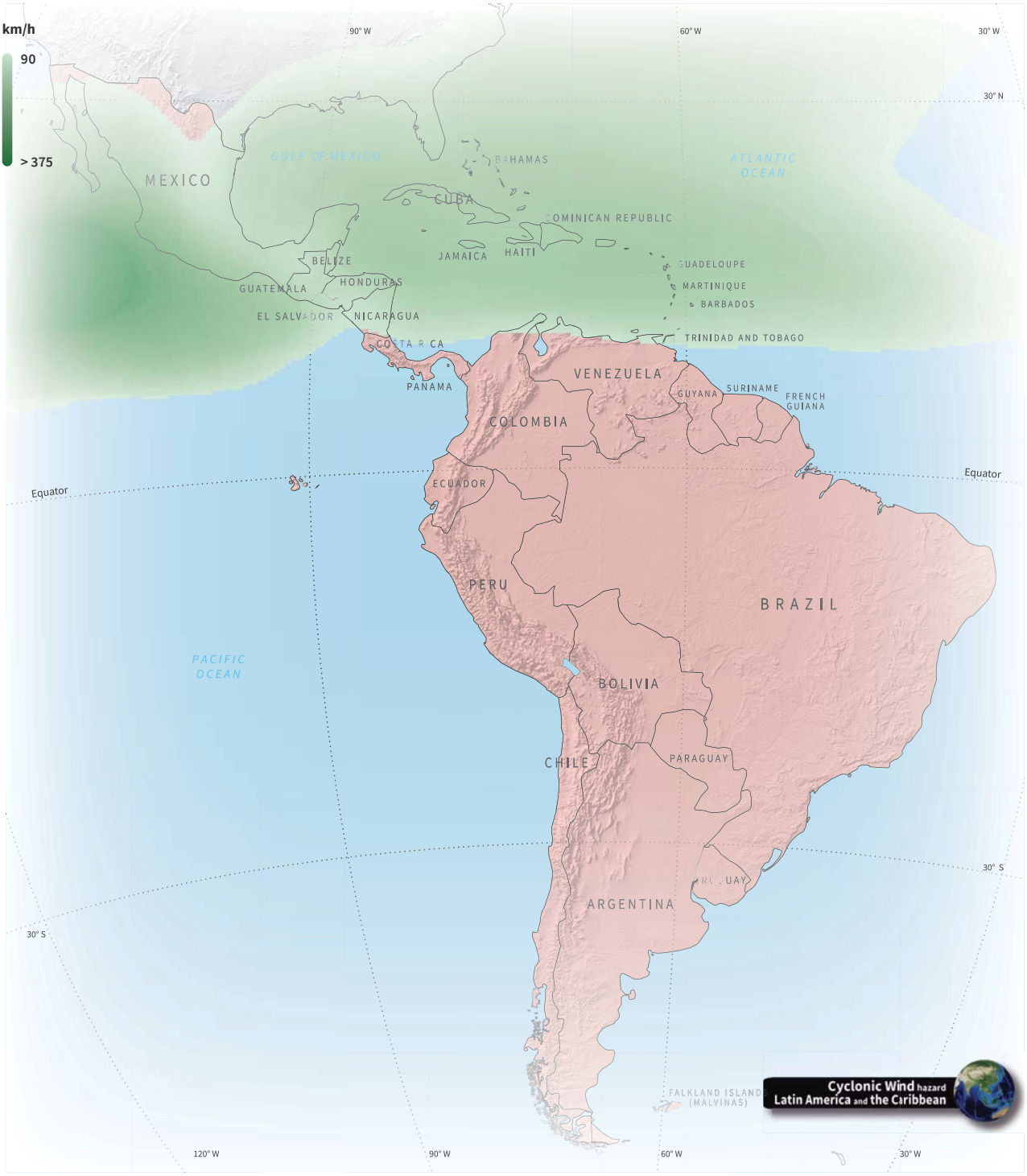

Map 5.22 Tropical cyclones (Storm surge) hazard-Latin America and the Caribbean (Run-up height 100 years return period)

Map 5.23 Cyclonic wind hazard North America (wind speed 100 years return period)

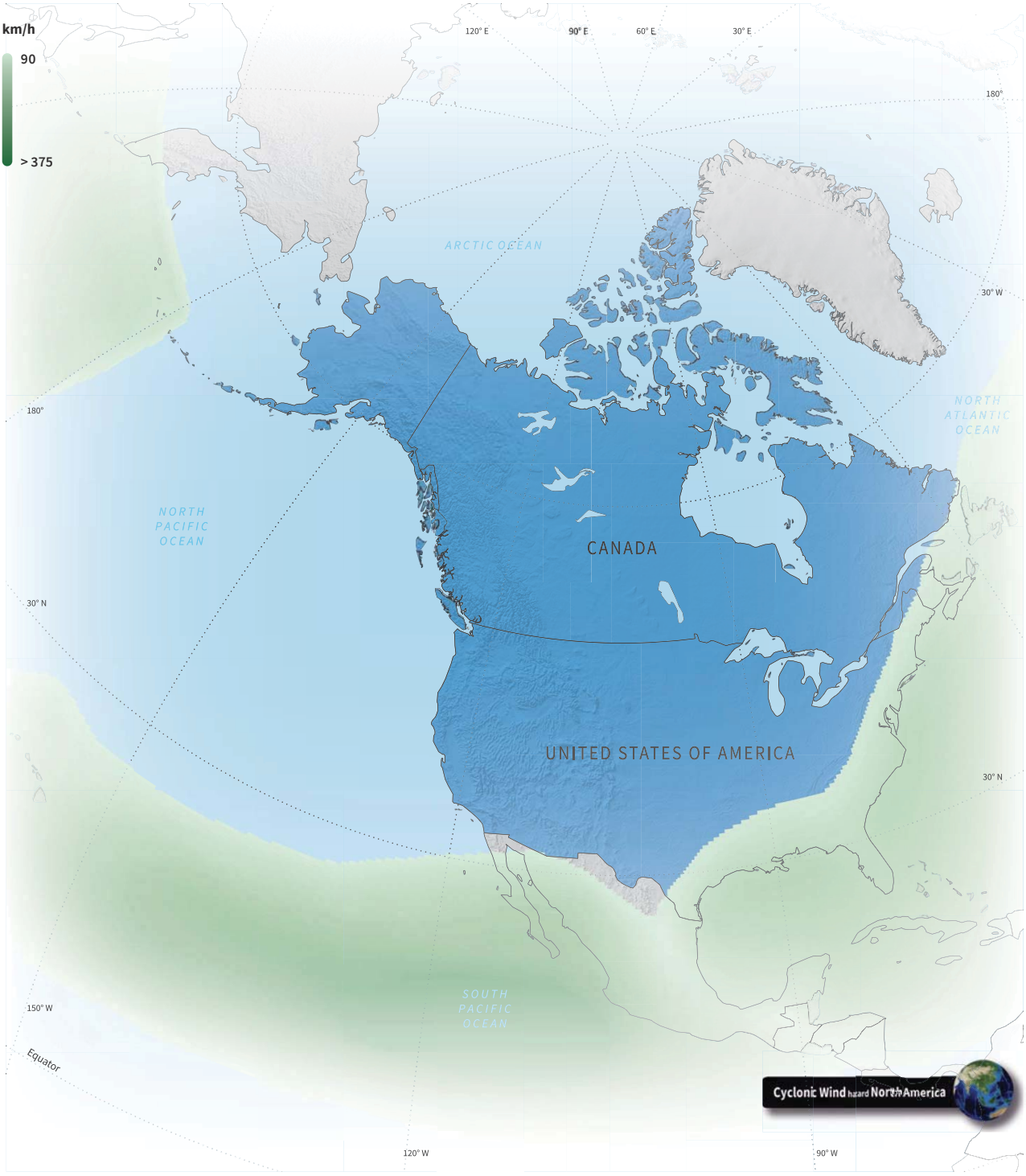

Map 5.24 Tropical cyclones (Storm surge) hazard-North America (Run-up height 100 years return period)

Map 5.25 Cyclonic wind hazard South Asia (wind speed 100 years return period)

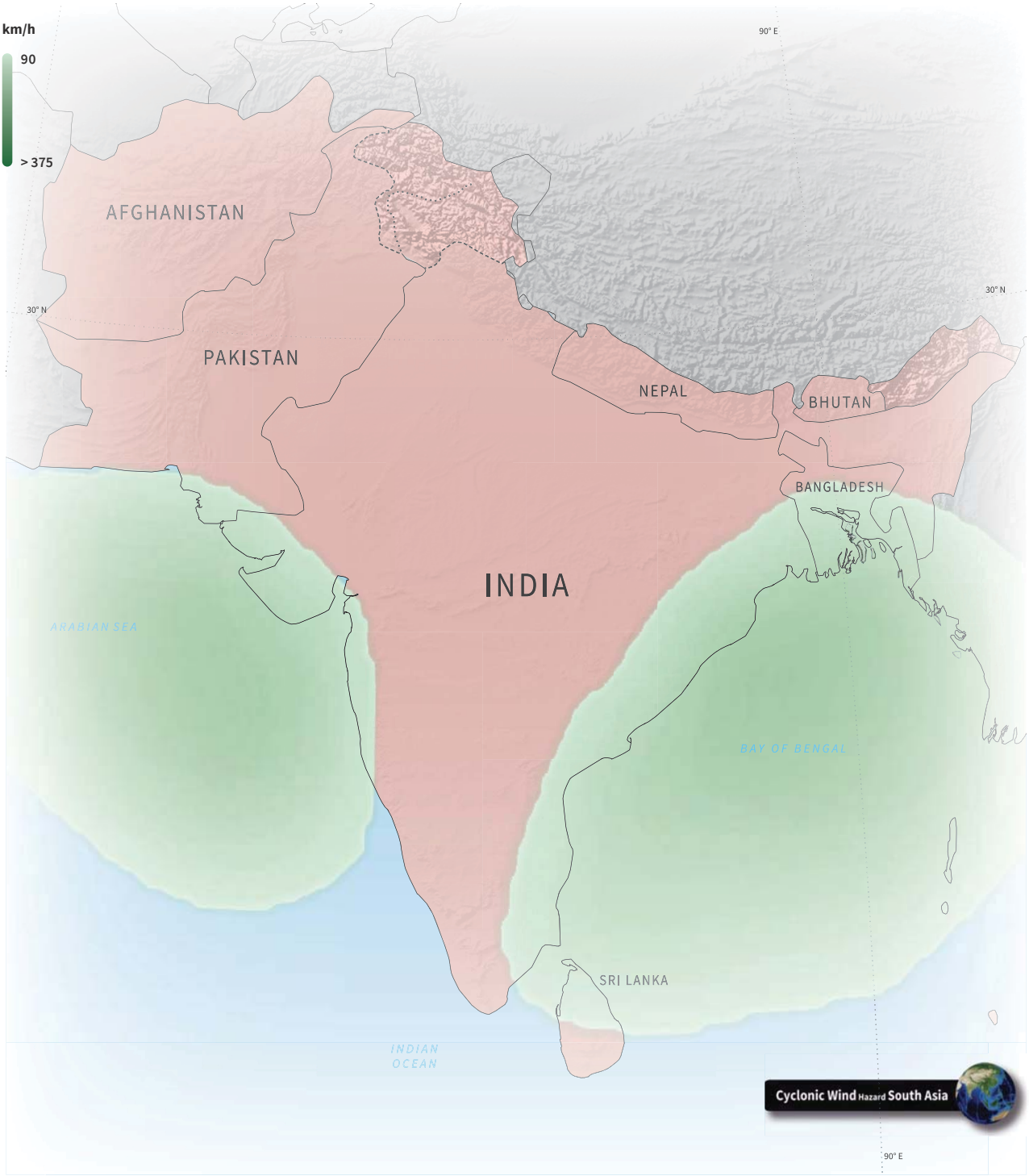

Map 5.26 Tropical cyclones (Storm surge) hazard-South Asia (Run-up height 100 years return period)

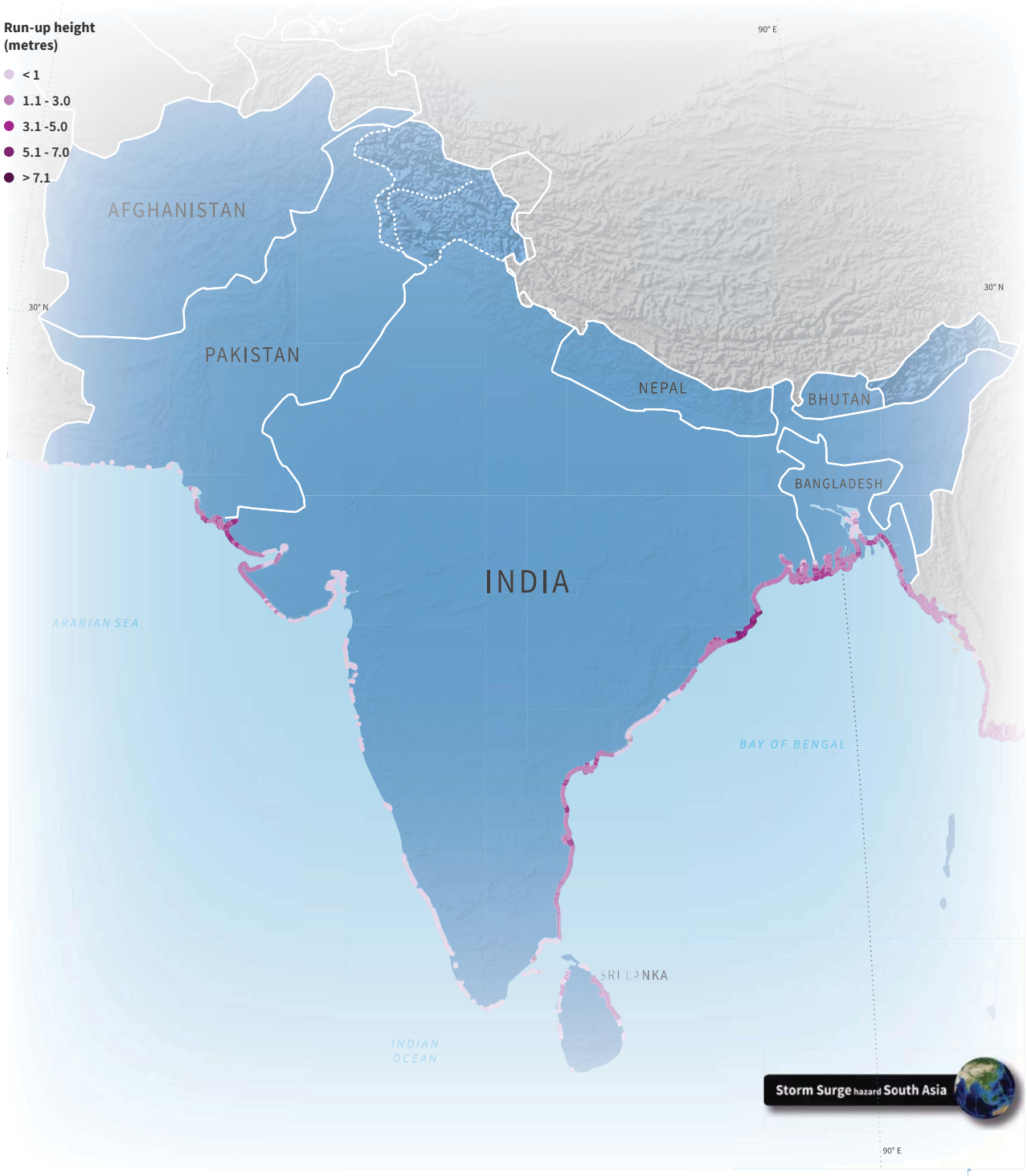

Map 5.27 Cyclonic wind hazard Sub Saharan Africa (wind speed 100 years return period)

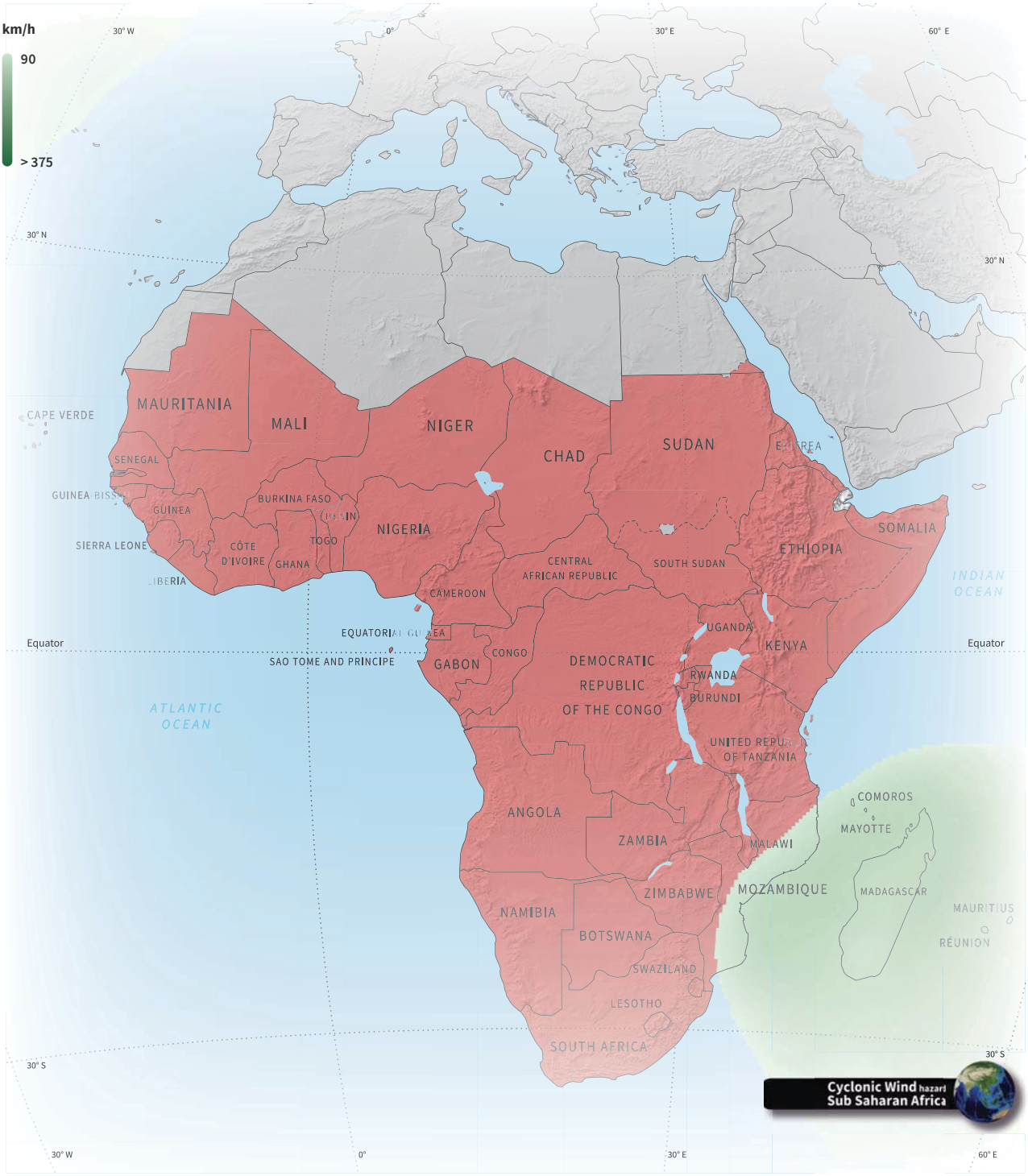

Map 5.28 Tropical cyclones (Storm surge) hazard-Sub Saharan Africa (Run-up height 100 years return period)

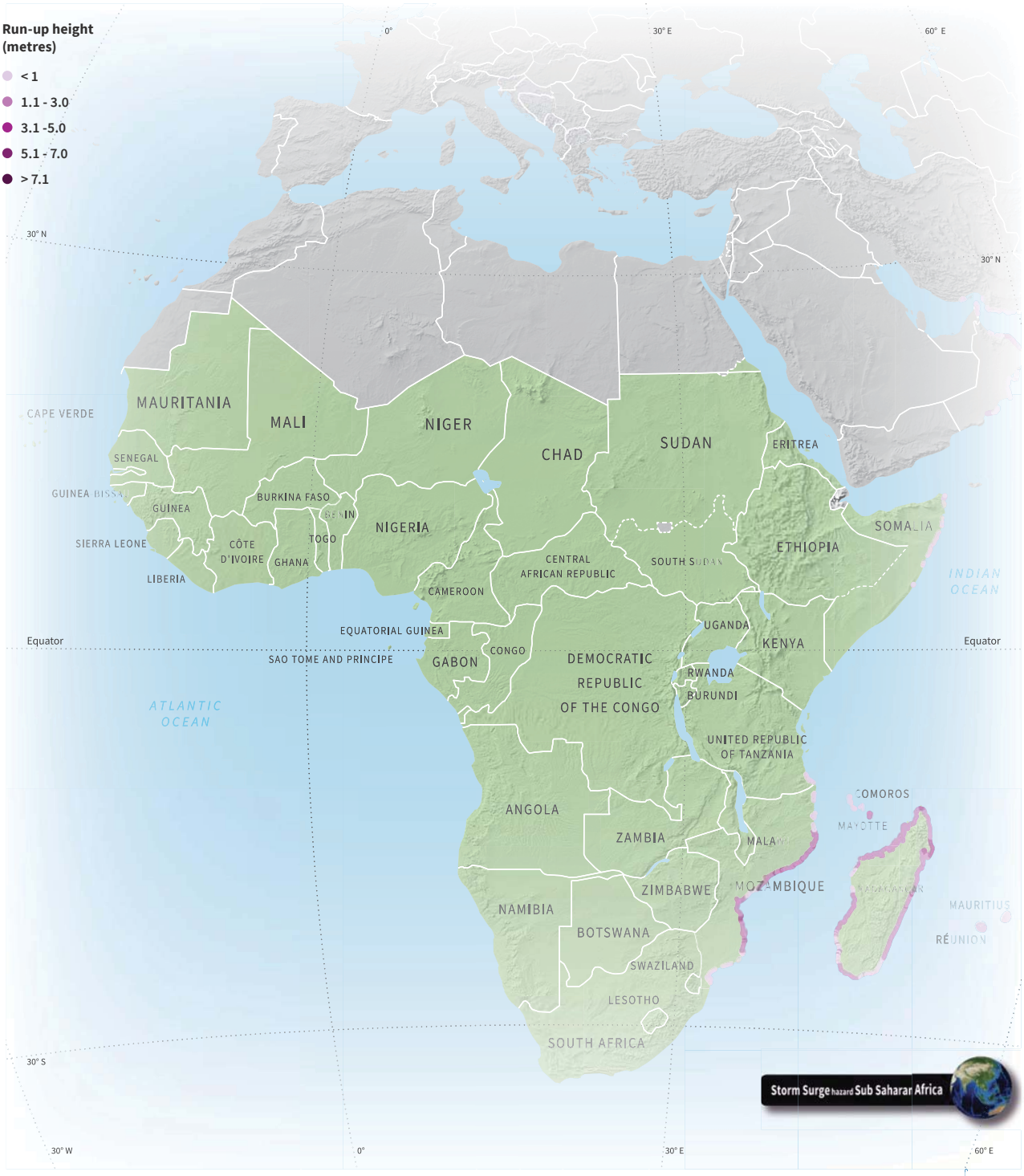

Map 5.29 Global riverine floods hazard (Water depth 50 years return period)

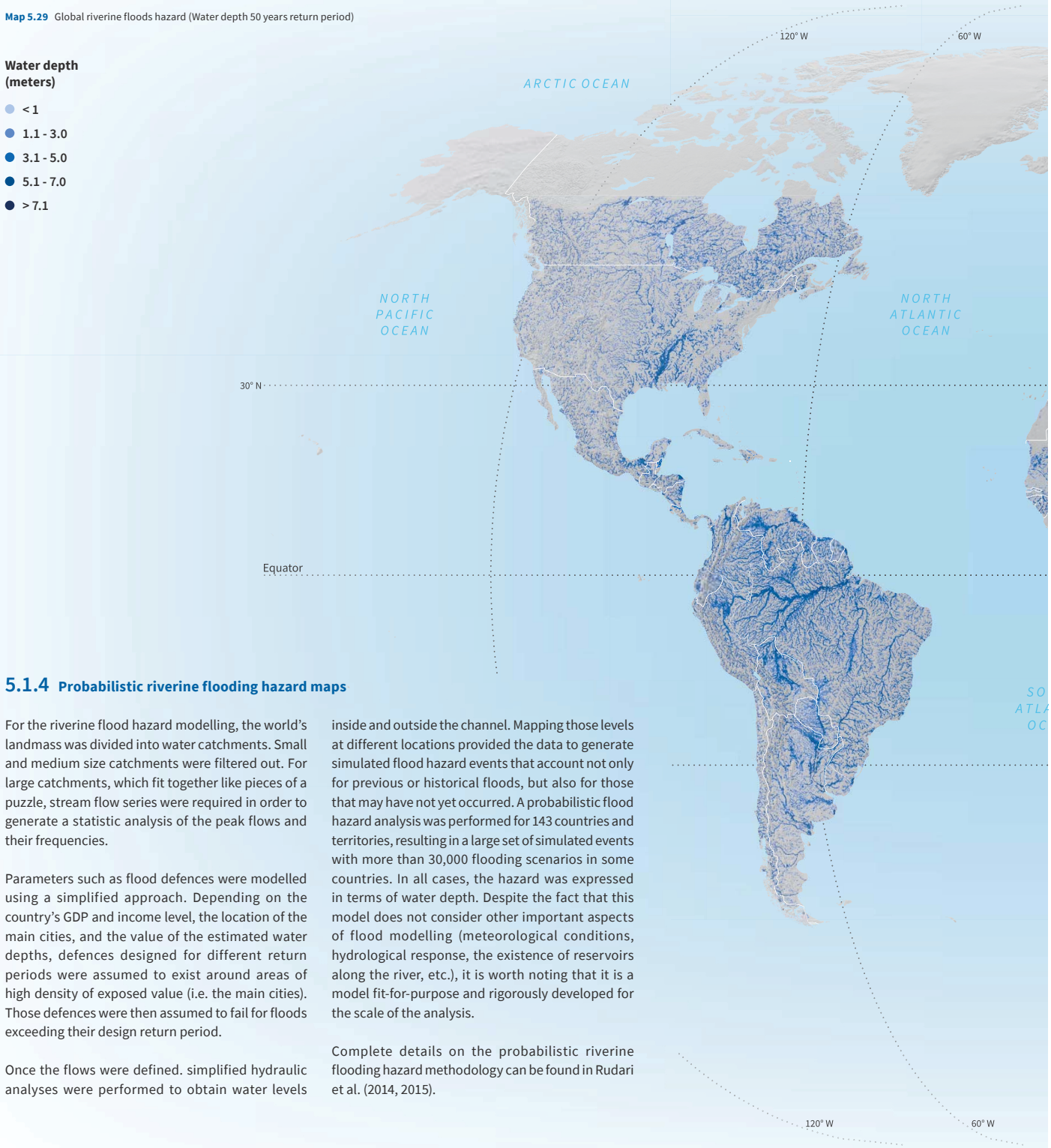

5.1.4 Probabilistic riverine flooding hazard maps

For the riverine flood hazard modelling, the world's landmass was divided into water catchments. Small and medium size catchments were filtered out. For large catchments, which fit together like pieces of a puzzle, stream flow series were required in order to generate a statistic analysis of the peak flows and their frequencies.

Parameters such as flood defences were modelled using a simplified approach. Depending on the country's GDP and income level, the location of the main cities, and the value of the estimated water depths, defences designed for different return periods were assumed to exist around areas of high density of exposed value (i.e. the main cities). Those defences were then assumed to fail for floods exceeding their design return period.

Once the flows were defined. simplified hydraulic analyses were performed to obtain water levels inside and outside the channel. Mapping those levels at different locations provided the data to generate simulated flood hazard events that account not only for previous or historical floods, but also for those that may have not yet occurred. A probabilistic flood hazard analysis was performed for 143 countries and territories, resulting in a large set of simulated events with more than 30,000 flooding scenarios in some countries. In all cases, the hazard was expressed in terms of water depth. Despite the fact that this model does not consider other important aspects of flood modelling (meteorological conditions, hydrological response, the existence of reservoirs along the river, etc.), it is worth noting that it is a model fit-for-purpose and rigorously developed for the scale of the analysis.

Complete details on the probabilistic riverine flooding hazard methodology can be found in Rudari et al. (2014, 2015).

Riverine Floods hazard World

Map 5.30 Riverine floods hazard-East Asia and The Pacific (Water depth 50 years return period)

Map 5.31 Riverine floods hazard-Europe and Central Asia (Water depth 50 years return period)"

Map 5.32 Riverine floods hazard-LA and The Caribbean (Water depth 50 years return period)

Map 5.33 Riverine floods hazard-Middle East and North Africa (Water depth 50 years return period)

Map 5.34 Riverine floods hazard-North America Water depth 50 years return period (Water depth 50 years return period)

Map 5.35 Riverine floods hazard-South Asia (Water depth 50 years return period)

Map 5.36 Riverine floods hazard-Sub-Saharan Africa (Water depth 50 years return period)

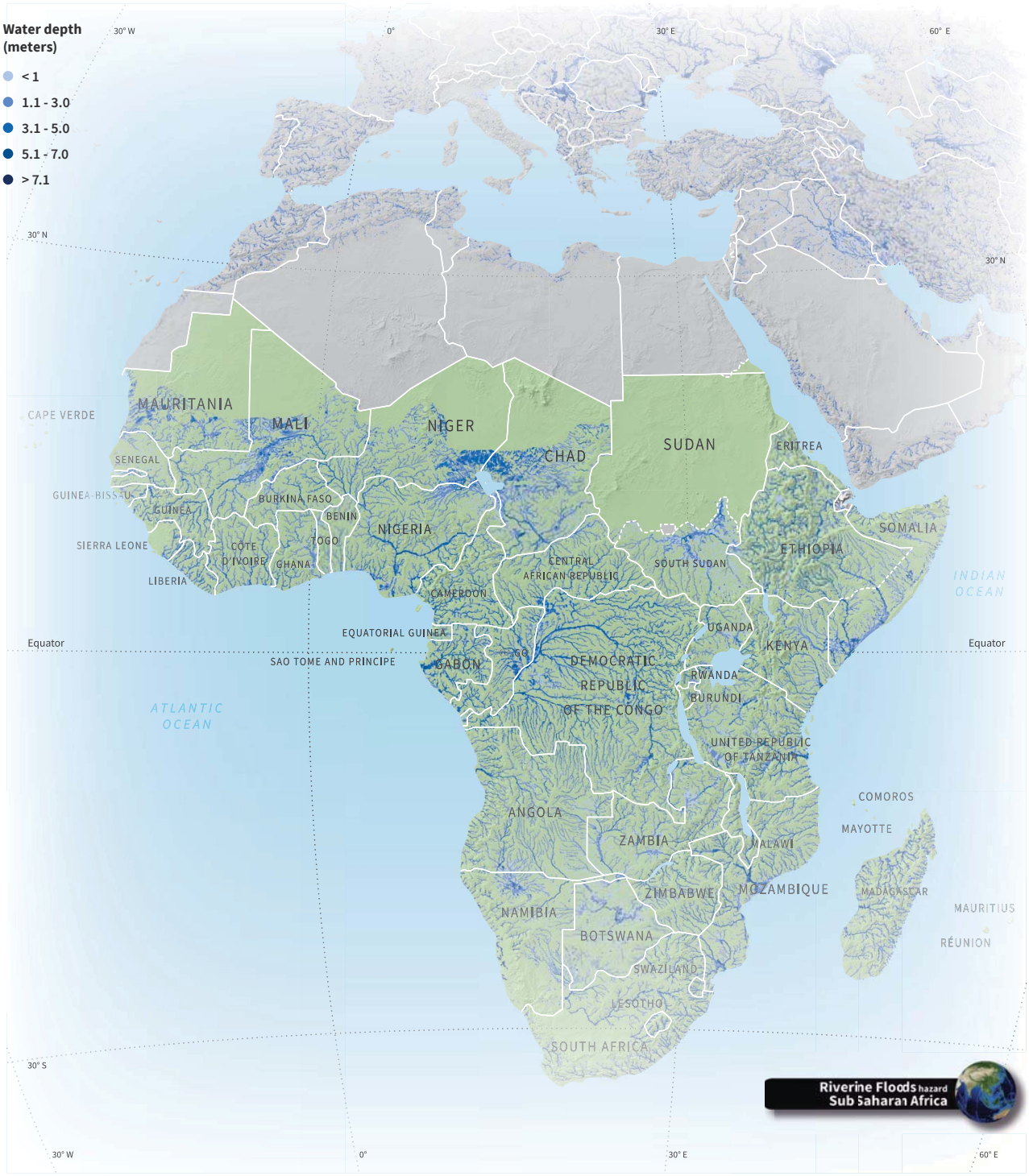

5.2 Development of the Global Exposure Database

The Global Exposure Database (GED) was developed with the aim of accounting for the built environment. The GED was developed using a top-down or "downscaling" approach, as shown in Figure 5.3. A spatial disaggregation of different data sources with global coverage of information related to national socio-economic indicators, building types and capital stock was performed on a regular grid using GIS data such as population distribution and proxies based on GDP distribution models[vii].

The GED was developed using a 5x5km level of resolution (see Figure 5.4), with the exception of the coastal areas, where the spatial resolution level was set to 1x1km. Both levels of spatial distribution use the same input indicators and information. The difference between the 5x5km and 1x1km levels of resolution is that the latter provides better information on the spatial distribution of the exposed assets. The 5x5km level of spatial resolution was chosen in order to balance aspects such as an acceptable size, in order to capture the effects of large scale hazards like earthquakes, floods and cyclonic winds, consistency with the openly available socio-economic datasets from national and/or global sources, and to optimise computation time. The 1x1km spatial distribution helped to capture the effects of more localised hazards such as storm surge and tsunami.

The main challenge in the development of the GED was to have uniform information at all locations so that risk results are consistent and comparable among different countries. The GED has a coarse grain resolution level but it is considered acceptable and fully compatible with the resolution of the hazard information and with the global purpose and scope of the assessment.

More details on the development of the GED can be found in De Bono and Chatenoux (2014).

Figure 5.4 Example of the 5x5km GED.

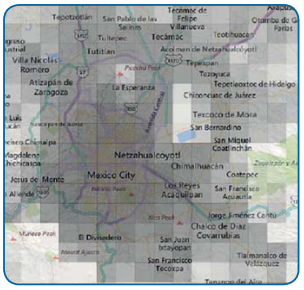

Source: UNISDR

5.3 Physical vulnerability of exposed assets

Different sets of vulnerability functions were developed to consider and capture regional differences in construction practices. Expert groups were convened to define different vulnerability functions for Latin America, the Caribbean, Europe, Asia and the Pacific[viii].

Many factors influence the damage and loss of exposed assets, including differences in construction practices, the quality of the materials used, and labour skills. For example, two neighboring and identical looking buildings do not necessarily end up with exactly the same damage and loss even when subjected to the same hazard intensity levels. Because of this, the damage ratio for each hazard intensity does not correspond to a single value but needs to be considered as a random variable that accounts for the distribution of possible losses. In other words, it is necessary to define each function according to the expected value and a variance measure of the mean damage ratio, as shown in Figure 5.5.

The hazard intensities used in the vulnerability functions are the same as those obtained in the hazard analysis described above, such as spectral ground accelerations for earthquakes, speed for cyclonic wind, water depth in case of riverine flooding, ash thickness for volcanic ash fall and run-up height for storm surge and tsunami. Figures 5.6 and 5.7 provide a schematic explanation of seismic and flooding vulnerability functions in order to show the relationships between hazard intensities and damage ratios.

Figure 5.3 Top-down approach global exposure database

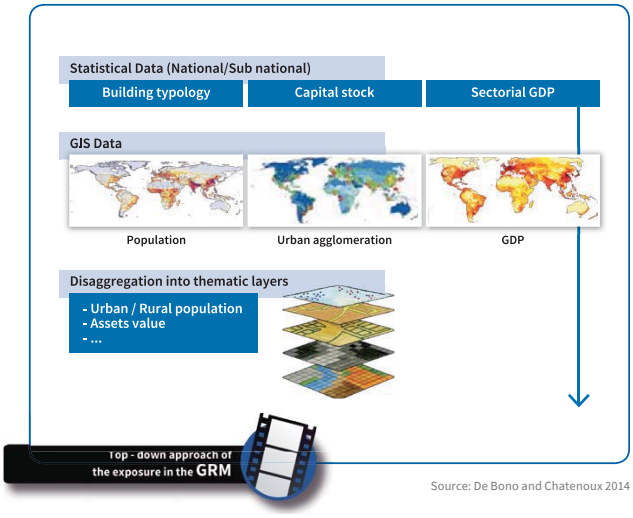

Source: De Bono and Chatenoux 2014

Figure 5.5 Schematic explanation of a vulnerability function Adapted from Cardona et al. 2015

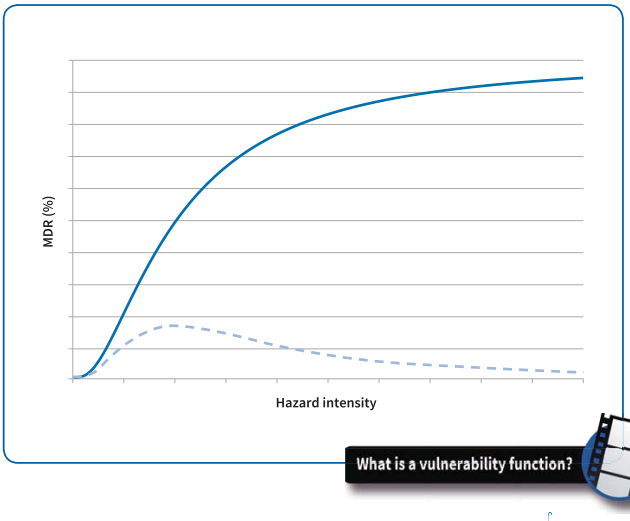

Figure 5.6 Schematic representation of a seismic vulnerability function. Adapted from Cardona et al. 2015

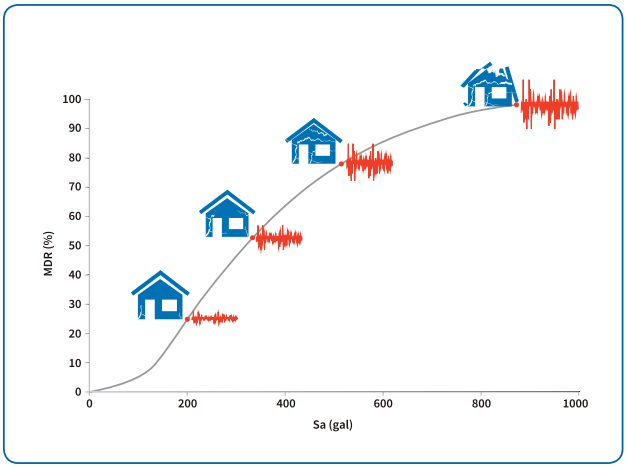

Figure 5.7 Schematic representation of a flood vulnerability function. Adapted from Cardona et al. 2015

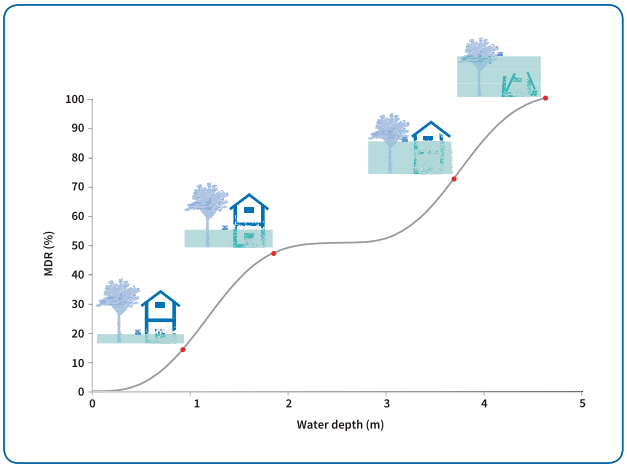

5.4 Probabilistic multi-hazard risk assessment

For the GRM, physical risk was calculated with the CAPRA Team RC+ programme, which is the updated risk module of the CAPRA suite. The methodology[ix] follows a state-of-the-art procedure for risk estimation and uses an event-based approach that allows a fully probabilistic risk assessment, the flowchart of which is illustrated in Figure 5.8. For each component included in the exposure database which has been grouped in a class of buildings with similar structural, material and height characteristics, damages and losses are estimated by convoluting hazard and vulnerability. This is done repetitively for each simulated event and for each considered hazard.

The objective of the probabilistic risk assessment is to obtain the losses that could feasibly occur in public and private buildings located in urban and rural areas of the 216 countries and territories included in the exposure database. These losses are associated with events such as earthquakes, tsunamis, cyclones and riverine floods. A critical innovation of the GRM is that they have been quantified by applying the same methodology. The results across all hazards and countries are therefore directly comparable.

The result obtained from the probabilistic risk assessment is the Loss Exceedance Curve (LEC). From it, different risk metrics can be obtained, such as Probable Maximum Loss (PML), Average Annual Loss (AAL) or Occurrence Exceedance Probability (OEP).

Risk metrics provide relevant information that helps paint a complete picture of risk, from a specific hazard, for each country. Quantifying risk provides decision-making support for disaster risk management. It is worth noting that the risk metrics provide the probability of certain losses and not the probability that a specific event will occur, and the loss values must be understood as orders of magnitude instead of exact values.

The LEC represents the annual exceedance rates of different loss levels since it considers the associated loss values associated with all simulated events of the hazard, or hazards, evaluated. An example of an LEC is shown in figure 5.9. Smaller losses have higher annual exceedance rates, whereas higher losses are related to lower annual exceedance rates. An LEC can be obtained for each of the hazards considered (in this example earthquakes, cyclonic wind and flood) in the risk assessment, and after identifying any loss value of interest, its corresponding exceedance rate and/or mean return period can be read.

Another possible way to communicate risk results is through exceedance probability curves. In this case, the probabilities need to be associated with a timeframe, meaning that the information in the plots is the probability of exceeding a certain loss level during the defined timeframe. It is common practice to set timeframes for one year so that occurrence exceedance probability (OEP) plots, such as that shown in Figure 5.10, are obtained.

The mean return period of the loss corresponds to the inverse value of the loss exceedance rate. Mean return periods of 50, 100, 200 or 500 years correspond to 0.02, 0.01, 0.005 and 0.002 annual exceedance rates. Expressed in another way, the annual exceedance probabilities are 2 per cent, 1 per cent, 0.5 per cent and 0,2 per cent respectively. By rearranging the data in the LEC, the Probable Maximum Loss (PML) plot can be obtained, as shown in Figure 5.11. A PML provides information about expected losses always associated with a specific mean return period (e.g. 50, 100, 200 or 500 years) and the losses associated to any mean return period of interest can therefore be read directly from it.

It is important to highlight that loss values associated with an annual exceedance rate (or mean return period if read from the PML plots) obtained for some areas are not necessarily related to a single hazard event but to the contribution of several events that can equal or exceed a given loss level. Since spatial correlation between losses caused by the same event is accounted for in the risk assessment process, the mean return period of the loss is not necessarily the same as for one of the hazardous events.

The average annual loss (AAL) or expected annual loss (EAL) is the mean value of all the expected losses during a sufficiently long timeframe and provides an annualised overview of the risk levels. The AAL is not a value indicating that all future losses will cost the

Figure 5.8 Probabilistic disaster risk assessment flowchart. Adapted from Marulanda 2013

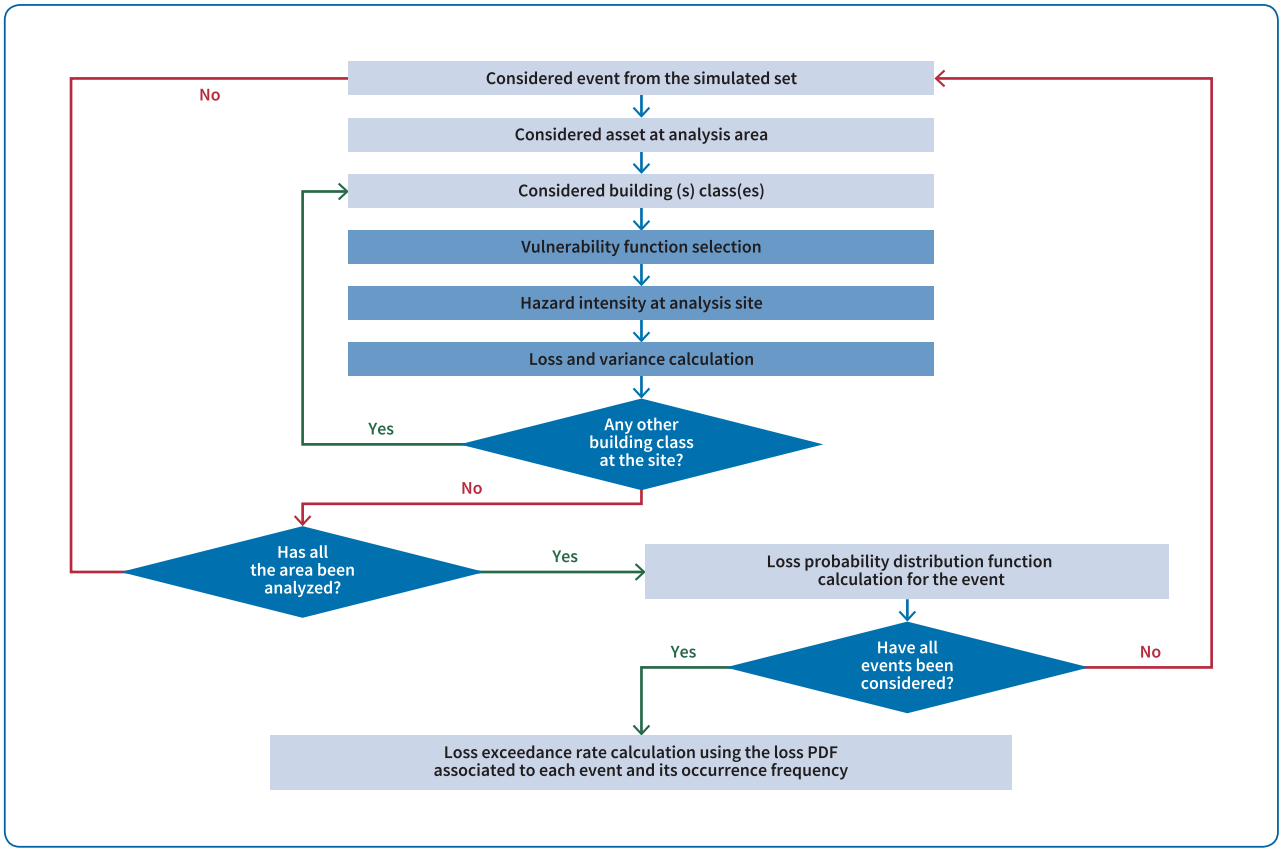

Figure 5.9 Example of a loss exceedance curves (LEC). Adapted from Ordaz 2000

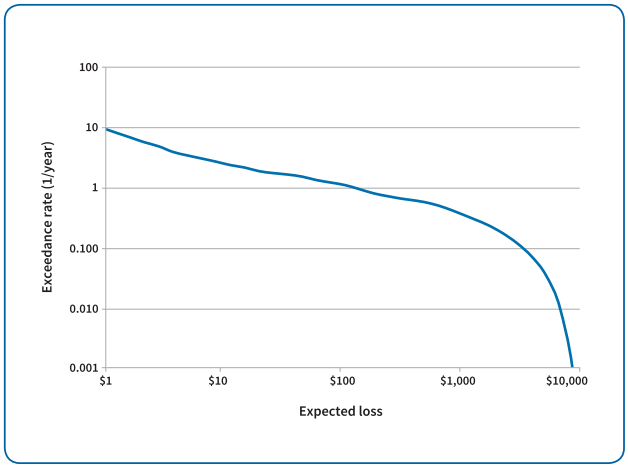

Figure 5.10 Example of occurrence exceedance probability plot. Adapted from Ordaz 2000

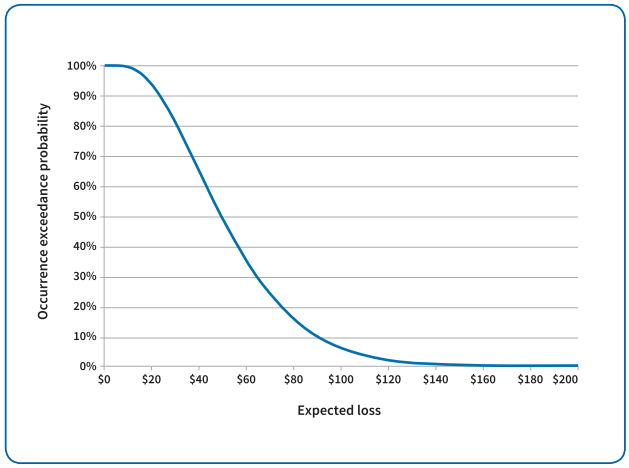

same every year. Given that it is an average value, losses may be lower in some years and higher in others. The AAL is a compact metric which accounts for the potential occurrence of small, medium and extreme events, with their associated losses. It has been used for many applications in the GAR Atlas. Figure 5.12 provides an explanation of the AAL concept.

The multi-hazard AAL can be obtained by adding up the AAL of each individual hazard. The AAL is obtained by multiplying the product of the expected loss by the annual occurrence frequency of each simulated event, or by calculating the area under the LEC.

Even if the AAL is a robust risk metric, it does not reflect which events have the greatest influence on its final value. In some cases, infrequent but high impact hazards such as earthquakes contribute more to the AAL than hazards with higher frequency but less severity. In other cases, extreme events are very infrequent, meaning that more recurrent events contribute a greater share of the AAL. This shows that using only a single metric is insufficient to have a complete overview of risk. A range of different metrics are required for comprehensive disaster risk assessment and communication. Risk information must be part of a decision context, establishing what it is considered as acceptable within different options, as well as being appropriate for the needs of different users.

Figure 5.11 Example of PML plots for different hazards. Adapted from Ordaz 2000

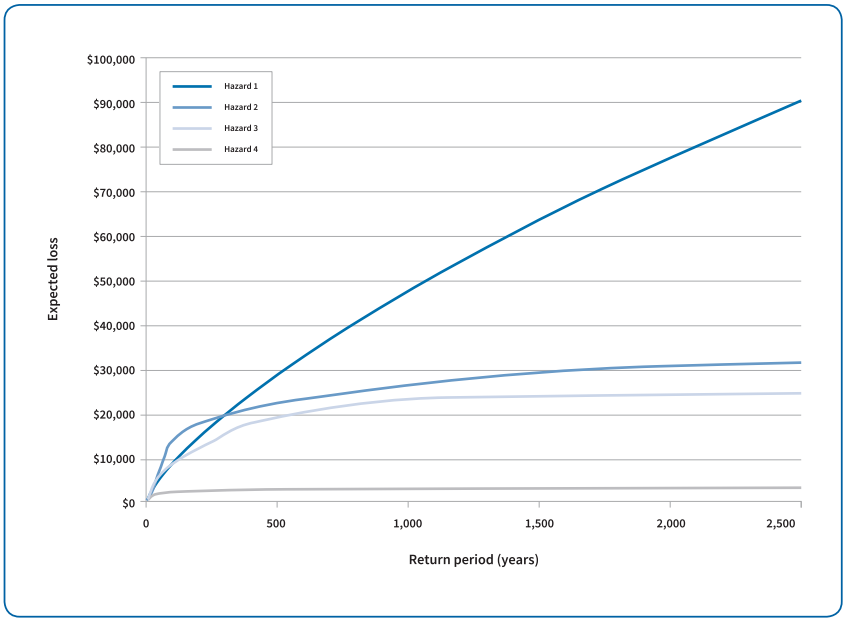

Figure 5.12 Explanation of the AAL concept. Adapted from Marulanda 2013

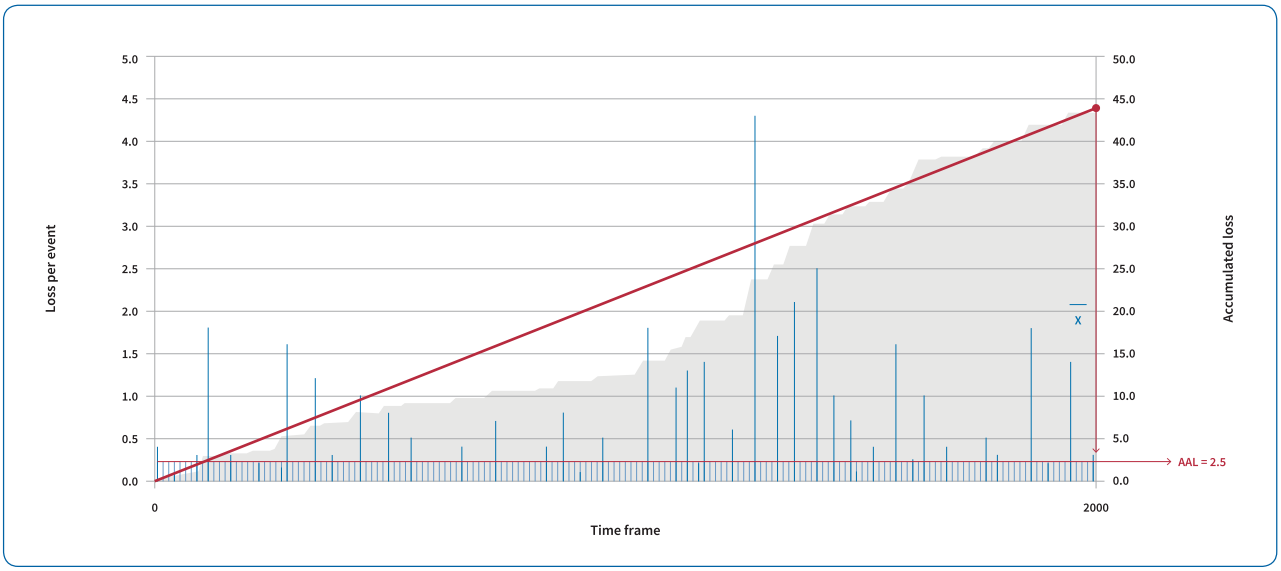

For the purposes of comparison, it is common practice to normalise the AAL and PML by exposed value or capital stock. This is done in order to identify levels of high relative risk. High absolute values may be caused by low levels of damage in high value exposed assets.

Maps 2.1 to 2.45 in section 2 present the relative multi-hazard AAL for the 216 countries and territories as well as its disaggregation by hazard. The LEC, OEP curve or PML plots are available through the augmented reality function of the GAR Atlas using the GAR for Tangible Earth application.

5.5 Aggregated multi-hazard probable maximum losses

Many countries have a multi-hazard context. It is therefore important to understand the potential magnitude of losses from a range of hazards, not just individually but in a combined manner. While the AAL can be calculated in a multi-hazard approach, it is not as straightforward to do so for other risk metrics such as the PML.

The AAL is a robust metric that offers a long-term view of disaster risk in a country, but it does not provide information about how often losses of different scales occur. Comprehensive disaster risk management requires an overview of the complete spectrum of risk, as well as knowing where risk is concentrated and the levels of contribution to overall risk by an individual hazard. This information is usually included in the LEC and the probable maximum loss plot of specific hazards. Presenting this jointly for multiple hazards is extremely useful for the development of disaster risk reduction plans and the design of financial protection strategies.

In order to aggregate results for multi-hazard PML assessments, a number of requirements need to be met. These include the use of the same exposure database for all hazards considered in the analysis and the identification of hazards with simultaneous occurrences (e.g. cyclonic wind and storm surge). This information is not yet available at the global level due to the lack of available homogeneous data. Local and regional case studies can be developed, however. As a pilot study, a multi-hazard estimation of all relevant risk metrics, using the GRM, has been developed successfully for a number of small island developing states (SIDS) in the Caribbean.

The results provide a wider panorama of risk, increasing the available information to stakeholders and decision-makers in an area that is of high relevance for countries that are exposed to more than one natural hazard (Figure 5.13).

In Grenada and Saint Lucia, larger though less frequent losses are expected to occur due to cyclonic activity, whereas the contribution of seismic hazard to overall risk is reflected mainly in small and recurrent events. And although tsunami risk is significantly lower than other hazard-related risk, it is not negligible.

Calculations of relevant risk metrics such as these, using a multi-hazard approach, are expected to be performed in the future for all countries covered by the GRM. This would create another layer of illustrative risk information, thereby increasing the understanding of the distribution of risk.

i. Woo 1996

ii. Ordaz et al. 2014a

iii. The maps are showing the hazard intensities that buildings of approximately five stories can be subjected to. They have fundamental periods of around 0.5 seconds

iv. Knapp et al. 2010

v. Center for International Earth Science Information Network – CIESIN et al. 2011, Shuttle Radar Topography Mission (SRTM) (NASA 2014), British Oceanographic Data Centre 2009

vi. Bernal 2014

vii. Pesaresi and Freire, Tolis et al. 2013

viii. Cardona et al. 2015, Maqsood et al. 2014

ix. Ordaz 2000

Figure 5.13 Multi-hazard loss exceedance curves for Grenada and Saint Lucia

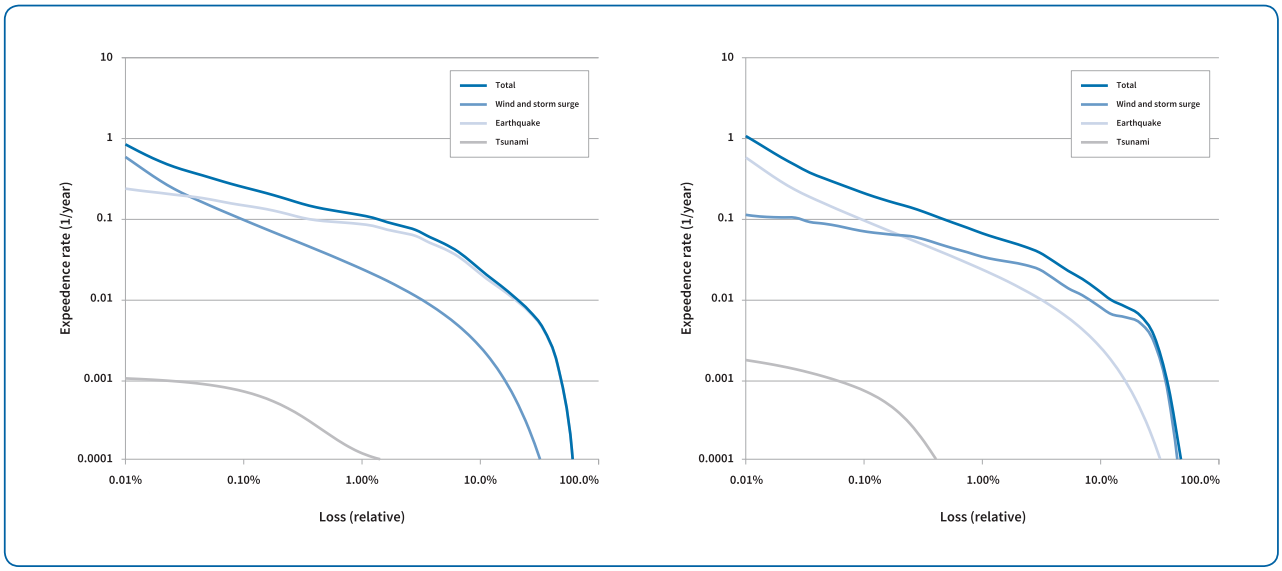

Source: UNISDR

References

AIR (2002). Ten Years after Hurricane Andrew: What should we be preparing for now. AIR Special Report. Boston, USA.

Bear-Crozier A.N., Miller V., Newey V., Horspool N. and Weber R. (2014). Emulating volcanic ash fall for multi-scale analysis - Development of the VAPAHR tool and application to the Asia-Pacific region Geoscience Australia. Canberra, Australia.

Bernal G.A. (2010). VHAST. A computer program for probabilistic volcanic hazard assessment. Bogotá D.C., Colombia. Available at: http://www.vhast.org

Bernal G.A. (2014). TCHM - Tropical Cyclones Hazard Modeler. Computer program for the probabilistic assessment of strong winds and storm surge from tropical cyclones. Bogotá D.C., Colombia.

Bernal G.A. and Cardona O.D. (2011). Probabilistic hazard and risk analyses of the Galeras Volcano in Nariño, Colombia. Technical Note Ingeniar Ltda. Bogotá D.C., Colombia.

Bernstein P.L. (1996). Against the Gods. The remarkable story of risk. John Wiley & Sons. New York, USA.

Bohm D. and Peat F.D. (1987). Science, Order and Creativity Bantam Books. New York, USA.

British Oceanographic Data Centre (2009). General Bathymetric Chart of the Oceans (GEBCO).

Brown S.K., Sparks R.S.J., Mee K., Vye-Brown C., Ilyinskaya E., Jenkins S. and Loughlin S.C. (2015). Regional and country profiles of volcanic hazard and risk. Report IV of the GVM/IAVCEI contribution to the GAR15.

Cardona O.D. (2001). Estimación Holística del Riesgo Sísmico Utilizando Sistemas Dinámicos Complejos, Ph.D. Thesis, Universidad Politécnica de Cataluña. Barcelona, Spain.

Cardona O.D., Ordaz M.G., Reinoso E., Yamín L.E. and Barbat A.H. (2012). CAPRA – Comprehensive Approach to Probabilistic Risk Assessment: International Initiative for Risk Management Effectiveness Lisbon, Portugal. Proceedings of the 15th World Conference on Earthquake Engineering.

Cardona O.D., Bernal G.A., Ordaz M.G., Salgado-Gálvez M.A., Singh S.K., Mora M.G., Yamín L.E. and A.H. Barbat (2013). Probabilistic Modelling of Natural Risks at the Global Level: Global Risk Model. Global earthquake and cyclone models and Disaster risk assessment of countries for seismic, cyclone and flood hazards. Consortium CIMNE, INGENIAR, ITEC and EAI. Background paper for GAR13. Barcelona, Spain - Bogotá D.C., Colombia.

Cardona O.D., Ordaz M.G., Mora M.G., Salgado-Gálvez M.A., Bernal G.A., Zuloaga-Romero D., Marulanda M.C., Yamín L. and González D. (2014). Global risk assessment: A fully probabilistic seismic and tropical cyclone wind risk assessment. International Journal of Disaster Risk Reduction. 10(B):461-476.

Cardona O.D., Bernal G.A., Ordaz M.G., Salgado-Gálvez M.A., Singh S.K., Mora M.G. and C.P. Villegas (2015). Update on the Probabilistic Modelling of Natural Risks at Global Level: Global Risk Model - Global Earthquake and Tropical Cyclone Hazard Assessment. Disaster Risk Assessment at Country Level for Earthquakes, Tropical Cyclones (Wind and Storm Surge), Floods, Tsunami and Volcanic Eruptions. CIMNE & INGENIAR Consortium. Background paper for GAR15. Barcelona - Bogotá D.C., Colombia.

Carreño M.L., Cardona O.D. and Barbat A.H. (2007). Urban seismic risk evaluation: A holistic approach. Natural Hazards. 40(1):137-172.

Cauzzi C. and Faccioli E. (2008). Broadband (0.05 to 20s) prediction of displacement response spectra based on worldwide digital records. Journal of Seismology 12(4):453-475.

CIESIN - Center for International Earth Science Information Network, Columbia University, IFPRI - International Food Policy Research Institute, The World Bank, and CIAT - Centro Internacional de Agricultura Tropical (2011). Global Rural-Urban Mapping Project, Version 1 (GRUMPv1): Urban Extents Grid. Palisades, NY. NASA Socioeconomic Data and Applications Center (SEDAC).

Chaulagain H., Rodrigues H., Silva V., Spacone E. And Varum H. (2015). Seismic Risk Assessment and Hazard Mapping in Nepal. Natural Hazards 78(1):583-602.

CIMNE and INGENIAR Ltda. (2015). Indicators of Disaster Risk and Disaster Risk Management (IDB-IDEA). Update of the System of Indicators of Disaster Risk and Disaster Risk Management International Center for Numerical Methods in Engineering and INGENIAR Ltda. Barcelona, Spain - Bogotá D.C., Colombia.

De Bono A. Chatenoux, B. (2015). A Global Exposure Model for GAR 2015, UNEP-GRID. Background paper for GAR15.

DesInventar. Disaster loss databases platform. Available at: www.desinventar.net

García Márquez G. (1984). El Olor de la Guayaba Oveja Negra. Bogotá D.C., Colombia.

GFDRR – Global Facility for Disaster Reduction and Recovery (2016). ThinkHazard! Available at: www.thinkhazard.org

Hallegate S., Vogt-Schilb A.; Bangalore M. and Rozenberg J. (2017). Unbreakable: Building the Resilience of the Poor in the Face of Natural Disasters. Climate Change and Development World Bank. Washington DC, USA.

Harvey D. (1989). The Condition of Postmodernity Basil Blackwell. Oxford, United Kingdom.

Hsu A. et al. (2016). Environmental Performance Index. Yale University, New Haven, USA.

IASC- Inter-Agency Standing Committee and European Commission (2015). Inform: Index for risk management. Available at: www.inform-index.org

IDEA (2005). Indicadores de riesgo de desastre y gestión de riesgos. Informe técnico principal Manizales, Colombia. Inter-American Development Bank, Manizales, Colombia.

INGENIAR Ltda. (2014). Perfil de riesgo de desastres de Venezuela Inter-American Development Bank.

INGENIAR Ltda. (2016). Hurricane Loss Track in the Caribbean using the Global Risk Model. Bogotá D.C., Colombia. Available at: http://ingeniar-risk.com

INGENIAR Ltda., International Center for Numerical Methods in Engineering, CIMNE and ITEC S.A.S (2014). Desarrollo del Perfil de Riesgo de Desastres a Nivel Nacional El Salvador, Peru and Venezuela. Inter-American Development Bank.

IPCC - Intergovernmental Panel on Climate Change (2014). Climate Change 2014: Impacts, Adaptation, and Vulnerability. Working Group II. Cambridge University Press, United Kingdom.

Knapp K.R., Kruk M. C., Levinson D.H., Diamond H.J., and Neumann C. J. (2010). The international best track archive for climate stewardship (IBTrACS) unifying tropical cyclone data. Bulletin of the American Meteorological Society. 91(3):363-376.

Løvholt F., Griffin J. and Salgado-Gálvez M.A. (2015). Tsunami Hazard and Risk Assessment on the Global Scale. Encyclopedia of Complexity and Systems Science. Springer Science+Business Media. New York, USA.

Maqsood T., Wehner M., Ryu H., Edwards M., Dale K. and Miller, V. (2014). GAR15 Vulnerability Functions: Reporting on the UNISDR/GA SE Asian Regional Workshop on Structural Vulnerability Models for the GAR Global Risk Assessment, 11–14 November, 2013 Geoscience Australia. Canberra, Australia.

Marulanda M.C. (2013). Modelación probabilista de pérdidas económicas por sismo para la estimación de la vulnerabilidad fiscal del Estado y la gestión financiera del riesgo. Ph.D. Thesis. Universidad Politécnica de Cataluña. Barcelona, Spain.

Marulanda M.C., Carreño M.L., Cardona O.D., Ordaz M.G. and Barbat A.H. (2013). Probabilistic earthquake risk assessment using CAPRA: application to the city of Barcelona, Spain. Natural Hazards. 69(1):59-84.

McChristian L. (2012). Hurricane Andrew and Insurance: the Enduring Impact of an Historic Storm Insurance Information Institute. Florida, USA.

References

NASA (2014). Shuttle Radar Topography Mission: The mission to map the world.

NGI – Norwegian Geotechnical Institute and GA – Geoscience Australia (2014). Tsunami methodology and result overview. Background paper for GAR15.

Noy I (2014). A New Non-Monetary Global Measure of the Direct Impact of Natural Disasters. Background paper for GAR15.

Noy I. (2015). Comparing the direct human impact of natural disasters for two cases in 2011: The Christchurch earthquake and the Bangkok flood. International Journal of Disaster Risk Reduction. 13:61-65.

Oliver-Smith A., Alcántara-Ayala I. Burton I. and Lavell A.M. (2016). Forensic Investigations of Disasters (FORIN): a conceptual framework and guide to research (IRDR FORIN Publication No.2) Integrated Research on Disaster Risk. Beijing, China.

Ordaz M.G. (2000). Metodología para la evaluación del riesgo sísmico enfocada a la gerencia de seguros por terremoto. México D.F. Universidad Nacional Autónoma de México.

Ordaz M.G., Martinelli F., Aguilar A., Arboleda J., Meletti C. and D'Amico V. (2014a). CRISIS 2014 V1.2. Program for computing seismic hazard. México D.F. Insitituto de Ingeniería. Universidad Nacional Autónoma de México. Mexico City, Mexico.

Ordaz M.G., Cardona O.D., Salgado-Gálvez M.A., Bernal-Granados G.A., Singh S.K. and Zuloaga-Romero D. (2014b). Probabilistic seismic hazard assessment at global level. International Journal of Disaster Risk Reduction. 10(B):419-427.

Pesaresi M. and Freire S. (2014). BUREF – Producing a Global Reference Layer of Built-up by Integrating Population and Remote Sensing Data. Background paper for GAR15.

Rudari R., Gabellani S. and Delogu F. (2014). A simple model to map areas prone to Surface water flooding. International Journal of Disaster Risk Reduction. 10(B):428-441.

Rudari R., Silvestro F., Campo L., Rebora N., Boni, G. and Herold, C. (2015). Improvement of the Global Flood Model for the GAR15 CIMA Research Foundation and UNEP-GRID. Savona – Geneva. Background paper for GAR15.

Salgado-Gálvez M.A. (2015). Comparison of fatalities and direct economic losses for the Nepal (Gorkha) M7.8 earthquake using the GAR15 Global Exposure Dataset and the CAPRA risk assessment tool. Technical Note. Barcelona, Spain.

Salgado-Gálvez M.A. (2016a). Probabilistic assessment of earthquake losses at different scales considering lost economic production due to premature loss of lives. Ph.D. Thesis Universidad Politécnica de Cataluña. Barcelona, Spain.

Salgado-Gálvez M.A. (2016b). Prospective estimation of the number of life-lost years associated to natural hazards using the datasets of the Global Risk Assessment of GAR15. Geneva, Switzerland. UNISDR Risk Knowledge Section internal report.

Salgado-Gálvez M.A., Zuloaga D., Bernal G., Mora M.G. and Cardona O.D. (2014). Fully probabilistic seismic risk assessment considering local site effects for the portfolio of buildings in Medellín, Colombia . Bulletin of Earthquake Engineering. 12:671-695.

Salgado-Gálvez M.A., Bernal G.A., Barbat A.H., Carreño M.L. and Cardona O.D. (2016a). Probabilistic estimation of annual los economic production due to premature mortality because of earthquakes. Human and Ecological Risk Assessment. 22(2):543-557.

Salgado-Gálvez M.A., Zuloaga D., Velásquez C.A., Carreño M.L., Cardona O.D. and Barbat A.H. (2016b). Urban seismic risk index for Medellín, Colombia, based on probabilistic loss and casualties estimations. Natural Hazards. 80(3):1995-2021.

Salgado-Gálvez M.A., Barbat A.H., Cardona O.D. and Carreño M.L. (2016c). Comparing observed damages and losses with modeled ones using a probabilistic approach. The Lorca 2011 case. International Journal of Disaster Risk Reduction. 19:355-365.

Salgado-Gálvez M.A., Ordaz M.G. and Cardona O.D. (2016d). Preliminary estimation of Amatrice's Earthquake (August 24th 2016) direct economic losses and fatalities using GAR15 seismic hazard and risk datasets and tools. Technical Note. Geneva, Switzerland.

Stern S., Wares A. and Hellman T. (2016). The Social Progress Index Methodology 2016. Social Progress Imperative. Washington D.C., USA.

The Economist Intelligence Unit (2016). Towards disaster-risk sensitive investments: the Disaster Risk- Integrated Operational Risk Model. London. The Economist Intelligence Unit. London, United Kingdom.

Tolis S., Rosset P. and Wyss M. (2013). Detailed Building Stock at Regional Scale in Three Size Categories of Settlements for 18 Countries Worldwide. WAPMERR. Background paper for GAR15.

UNISDR – United Nations Office for Disaster Risk Reduction (2005). Hyogo Framework for Action. Geneva, Switzerland.

UNISDR (2009). Risk and poverty in a changing climate. Invest today for a safer tomorrow Global Assessment Report on Disaster Risk Reduction 2009. Geneva, Switzerland.

UNISDR – United Nations Office for Disaster Risk Reduction (2011). Revealing Risk, Redefining Development. Global Assessment Report on Disaster Risk Reduction 2011. Geneva, Switzerland.

UNISDR – United Nations Office for Disaster Risk Reduction (2013). From Shared Risk to Shared Value: The Business case for Disaster Risk Reduction. Global Assessment Report on Disaster Risk Reduction 2013. Geneva, Switzerland.

UNISDR – United Nations Office for Disaster Risk Reduction (2015a). Sendai Framework for Disaster Risk Reduction 2015 - 2030. Geneva, Switzerland.

UNISDR – United Nations Office for Disaster Risk Reduction (2015b). Making Development Sustainable: The Future of Disaster Risk Management. Global Assessment Report on Disaster Risk Reduction 2015. Geneva, Switzerland.

United Nations (2015a). World Urbanization Prospects: The 2014 Revision. Department of Economic and Social Affairs, Population Division. ST/ESA/SER.A/366.

United Nations (2015b). Transforming our world: the 2030 Agenda for Sustainable Development. United Nations General Assembly A/RES/70/1 September 2015. New York, USA.

United Nations (2016). Report of the open-ended intergovernmental expert working group on indicators and terminology relating to disaster risk reduction United Nations General Assembly A/71/644. 1 December 2016. New York, USA.

Veal M. (2007). Dub: Soundscapes and Shattered Songs in Jamaican Reggae Wesleyan University Press. Connecticut, USA.

Velásquez C.A., Cardona O.D., Mora M.G., Yamín L.E., Carreño M.L. and Barbat A.H. (2014). Hybrid loss exceedance curve (HLEC) for disaster risk assessment. Natural Hazards 72(2):455-479.

Williges K., Hochrainer-Stigler S., Mochizuki J. and Mechler R. (2015). Modeling the indirect and fiscal risks from natural disasters: Emphasizing resilience and "building back better". Background paper for GAR15.

Woo G. (1996). Kernel Estimation Methods for Seismic Hazard Area Source Modeling. Bulletin of the Seismological Society of America. 68(2):353-362.

World Bank (2016). World Bank Open Data. Available at: data.worldbank.org

Wulf A. (2015). The Invention of Nature: Alexander von Humboldt's New World Random House. New York, USA.

Acknowledgements

The GAR Atlas has been produced by UNISDR in collaboration with INGENIAR LTDA, Earth Literacy Programme and AXIS.

Editor: Andrew Maskrey.

Coordination: Mabel Marulanda Fraume, Bina Desai.

Lead authors: Andrew Maskrey, Bina Desai, Mabel Marulanda Fraume, Mario A. Salgado-Gálvez.

Cartography: Stéphane Kluser (Komplo), Johoner Correa.

Figures: Paula Marulanda Fraume.

Technical support and concept development: Omar-Dario Cardona, Gabriel Bernal, Paula Marulanda Fraume, César Velásquez, Martha-Liliana Carreño, Pascal Peduzzi, Claudia Villegas.

Augmented reality and GAR for Tangible Earth (GfT) application: Tangible Earth (TE)platform design and GfT scenario development: Shin'ichi Takemura; TE systems architecture: Ryuichi Iwamasa, Takahiro Shinkai and Jun Nishimura; GfT scenario development: Yoshiyuki Inaba; Production management: Shin'ichi Takemura ; Case studies for GfT: Sylvain Ponserre (UNISDR); GfT interface design: Jun Nishimura, Masashi Tomura (AXIS).

Proof reading and correction: Frédéric Delpech, Jonathan Fowler.

Production coordination: Frédéric Delpech.

Design and Layout: Masashi Tomura, Mitsuhiro Miyazaki (AXIS), Takae Ooka, Earth Literacy Program (NPO).

Online GAR Atlas: Sylvain Ponserre, Mario A. Salgado-Gálvez, Mabel Marulanda Fraume.

GAR Atlas risk data platform: Julio Serje, Mario A. Salgado-Gálvez.

Printing: Imprimerie Gonnet (Belley, France).

Procurement: United Nations Office at Geneva (UNOG).

The GAR Global Risk Model (GRM) has been developed by UNISDR in collaboration with the following institutions:

Coordination (UNISDR): Andrew Maskrey, Mabel Marulanda Fraume, Mario A. Salgado-Gálvez, Manuela di Mauro, Julio Serje, Sylvain Ponserre, Bina Desai.

INGENIAR LTDA & CIMNE: Omar-Darío Cardona, Gabriel Bernal, Mario A. Salgado-Gálvez, Cesar Velásquez, Claudia Villegas, Diana González, Daniela Zuloaga & Alex Barbat, Martha Liliana Carreño.

CIMA Foundation: Roberto Rudari, Lorenzo Campos, Francesco Gaetani, Giorgio Boni.

Geoscience Australia: Adele Bear-Crozier, Ken Dale, Gareth Davis, Mark Edwards, Jonathan Griffin, Nick Horspool, Andrew Jones, Tariq Maqsood, Steve Newey, Victoria Miller, Hyeuk Ryu, John Schneider, R. Weber, Martin Wehner.

Norwegian Geotechnical Institute (NGI): Farrokh Nadim, Carl Harbist, Finn Løvholt, Sylfest Glimsdal, Helge Smebye, Jose Cepeda.

Universidad Nacional Autonoma de Mexico (UNAM): Mario Ordaz and Krishna Singh.

United Nations Environment Programme (UNEP-GRID Geneva): Pascal Peduzzi, Andrea de Bono, Christian Herold, Bruno Chatenoux.

WAPMERR: Max Wyss, Philippe Rosset, Stavros Tolis.

Global Volcano Model (GVM) and International Association of Volcanology and Chemistry of the Earth's Interior (IAVCEI): Susan C. Loughlin, British Geological Survey; Sarah. K. Brown, Steve Sparks, and Susanna Jenkins, University of Bristol; Charlotte Vye-Brown, British Geological Survey; Thomas Wilson, University of Canterbury; Christina Magill, Macquarie University; Victoria Miller, Geoscience Australia; C. Stewart, Joint Center for Disaster Research, GNS Science, Massey University.

International Institute for Applied Systems Analysis (IIASA): Stefan Hochrainer; Reinhardt Mechler; Junko Mochizuki; Keith Williges.

The Global Assessment Report (GAR) brand iconography is based on an image of a person holding an inverted umbrella.
The inverted "A" in the GAR 2015 logo is a resonance of this motif.

Thus, the inverted umbrella is an icon of positive empowerment, advocating disaster risk management as an opportunity rather than a cost, and as something which makes human and planetary well-being possible.

Inverted umbrella symbol: Taku Satoh and Shin'ichi Takemura, inspired by the work of Makoto Murase and the Institute on Sky Water Harvesting

120° W
60° W
ARCTIC OCEAN
NORTH PACIFIC OCEAN
NORTH ATLANTIC OCEAN
30° N
Equator
30° S
SOUTH PACIFIC OCEAN
SOUTH ATLANTIC OCEAN
SOUTHERN OCEAN
120° W
60° W
East Asia and the Pacific
South Asia
North America
Latin America and the Caribbean
Middle East and North Africa
Sub-Saharan Africa
Europe and Central Asia

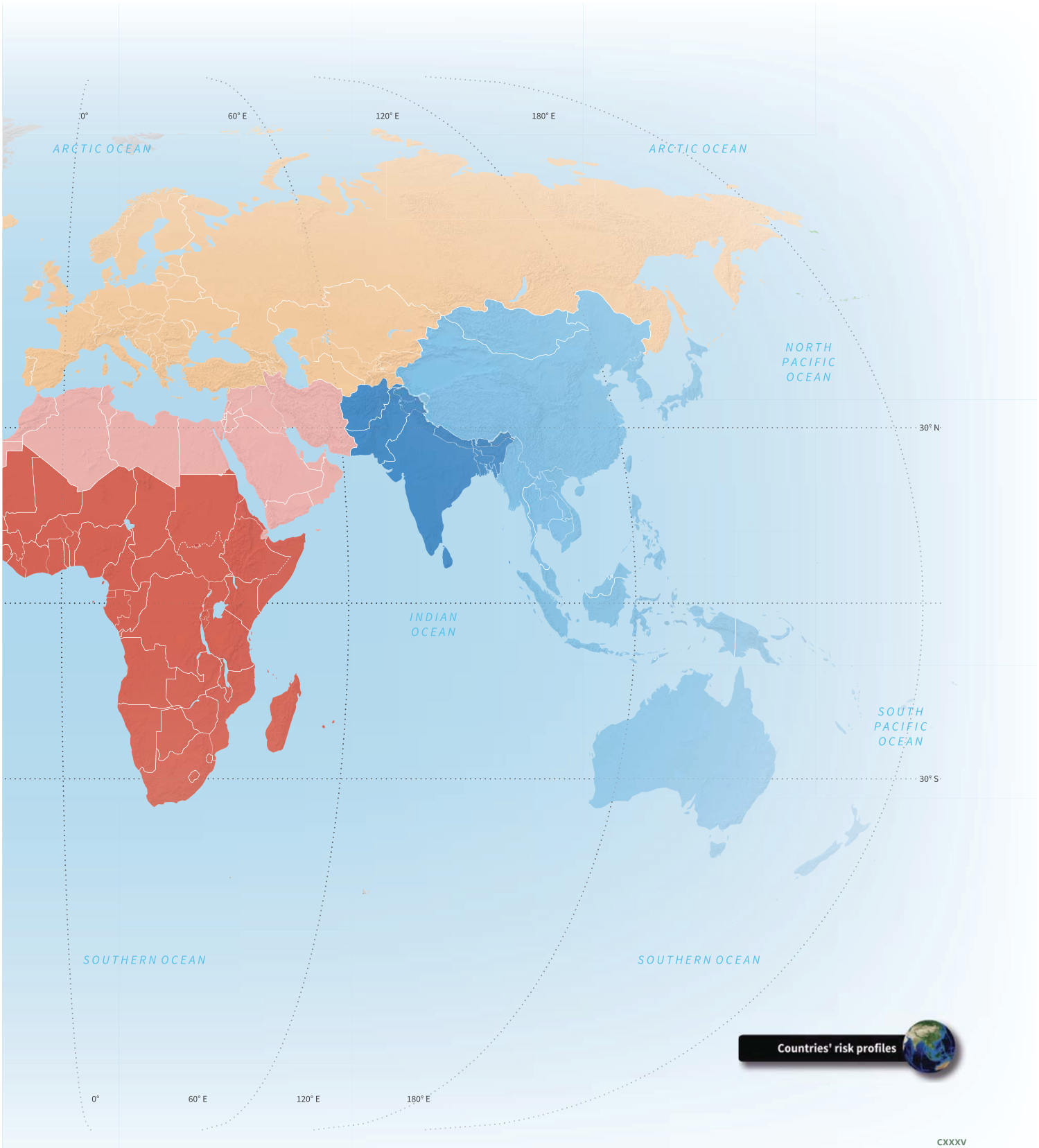

Countries' risk profiles

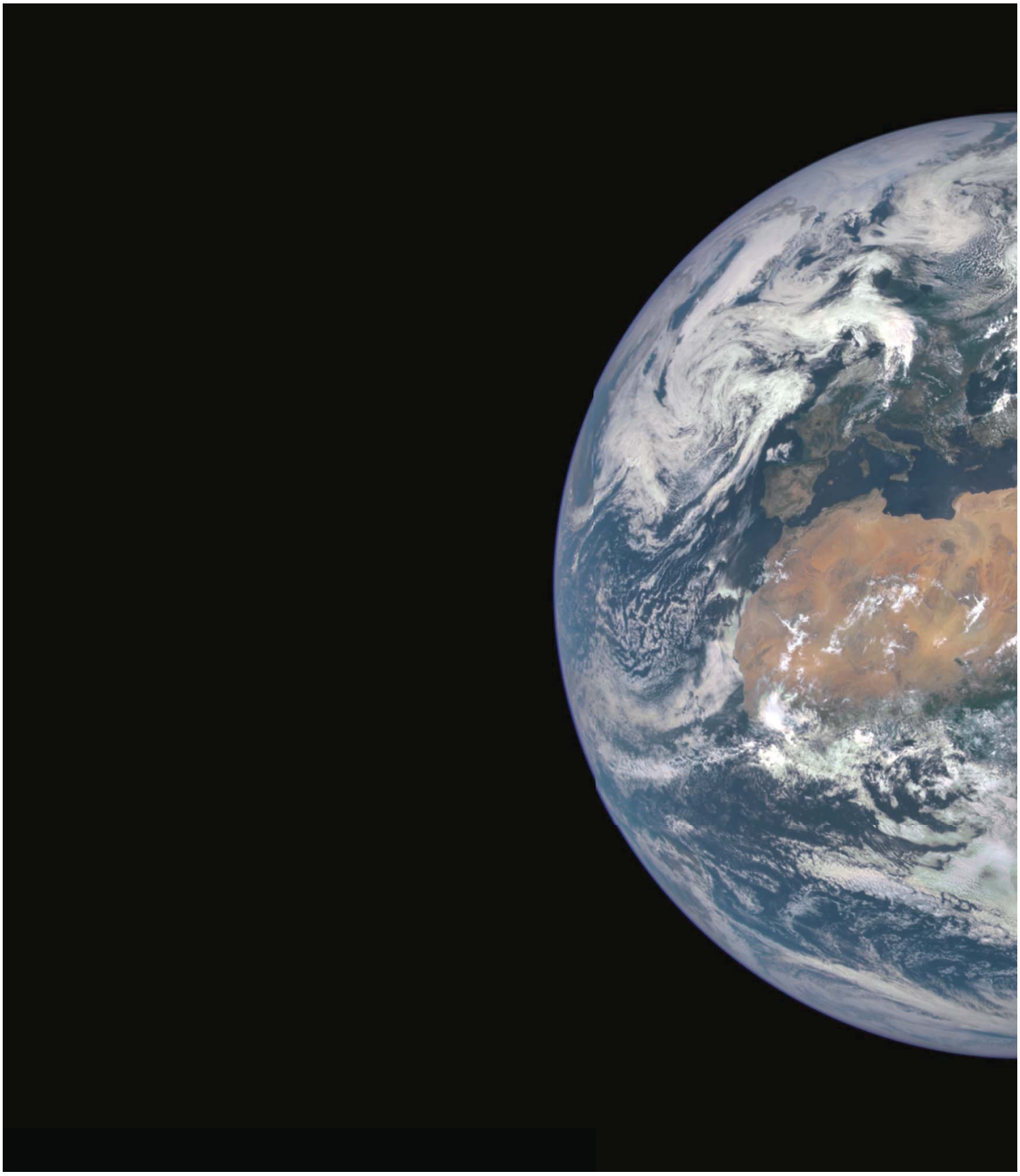

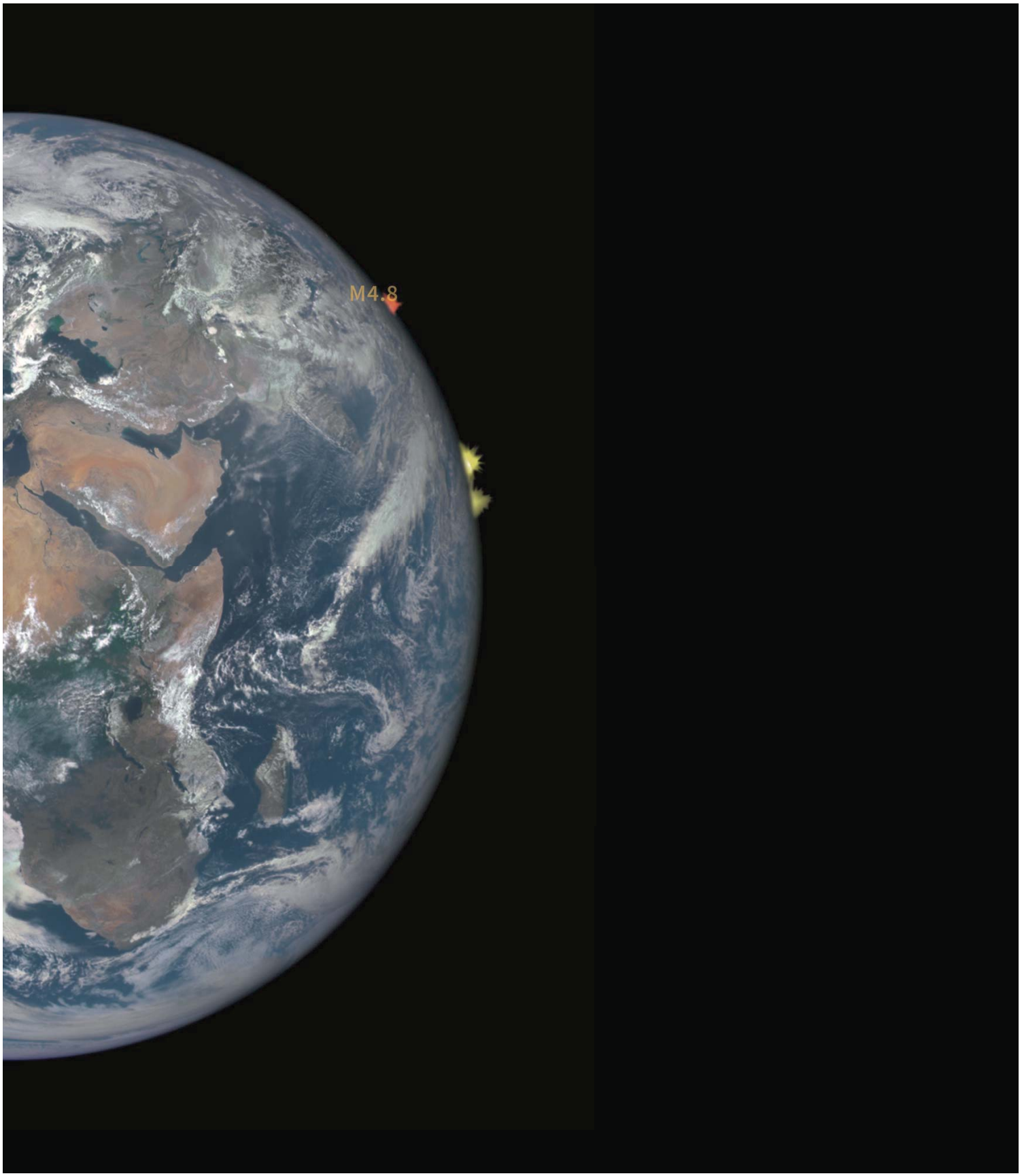
M4.8

GAR Atlas Products

• The GAR Atlas contains risk indicators and hazard maps and further enhanced content links which provide access to maps, videos, dynamic figures, photos, case studies and country risk profiles for users with tablets.

• Tablet computer users can also enjoy the free GAR for Tangible Earth (GfT) application. The GfT (or "gift) This includes a detailed risk profile, including the absolute and relative Annual Average Loss (AAL), a Loss Exceedance Curve (LEC) and, where available, data on historical disaster losses. Furthermore, additional information is provided on Average Annual Mortality for earthquakes, financing gaps as well as on the social, economic and environmental drivers of risk and resilience.

• GAR Atlas platform is also available in the web which allows access to hazard, exposure and risk maps and to all the datasets (hazard, exposure, vulnerability) used in the multi-hazard probabilistic risk assessment to obtain the different risk metrics.

• GAR Atlas is also available as a web version, with much of the functionality available in products such as:

- Interactive GAR Atlas (in English only)
- PDF of the GAR Atlas
- Background papers
- Access to the GAR Atlas platform

• All GAR Atlas products can be accessed via:

www.preventionweb.net/gar/

UNISDR
United Nations Office for Disaster Risk Reduction